Development of alkali-activated slag concrete for potential application in pavements using municipal solid waste incineration bottom ash aggregates

Ivana Mariam Paul

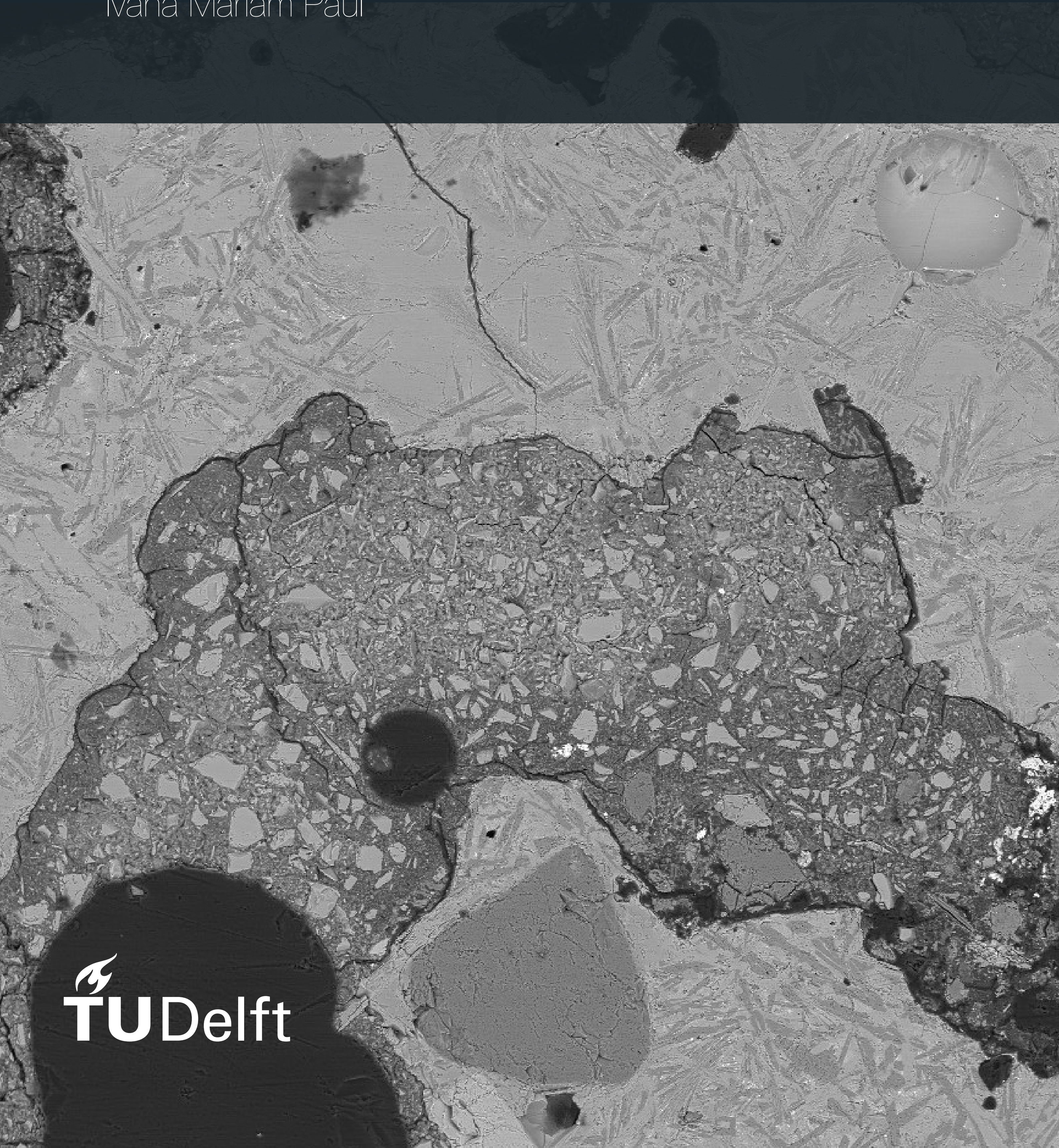

DEVELOPMENT OF ALKALI-ACTIVATED SLAG CONCRETE FOR POTENTIAL APPLICATION IN PAVEMENTS USING MUNICIPAL SOLID WASTE INCINERATION BOTTOM ASH AGGREGATES

AN EXPERIMENTAL INVESTIGATION

by

IVANA MARIAM PAUL

to obtain the degree of Master of Science
at the Delft University of Technology,
to be defended publicly on Friday 23 June, 2023

Student number:	5263050	
Project duration:	January 1, 2022 – June 31 , 2023	
Thesis committee:	Dr. G. (Guang) Ye,	Chairman
	Prof. dr. ir. M.A.N. (Max) Hendriks,	Supervisor
	Dr. Xueyan Liu,	Supervisor
	Dr. Ir. Boyu Chen,	Daily Supervisor
	Ir. Luiz Cezar Miranda de Lima Junior,	Daily Supervisor

To my loving parents , sister
and grandmother

SUMMARY

The development of an efficient and sustainable transportation system is crucial for the effective functioning of economies. The demand for sustainable roadways and functional connectivity is increasing with the growing population and urbanisation. Concrete, a widely used material for construction purposes, poses significant environmental challenges. As a result, researchers are continuously exploring sustainable alternatives to traditional concrete (ordinary Portland cement concrete), and alkali-activated concrete is a sustainable alternative. However, the aggregates used in alkali-activated concrete are typically mined, contributing to negative environmental impact. To address this concern, municipal solid waste incineration bottom ash (MSWI BA) obtained through the incineration of municipal solid waste can be utilised to replace natural aggregates. Thus the construction of pavements using sustainable concrete facilitates its growing demand without burdening the environment.

This research focuses on the utilisation of MSWI BA aggregates in alkali-activated concrete for potential application in pavements. The study is divided into five phases: aggregate characterisation, mechanical properties evaluation, long-term performance study, microstructure analysis, and life cycle assessment (LCA) analysis. The physical properties of MSWI BA aggregates indicated higher water absorption and lower density compared to natural aggregates, attributed to their production process. Nonetheless, these aggregates showed almost comparable properties to natural aggregates and can still be used for pavement application. However, the metallic aluminium in the MSWI BA aggregates releases hydrogen gas when it reacts with the alkali leading to concrete cracking and swelling, thus, hindering its use in various applications. To address this concern, alkaline pre-treatment using sodium hydroxide solution was employed in this research. The effectiveness of the treatment was observed to be higher for lower replacement levels (30%) of MSWI BA aggregates in alkali-activated concrete compared to higher levels (50% and 75%). Thus, an optimal replacement level of 30% was chosen based on the effectiveness of the pre-treatment in removing metallic aluminium and the compressive strength. Further tests (mechanical, durability, microstructure and environmental impact) were conducted only on the optimum replacement level.

In the next phase of the research, the mechanical and long-term performance of alkali-activated concrete with 30% MSWI BA replacement was evaluated. The results demonstrated that the concrete satisfied the mechanical performance requirements for pavements, with compressive and tensile strength exceeding the minimum requirements after 28-days. However, the freeze-thaw resistance of the alkali-activated concrete was below the norm requirement due to air voids and associated cracking. Microstructure analysis using X-ray computed tomography and scanning electron microscopy confirms the higher porosity and presence of larger-sized air voids in the sample, potentially caused by the release of hydrogen gas and inherent porosity.

Scanning electron microscopy revealed reactive phases in the MSWI BA aggregates and poor aggregate-matrix bonding for the coarser fraction compared to the finer aggregate fraction, leading to decreased mechanical performance. Despite these findings, the alkali-activated concrete containing MSWI BA aggregates satisfied the majority of the norm requirements for pavement applications, indicating its potential for road pavements. However, evaluating the environmental impact of adding MSWI BA aggregates in concrete is essential. The conducted life cycle assessment demonstrated that the optimal replacement MSWI BA sample exhibited better environmental effects, indicated by a lower environmental cost indicator value compared to alkali-activated concrete and ordinary Portland cement concrete samples with similar 28-day compressive strength obtained from the literature.

In conclusion, the pre-treatment method utilised in this research is optimal for a replacement level of 30% of gravel with MSWI BA aggregates. The alkali-activated concrete with 30% replacement level meets all the mechanical property requirements stipulated by the norm for pavement application, exhibits good air void distribution, and has limited environmental impact owing to the lower ECI value. This study evaluated the feasibility of applying MSWI BA aggregates for pavement application and showed promising results. Further, recommendations were provided for the upscaling of the alkali-activated concrete containing MSWI BA aggregates in pavement application.

PREFACE

This thesis presents my research on the development of alkali-activated slag concrete for potential application in pavements using municipal solid waste incineration bottom ash aggregates. It is written for the fulfilment of my master's in Structural Engineering with a specialisation in Concrete Structures at TU Delft, Netherlands. This research, for me, has been an enriching journey with invaluable insights and memorable experiences.

First and foremost, I thank God for His grace and blessings all through my study and research.

I would like to extend my deepest appreciation to my chair, Dr. Guang Ye, for his unwavering support and guidance during the course of my research. I am truly grateful to Dr. Boyu Chen and Ir. Luiz Cezar Miranda de Lima Junior for their supervision, assistance, and valuable insights that have guided me through the various stages of my work and in the preparation of this thesis. I also extend my gratitude to Prof. Max Hendriks and Dr. Xueyan Liu for their valuable suggestions and critical evaluation of my research work.

I am indebted to my parents, my sister, and my family for their unconditional support and constant faith in my abilities, which enabled me to complete this research successfully. I am truly fortunate to have such a loving and supportive family. A special mention goes to my grandmother and Gemi for their unwavering faith and support during this crucial phase of my life. I extend my sincere gratitude to my best friend, Rahul, for going above and beyond to assist and support me in this endeavour. I also express my gratitude to Kanhai, Vivian, Srijit, Rohan, Varsha, Reuben, Ashwin and Riley for their caring and supportive friendship, which provided me with comfort during challenging times throughout this research.

I would like to thank Farnaz Aghabeyk, Patrick Holthuizen, Hu Shi, Ali Ghaderiaram, Zhiyuan Xu, and Ahmad Fathi for their support during my research. I am also grateful to the technicians for their assistance during the experimental phase of this research. There are many more individuals whose contributions helped me to complete this research, and I sincerely thank them for their support.

Once again, I extend my heartfelt gratitude to everyone who has supported me in this academic endeavour.

Ivana Mariam Paul
Delft, June 2023

CONTENTS

LIST OF FIGURES

LIST OF TABLES

LIST OF ABBREVIATIONS

AAB	Alkali Activated Binders
AAC	Alkali Activated Concrete
AASC	Alkali Activated Slag Concrete
ASR	Alklai Silica Reaction
BCC	Blended Cement Concrete
BFS	Blast Furnace Slag
CT	Computed Tomography
ECI	Environmental Cost Indicator
EDS	Energy Dispersive Spectrometer
EDX	Energy Dispersive X-Ray Spectroscopy
EPD	Environmental Product Declaration
GGFBS	Ground Granulated Blast Furnace Slag
ITZ	Interface Transition Zone
LCA	Life Cycle Assessment
LCI	Life Cycle Inventory
LCIA	Life Cycle Impact Assessment
MSWI BA	Municipal Solid Waste Incineration Bottom Ash
NaOH	Sodium Hydroxide
Na_2SiO_3	Sodium Silicate
OPC	Ordinary Portland Cement
PSD	Particle Size Distribution
RPM	Revolutions Per Minute
SCM	Supplementary Cementitious Materials
SEM	Scanning Electron Microscopy
SSD	Saturated Surface Dry

1

INTRODUCTION

1.1. RESEARCH BACKGROUND

An efficient transportation system plays a vital role in economic development, necessitating the construction of structurally and functionally sound roadways [1]. Road pavements are typically classified as: flexible pavements; constructed using bitumen, and concrete pavements. Concrete pavements, characterised by their ability to withstand the wear caused by moving loads, extended service life, and reduced maintenance costs, are preferred to flexible pavements [1, 2]. Despite the superior durability properties of rigid pavements, the use of concrete in it is concerning due to its adverse effects on the environment [3].

Traditional concrete is composed of aggregates, binder and water. The binder combines the aggregates, and ordinary Portland cement (OPC), is the commonly used binder in concrete [4, 5, 6]. However, OPC is responsible for significant carbon dioxide emissions, with its production alone contributing to 5-7% of the global CO_2 emissions [4, 7, 8, 9]. Further, natural aggregates constitute a major part of the concrete and are extracted from quarries or sandpits [10, 7]. Hence, its increased mining is affecting the ecological equilibrium by threatening the biodiversity, landscape and water sources [11, 12]. To address these environmental concerns, the exploration of alternative materials for producing eco-friendly concrete has gained attention.

The pursuit of finding alternative binders for concrete revealed promising potential in pozzolanic industrial and agricultural wastes. These supplementary cementitious materials (SCM's) can be used as binder along with cement and aggregates to produce blended cement concrete (BCC)[13]. Fly ash, ground granulated blast furnace slag (GGFBS) and silica fume are the most prominent SCM's utilized in concrete [13, 14]. BCC exhibited improved mechanical and durability properties compared to OPC concrete while allowing partial cement replacement and better environmental impact [15, 16].

The drive to provide a more environmentally friendly concrete which can fully replace OPC led to the extensive development of alkali-activated concrete (AAC). Alkali-activated concrete (AAC) has emerged as a sustainable alternative having good mechanical characteristics while entirely substituting cement [17]. The mineral binder in AAC incorporates industrial by-products resulting in sustainable management of these waste products while fully diminishing the effect of CO_2 emission related to the use of OPC. Despite the progress made by AAC to use sustainable binders, the use of natural aggregates in it remains a challenge. An alternative approach is required to replace natural aggregates and mitigate the environmental impact associated with their extraction.

While the extraction of natural aggregates poses a threat to the environment, the growing population and the solid waste generated as a result further contribute to the negative impact on the environment. Municipal solid waste (MSW) generated globally from commercial, residential and industrial activities is approximately 3.5 million tons per day. However, with increasing urbanisation and population growth, this amount is expected to reach 6.1 million tons per day by 2025 [11]. To tackle the negative impact on the ecological environment, most countries adopt the incineration of MSW. But these MSWI ashes are still mostly landfilled, posing the risk of soil and environmental contamination caused by heavy metals leaching [18]. Utilising these ashes in concrete provides a more sustainable management of these ashes, and its potential for application in concrete is receiving increasing attention.

The incineration of municipal solid wastes produces bottom ash and fly ash. Bottom ash constitutes about 80-85% by mass of the incinerated ash[19]. The presence of harmful metals, including lead, zinc and antimony in bottom ash is comparatively lower than in fly ash, making it a more suitable material. Previously, MSWI BA was used as loose aggregates in base layers for road construction and embankments [20]. Extending the utilisation of MSWI bottom ash as aggregates in concrete aids in reducing the waste material in landfills and serves as a viable substitute for natural aggregates in concrete.

Concrete pavements are mostly cement despite their negative environmental impact. Further, concrete pavements can be subjected to freeze-thaw deterioration in cold regions [21]. De-icing salts are used on road pavements to prevent the freezing of water on the surface, which leads to increased damage of the concrete. The road pavements in the Netherlands are also affected by the freeze-thaw mechanism, which further deteriorates in the presence of de-icing salts [22]).

Currently, municipal solid waste incineration bottom ash (MSWI BA) are used as aggregates in OPC concrete, and its use in AAC is yet to be explored [23]. Hence, information on the performance and challenges involved in the utilisation of MSWI BA aggregates in AAC is lacking. Further, the application of alkali-activated concrete for concrete pavements is limited owing to the absence of convincing evidence on its feasibility to replace OPC concrete [24]. The study aims to evaluate the possibility of applying alkali-activated concrete with MSWI BA aggregates in concrete pavements in the Netherlands.

1.2. KNOWLEDGE GAPS

MSWI BA aggregates are commonly used in ordinary Portland cement concrete for road constructions, particularly in unbound sub-base or base layers. However, their utilisation in the top layers is restricted due to the harmful materials in the aggregates, which can negatively impact the performance of concrete. To address this limitation pre-treatment of the aggregates are conducted using methods including weathering, solidification, magnetic separation, and alkaline pre-treatment. However, most of the pre-treatment methodologies can adversely impact the environment. Considering these details in the literature, this research addresses the following knowledge gap:

- Concrete pavements largely use cement binders. An alternate sustainable option is to adopt alkali-activated concrete for pavements which are cement free. The possibility of the application is yet to be fully evaluated for the application in pavements.

- MSWI BA aggregates are a sustainable alternative to natural aggregates but require treatment to overcome the limitations related to harmful metals and organic content. Existing treatment processes are either environmentally burdensome or not economically viable. A sustainable and cost-effective treatment process needs to be investigated to elevate the quality of the aggregates.

- The MSWI BA are currently used as aggregate replacement in Portland cement concrete systems. The numerous challenges involving the harmful metals in the MSWI BA aggregates, and the aggressive environment in the AAC due to the presence of alkalis have limited the application of the aggregates in the AAC. Hence, the mechanical and long-term performance of alkali-activated concrete containing coarse MSWI BA aggregates is yet to be explored.

- MSWI BA aggregates are regarded as environmentally burden-free. Nevertheless, a comprehensive understanding of the environmental impact of the AAC containing MSWI BA aggregates necessitates the quantification of the impact, which is lacking.

1.3. RESEARCH AIM

The research aims to develop an AAC mixture utilising MSWI BA aggregates for potential application in road pavements in the Netherlands. Further, it investigates the mechanical and long-term performance of the designed concrete. The feasibility of applying the concrete in pavements is established by comparing it against the norm requirements (NEN 1338 (2003) [25]). The research also provides insights into the microstructural changes with the introduction of MSWI BA aggregates in AAC. The environmental effects of this concrete are realised by conducting a life cycle assessment (LCA) analysis. The detailed objectives of the research are mentioned below:

1. To find the optimum replacement level of natural gravel with bottom ash aggregates in AAC with a minimum compressive strength of C30/37 after 28 days.
    - To find a suitable pre-treatment procedure for removing metallic Aluminium in the MSWI BA aggregates.
    - To study the effect of replacement levels of treated MSWI BA aggregates on the strength of AAC.

2. To investigate the mechanical properties (Compressive strength, splitting tensile strength and Flexural strength) and durability (Freeze-thaw resistance) of AAC after introducing MSWI BA aggregates.

3. To investigate the porosity and features of the concrete after introducing MSWI BA aggregates.

4. To analyse the environmental impacts of using the AAC concrete containing MSWI BA aggregates.

1.4. RESEARCH SCOPE

The scope of the research is to control the factors affecting the microstructure formation and to fully realize the effect of adding MSWI BA aggregates into concrete.

- The thesis involves the addition of MSWI BA coarse aggregates of size 4-11 mm; hence no paste or mortal-level studies are performed.

- No admixtures are added to fully realise the effect of MSWI BA aggregates on the mechanical and durability properties.

- Compressive strength is used as the parameter to evaluate the effectiveness of pretreatment to remove metallic aluminium from MSWI BA aggregates.

- All the control (reference) specimens are designed for similar 28-day compressive strength.

- The prepared AAC samples are sealed in a plastic cover and placed in the curing chamber at 20°C & Relative Humidity (RH)=99%.

1.5. THESIS OUTLINE

The thesis outline for this research is depicted in Figure 1.1. The outline entails a brief description of the chapter content.

Chapter 1: This chapter aims to give a general introduction to the research. The chapter entails the aim, objective and scope of the research.

Chapter 2: This chapter provides the state of the art and the background for designing the research methodology. It highlights the materials used in road pavements and the application of MSWI BA aggregates in concrete.

Chapter 3: This chapter presents the overview of the materials and the experimental methodology. The mix design and sample preparation for the concrete investigated in the later chapters are also provided.

Chapter 4: This chapter presents the detailed characteristics and pre-treatment of the MSWI BA aggregates. Particle size distribution, specific gravity, bulk density, water absorption, and Los Angeles Abrasion resistance are the physical properties measured. Based on the characteristics of MSWI BA aggregates, pre-treatment is conducted to enhance the quality by reducing the metallic Al present in it.

Chapter 5: This chapter investigates the mechanical properties and durability of AAC concrete containing MSWI BA aggregates. Compressive strength, tensile strength and flexural strength are the mechanical properties investigated. Along with the mechanical performance, the long-term performance of the concrete is also investigated. Freeze-thaw resistance is the durability property under investigation. Further, the feasibility of the AAC with MSWI BA aggregates is compared with the norm requirements for pavements.

Chapter 6: This chapter provides details on the microstructure of AAC with MSWI BA aggregates. X-ray computed tomography (CT) and scanning electron microscopy (SEM) tests are conducted to analyse the air voids, gel formations and aggregate-matrix bonding. Further, the influence of these properties on the mechanical and durability performance is indicated.

Chapter 7: This chapter presents the environmental impacts of using MSWI BA aggregates in AAC. Life cycle assessment (LCA) is used to quantify the impact of MSWI BA in AAC. The leaching of heavy metals and ions from the AAC containing MSWI BA aggregates are evaluated in this chapter.

Chapter 8: The thesis discussion, conclusion and recommendations for future research are presented in this chapter

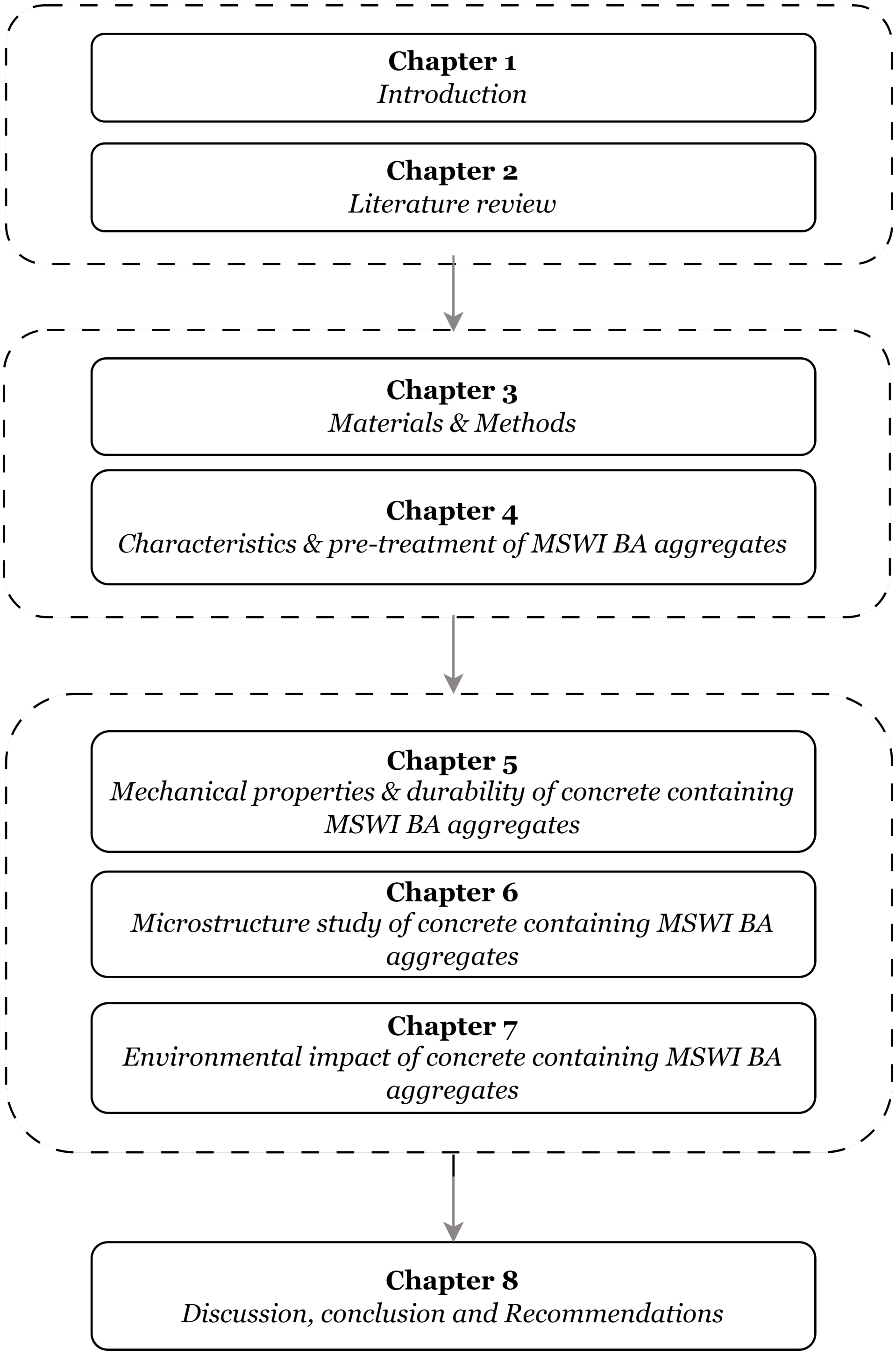

Figure 1.1: Thesis outline

2

LITERATURE REVIEW

2.1. CONCRETE PAVEMENTS

Concrete pavements are extensively used in constructing roadways, including national highways and expressways [2]. They are economical and durable, making them an attractive choice for construction [26]. These pavements are made either cast in situ or using precast concrete blocks.

The cast-in-situ rigid pavements are laid on the sub-base layer and have a square pattern for better load spreading. It generally consists of cement-bound or granular material. The precast concrete block pavements are placed on top of a bedding layer, a base course and a sub-base course later. The concrete pavement has a service life of 20 to 40 years [27, 26].

In the Netherlands, the road infrastructure is divided into a Main Road Network (MRN)and Secondary Road Network. The Main road network consists of the highways, which is maintained by the Rijkswaterstaat, while the secondary roads consist of the remaining road that does not belong to the main roads. The regional and local governments maintain it. The MRN consists of 95% of the roads and is made using asphalt. The secondary roads generally use concrete pavement blocks [26]. The pavement blocks used are about 8.5 cm in height.

2.2. BLENDED CEMENT CONCRETE (BCC)

Cement used in concrete contributes 5% to 7% of carbon dioxide emissions globally [4, 7]. Hence the need to shift from cement concrete roads is increasing. Blended cement is produced by incorporating waste products as substitutes for Portland cement.

The utilisation of blended cement effectively reduces the embodied greenhouse gas emissions associated with the production of concrete [28]. Ground granulated blast furnace slag (GGBFS) is a by-product in the production of metallic iron, and it contains the same oxides (SiO_2, Al_2O_3, CaO) as Portland cement [29]. Hence, blended cement can be made by partially replacing cement using GGBFS. Concrete pavements in the Netherlands are mainly constructed using CEM III/B, which is a blended cement (66 wt.% slag and 34 wt% OPC) [26, 30].

GGBFS has higher SiO_2 than CaO compared to OPC [31]. Hence, blending PC with GGBFS increases the amount of C-S-H formed, thus lowering the Ca/Si ratio [29]. The low Ca/Si C-S-H fills up the capillary pores leading to improved durability. It is observed that slags react relatively slowly compared to the PC clinkers in blended systems. Further, the hardening of slag is slower during the first 28 days, which then increases after that [29]. It was reported that the replacement of OPC with GGBFS reduced the early-age strength of the concrete since clinker contributed the most to the early-age hydration and early-age strength [29, 32, 33]

2.3. ALKALI-ACTIVATED CONCRETE (AAC)

The development of alkali-activated concrete (AAC) as an alternative to cement-based concrete has significantly reduced CO_2 emissions. Studies have shown that AAC can reduce CO_2 emissions by about 50-80% compared to Ordinary Portland Cement (OPC) concrete [34, 35, 36]. Further, AAC offers several advantages over OPC concrete, including excellent thermal stability, high early-strength, reduced shrinkage, low permeability, and superior resistance to chemical corrosion [37, 38, 39, 40]

AAC utilises aluminosilicate materials derived from geological sources or industrial by-products, combined with activators to form Alkali activated binders (AAB). These binders are then mixed with aggregates to produce concrete [16, 41]. These alumino silicate materials are called precursors, and the commonly used precursors are fly ash, blast furnace slag, and metakaolin [42, 43]. The most successful combination of activators in AAC involves sodium silicate and sodium hydroxide solutions [44, 36, 43]. The polymerisation process is depicted in Figure 2.1.

The stages in the geopolymerisation reaction involve the following;

- Alkaline hydrolysis causes the solid aluminosilicate source to dissolve, consuming water and producing aluminate and silicate species.
- The dissolved species and any existing silicate in the activating solution combine in the aqueous phase, forming a complex mixture of silicate, aluminate, and aluminosilicate species.
- Amorphous aluminosilicates dissolve rapidly at high pH, rapidly forming a supersaturated aluminosilicate solution. In concentrated solutions, this results in gel formation through condensation, releasing the water initially consumed during dissolution. Water acts as a reaction medium and resides within pores in the gel.
- The time it takes for the supersaturated aluminosilicate solution to form a continuous gel varies depending on the processing conditions of the raw materials, solution composition, and synthesis conditions.

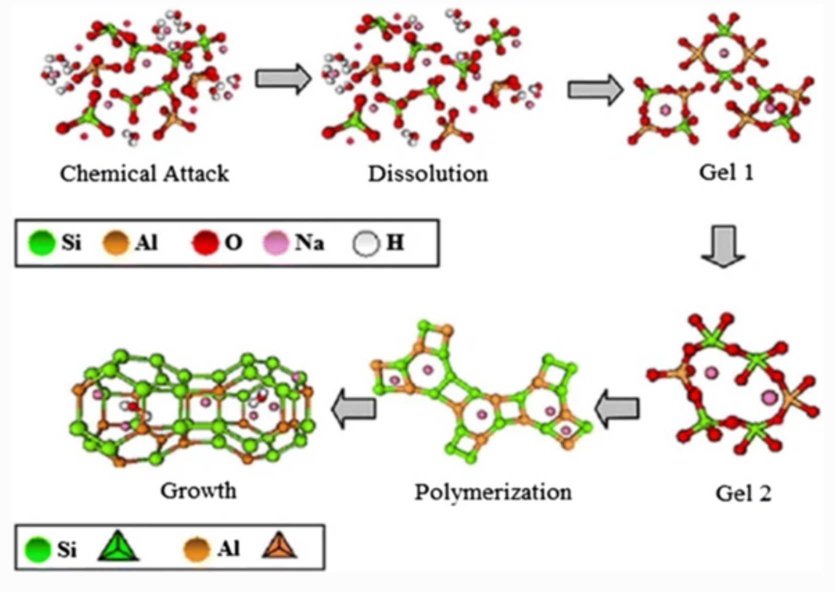

Figure 2.1: Geopolymerisation reaction [44]

- Following gelation, the system continues to undergo rearrangement and reorganisation as the connectivity of the gel network increases, ultimately resulting in the formation of a three-dimensional aluminosilicate network commonly observed in geopolymer [42, 44]

The alumino silicate source used in the geopolymerisation reaction is a high calcium system (GGBFS) or a low calcium system (Fly ash & metakaolin). The main reaction product of a high calcium system is a C-(A)-S-H gel with a lower Ca/Si ratio compared to an OPC system [43, 45]. However, the gel shows few features similar to the dominant C-S-H gel in OPC concrete [5, 45]. While a low calcium system majorly produces N-A-S-H gel that possesses a three-dimensional structure [16]. It was reported that precursor materials with high amounts of calcium oxide (CaO) give higher strength geopolymer concrete, reduce the setting time and improve mechanical properties when cured at ambient temperature [46]

The aluminosilicate source, curing conditions, type of alkaline activator, combination and concentration of the activator, and the alkaline activator to binder ratio primarily influence the properties of the geopolymers. These factors play a significant role in determining the final characteristics and performance of geopolymers [44, 47, 40, 48, 49].

2.3.1. PRECURSOR

Aluminosilicate-bearing raw materials, known as precursors, undergo dissolution by activators in alkali-activated materials (AAMs). These precursors often consist of waste products such as ground granulated blast furnace slag (GGBFS) and fly ash, which have a high amorphous content. When exposed to an alkaline medium, hydrolysis and condensation occur, resulting in the formation of new inorganic polymers capable of developing load-bearing capacity [50]

These precursors introduce dissolved and reactive elemental materials that undergo rearrangement during the hardening process [34]). These precursors' aluminium, calcium, and silicate contents significantly influence the outcomes of the geopolymerisation process. Factors like the Si/Al ratio, particle size (which affects the rate of monomer dissolution), calcium content, and other elemental compositions directly impact the resulting outcomes [44]

GGBFS is a widely used precursor in AAMs, obtained as a byproduct from pig iron production in blast furnaces. It has abundant Ca^{2+} and Mg^{2+} and is a cost-effective and easily available source of silica-rich material, with an estimated annual production of around 300 million tons globally [51]. Alkali-activated mortars based on GGBFS exhibit early high mechanical strength, durability against sulfate and acidic environments, reduced greenhouse gas emissions, and improved fire resistance [52, 44, 53]

The primary reaction product in the alkali activation of slag is a hydrated calcium silicate, such as C-S-H gel, which has a lower Ca/Si ratio compared to the one formed during Portland cement hydration [51]. The formation of additional phases or hydrated compounds depends on factors such as the type and quantity of activator used, the structure and composition of the slag, and the curing conditions during the hardening process [52].

Alkali-activated slag concrete (AASC) exhibits relatively high early strength and rapid strength development. However, a significant drawback is the high calcium content in GGBFS, which accelerates the reaction of alkaline binders and leads to early setting time [43]. The high mechanical strength of AASC is attributed to the fast rate of hydration reactions at elevated pH levels, resulting in high early-age strength, as well as a dense and homogeneous interface transition zone (ITZ) with minimal strength differences between the ITZ and the binders [16].

2.3.2. ACTIVATORS

Aluminosilicate precursors, crucial for geopolymers, have limited reactivity with water [34, 48]. Therefore, an alkaline medium is employed to dissolve the abundant silicate and aluminate, termed alkali activation, thus forming a gel that subsequently hardens [34]. This process involves ion exchange, hydrolysis of Si and Al, and the breakdown of their networks. The alkaline solution serves two primary roles:

1. Dissolving Si-O and Al-O bonds and facilitating their re-establishment in the geopolymer network
2. Charge-balancing the mixture with alkali-metal cations

The most commonly used alkaline solutions include alkali hydroxides (NaOH, KOH) and alkali silicates (Na_2SiO_3, K_2SiO_3) [54]. Sodium hydroxide, derived from brine electrolysis, is available in flakes, beads, and solid forms. The chemical composition remains the same, but particle sizes differ [43]. Sodium silicate, obtained from carbonate salts and silica, promotes the polymerisation process, resulting in a silica-rich reaction product and improved strength [40]

The concentration of alkaline activators in the geopolymer concrete matrix significantly influences the release of silica and alumina particles, with higher NaOH molarity resulting in increased release [35]. Studies have demonstrated that increasing the concentration of activators enhances the mechanical strength of alkali-activated slag (AAS) [40]. The dosage of Na_2O and the activator modulus (SiO_2/Na_2O) also impact the microstructure and mechanical properties of AAS concrete [48].

2.3.3. CURING CONDITION

Alkali-activated materials exhibit varying chemical compositions depending on the type of precursor utilised, often requiring specific techniques to enhance their reactivity. Thermal curing (through heating or oven), sealing (wrapping), steaming, and water immersion are commonly employed techniques to achieve optimal properties, depending on the alkali activated material system. Thermal curing is widely used initially to increase chemical reactivity during the early hardening stages, typically employing a temperature range of 60–80°C for the first 24 hours [44]. However, prolonged thermal curing has drawbacks such as drying shrinkage, increased porosity, and a loss of hardened state properties [16]. Water curing, on the other hand, has been reported to dilute the reaction, resulting in reduced pH, lower strength gain, and activator leaching [55]. Wrapping and sealing, as alternatives to water immersion, can minimise environmental effects such as evaporation, reducing porosity and overall shrinkage cracking [44].

2.4. MSWI BA AGGREGATES

Global municipal solid waste generation is projected to reach 3.4 billion tonnes by 2025 [56]. Waste generation and management strategies vary based on a country's development index. Recycling accounts for the reduction of approximately 19% of global waste, while 11% is incinerated. Although recycling is preferred, incineration becomes necessary for economically unrecyclable waste, allowing energy generation. Centralised incineration is widely employed to reduce waste volume, mitigate sanitary issues, and recover metals. This process reduces waste by 90% and produces bottom ash (coarse fraction) and fly ash (fine fraction) as residues. In Europe, approximately 16 million tonnes of bottom ash are generated annually from about 450 incinerators [56].

Municipal solid waste incineration bottom ash (MSWI BA) from municipal solid waste incineration, consists primarily of slag, black and non-ferrous metals, ceramic chips, glass, and other non-combustible organic matter as shown in Figure 2.2 [57, 58]. Its physicochemical and engineering properties' similarity to natural aggregates has led to its recognition as a potential substitute material in road construction [59, 60, 61]. However, the composition of bottom ash is influenced by factors such as the incineration technology employed and the type of solid waste being incinerated [62, 63].

2.4.1. PHYSICAL PROPERTIES

MSWI BA is an amorphous material with a grey to black appearance. Its quality is influenced by various factors, including the waste content, type of combustion unit, and the air

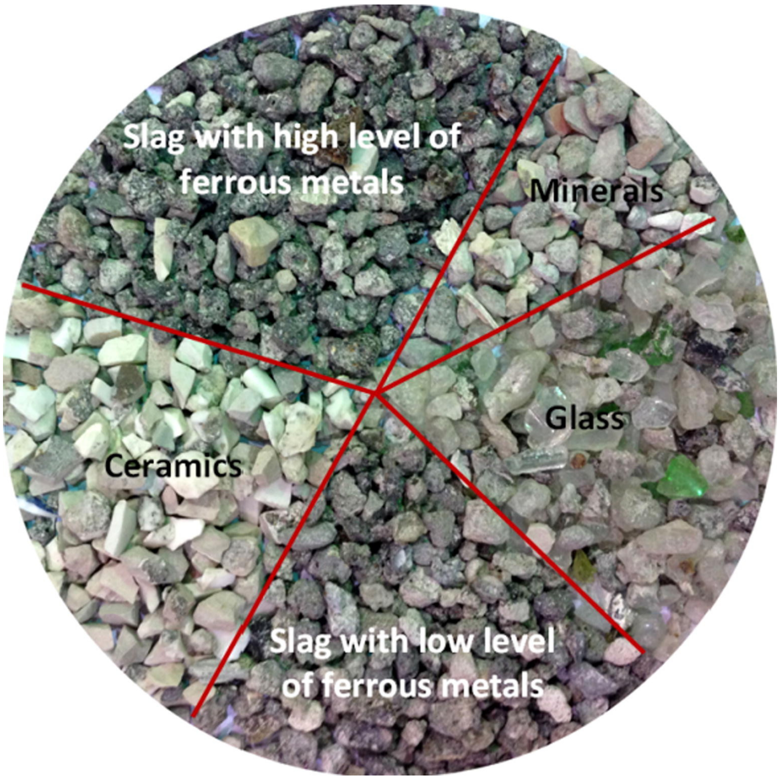

Figure 2.2: Composition of MSWI BA aggregates [58]

pollution control device employed in the incineration [11, 59].

Table 2.1: Physical properties of MSWI BA aggregates reported by researchers

Paper	**Particle size**	**Water absorption**	**Density**	**Loose bulk density**	**Los Angeles coefficient**
	(mm)	(wt %)	(kg/m^3)	(kg/m^3)	-
Ginés et al. (2009) [57]	3.2-5	15.75	2220	-	-
Ginés et al. (2009) [57]	5-25	2.72	2480	-	-
Kuo et al. (2013) [64]	0-12.5	1.94	2580	-	-
Kuo et al. (2013) [64]	0-9.5	4.21	2520	-	-
Huynh & Ngo (2022) [65]	0-5	7.71	2268	-	-
Bawab et al. (2021) [11]	0.02-10	1.5-2	1500-2400	-	29.6
Sorlini et al. (2011) [66]	9.5–19	6	2560	-	25.4
Sorlini et al. (2011) [66]	4.75–9.5	7.4	2411	-	-
Sorlini et al. (2011) [66]	2–31.5	-	2670	1600	33
Keulen et al. (2016) [67]	2-8	6.9	2400	-	31
Keulen et al. (2016) [67]	8-16	6.8	2250	-	

The physical properties of the MSWI BA aggregate from the literature show a wide range of density and water absorption values, as indicated in Table 2.1. As mentioned in the previous section, the type of waste material and the incineration process accounts for this. The water absorption is consistently higher for the coarser particles than the finer range. The density of the aggregates also reflects this. The Los Angeles coefficient is observed to be lower for the larger-sized particles compared to the smaller fraction. Table 2.1 clearly shows that the MSWI BA aggregates are produced in various size fractions depending on the production procedure and the treatment methodology adopted.

2.4.2. CHEMICAL PROPERTIES

The composition of MSWI BA can vary significantly depending on the source of waste and the incineration technology employed. Waste bottom ash characterisation shows that approximately 50% consists of glassy material, 37% comprises ceramic materials, and the remainder includes metals and a small percentage of unburned material [57]. However, regardless of the waste origin, the main oxides found in the characterisation are, Al_2O_3, CaO, and Fe_2O_3 [64, 11, 59]. These minerals, particularly SiO_2, exhibit similarities to the mineral composition of natural aggregates used in road construction [68, 69], indicating the potential for using MSWI BA as an aggregate in road construction [59].

Toxic elements, including heavy metals including Pb and Zn can also be present, potentially causing environmental leaching issues. The leachate pH plays a crucial role in the leaching behaviour of heavy metals in MSWI-BA. Ferrous metals account for approximately 7-15% of the composition, while non-ferrous metals make up around 2% [11, 70].

2.4.3. CURRENT APPLICATION

The extensive amount of bottom ash generated in waste incineration presents opportunities for circular economy practices. While it is currently used in minor applications such as filler or foundation material, it has the potential for higher-value applications in construction [56]. By incorporating recycled raw materials like bottom ash, the ecological footprint of building materials can be reduced.

One common practice is using it as a substitute for aggregate in road construction, adhering to specific requirements set by European countries [71]. Due to environmental concerns in the Netherlands, there is a shift away from using unbounded MSWI bottom ash in road construction and noise barriers. Various wet and dry treatment processes have been developed to improve the quality of the mineral fractions, making them suitable for concrete aggregates [72]. Experimental studies have also indicated that stabilised bottom ash can be incorporated at a percentage of 10% in cement-bound mixes and asphalt concretes for road pavements while meeting technical guidelines and leaching requirements [61]. To ensure compliance with technical and environmental requirements, MSWI ash used granular replacements in cement-based products must exhibit sufficient strength, durability, and leaching limits for toxic elements. Treatment of MSWI ash is often necessary to reduce the concentrations or mobilities of hazardous components [73].

However, improvements are necessary for MSWI BA to be effectively utilised in gravel-cement bases and concrete pavements. These improvements involve refining the particle size distribution and enhancing resistance to abrasion, which can be achieved by blending MSWI BA with a portion of natural aggregate [68].

2.4.4. CHALLENGES OF APPLYING MSWI BA AGGREGATES IN CONCRETE

Several research studies have highlighted various detrimental effects of using MSWI BA aggregates in concrete. These effects include:

- Strong and substantial decline of fresh concrete workability: Studies conducted have observed a significant reduction in the workability of fresh concrete when MSWI BA aggregates are incorporated[74]. This decrease in workability can pose challenges during the casting and placement of concrete.

- Severe matrix expansion and cracking by hydrogen gas production: MSWI BA aggregates can lead to hydrogen gas generation within the concrete matrix [70]. This gas production causes expansion and subsequent cracking, jeopardising the structural integrity of the concrete.

- Increase of matrix porosity and permeability due to gas bubble formation: Formation of gas bubbles within the concrete matrix as a result of hydrogen gas production from MSWI BA aggregates is observed by researchers [70, 75]. This gas bubble formation leads to a significant increase in matrix porosity and permeability, which can compromise the durability and long-term performance of the concrete.

- Moderate to high loss of mechanical strength: Research studies have shown a reduction in the mechanical strength of concrete containing MSWI BA aggregates [66, 75, 76]. The loss of mechanical strength can be attributed to factors such as cracking, increased porosity, and the presence of disturbing substances in the aggregates. These findings highlight the challenges associated with incorporating MSWI BA aggregates in concrete, prompting careful consideration and mitigation strategies to address these detrimental effects. The commonly used treatment methods to improve the quality of the MSWI BA aggregates are mentioned in the subsequent section

2.4.5. TREATMENT PROCESSES FOR MSWI BA AGGREGATES

WEATHERING

Heavy metals in bottom ash highlight the risk of soil, surface, and groundwater contamination if MSWI-BA is utilised as a granular material in road construction without pre-treatment [77]. To address this concern, ageing treatment in outdoor conditions is recommended as an effective pre-treatment method [59]. This treatment helps reduce carbonation, hydration, and organic bio-degradation reactions in MSWI-BA, leading to decreased mobility of certain heavy metals and improved environmental performance[78]

SEPARATION PROCESSES

Separation processes are commonly employed as the initial step in treating MSWI BA. Washing, electrochemical processes, magnetic density and eddy current are the separation techniques discussed. Washing uses leachate-like water to remove chlorides and heavy metals

[11]. Studies have shown that over 70% of chlorides can be removed with a liquid/solid ratio of 10:1, and a 15-minute water washing and shaking at a liquid/solid ratio of 2.5 can remove 77% of chlorides while dissolving highly soluble sulfates.

Metals may be present within the aggregate matrix of MSWI BA in the mineral form. To address this, leachates such as sodium carbonate (Na_2CO_3) or sodium hydroxide (NaOH) can increase the pH level and remove sulfates and remaining metallic aluminium [11]. A comprehensive description of the alkaline pre-treatment process is provided in the following section.

Electrochemical processes are another separation method used to extract and reduce the leaching of heavy metals. This technique creates an electric potential to facilitate reduction and oxidation reactions, resulting in metal accumulation on the cathode surface. The efficiency of this process was reported to be low; hence combining washing and remediation is also conducted to reduce the heavy metal leaching from the MSWI BA aggregates [11].

Magnetic density separation effectively separates metals in MSWI BA, particularly for the coarser aggregate fraction. This process can achieve recovery rates of up to 83% for ferrous metals [11, 79]. Typically, magnets are positioned above a conveyor belt to facilitate the extraction of magnetic particles from the bulk material stream. Subsequently, a different conveyor belt transports the separated particles either across or beyond the main material flow to a dedicated chamber [79]. Eddy current separation, on the other hand, is used for non-ferrous metal separation, especially aluminium and zinc. Eddy current separators generate magnetic fields within electrically conductive particles, in contrast to the alternating arrangement of permanent magnets found in a rotating magnet wheel. Non-conductive particles are influenced by gravity and velocity, causing them to fall off the conveyor belt, while conductive particles are attracted by repulsive forces [79]. The trajectory of particles is determined by various factors, including the size of the MSWI BA aggregates, with the efficiency of the process increasing with larger particles [11, 79].

SOLIDIFICATION AND STABILISATION METHODS

Solidification and stabilisation methods aim to immobilise the hazardous contents found in the MSWI BA by using additives, binders, or stabilisers. Solidification utilises certain binders, such as cement, to improve the physical properties and durability of the MSWI BA, creating a feasible aggregate for use in engineering applications. For example, it was reported that lightweight artificial aggregates suitable for use in structural concrete could be manufactured by the solidification of MSWI BA using cement. Solidification can also be done by hydrothermal treatment. It is based on solidifying MSWI BA at 150–200°C under high pressure. The main advantage of this process is that it can be applied on a large scale and significantly reduces heavy metals [11].

THERMAL TREATMENT

Thermal treatment methods involve treating MSWI BA at very high temperatures ranging from 700 °C to 1500 °C, transforming the ash into less heterogeneous slag. The reactions at such temperatures contribute to removing organic matter and immobilising heavy metals [11]. It also leads to the volatilisation of chlorides and the leaching levels of the products are much lower than that of untreated MSWI BA. The main concern of this method is its high cost, gas pollutants, and potential alkali-silica reaction (ASR) if used in concrete afterwards [11].

Another method that involves thermal treatment is sintering. This method can create a lightweight aggregate from MSWI BA, having properties comparable to lightweight NA after treating them at a temperature of around 1000 °C [11].

2.5. ALKALINE PRE-TREATMENT OF MSWI BA AGGREGATES

Metallic aluminium, originating from packaging materials, is a common component of MSWI BA and can be dissolved through chemical reactions in alkaline solutions. Alkaline pre-treatment is used by researchers due to its relatively simple and cost-effective process allowing large replacement of the aggregates, thus making it suitable for industrial application [80]. The effect of the alkaline pre-treatment investigated by researchers are as follows:

- Rübner et al. (2008) [75] utilised MSWI BA aggregates in the size range of 2-32 mm and subjected it to alkaline pre-treatment. The details of the pre-treatment process were lacking. However, the treatment had reported a reduction in the metallic Al content from an average of 1.4% to 0.2%. The research indicated promising results of the alkaline pre-treatment process.

- Kim et al. (2015) [80] used 1 M NaOH solution for the treatment of MSWI BA aggregates of size 0-4 mm. The author immersed the aggregates in the alkaline solution for 3-days after which no reaction was observed. The untreated MSWI BA aggregates had an initial metallic Al content of 0.03% which was reported to reduce to 0.004%.

- Van den Heede et al. (2016) [81] conducted alkaline pre-treatment using 1 M NaOH solution for 2 weeks with constant stirring for continuous release of hydrogen gas. The MSWI BA aggregates used in the research were in the size range of 2-20 mm. The pH before and after pre-treatment observed a reduction from 12.8 to 8-10.

- Xuan et al. (2018) [82] investigated the parameters that affect the quality of the alkaline pre-treatment of MSWI BA aggregates. The study reported that the concentration of the hydroxide ion and temperature mainly affected the effectiveness of the treatment and the L/S ratio had the least effect. It was concluded that the 1 M hydroxide ion concentration, 55°C temperature and a L/S ratio of 5 gave the best results.

2.6. MECHANICAL PROPERTIES OF MORTAR AND CONCRETE CONTAINING MSWI BA AGGREGATES

Depending on the chemical composition and size of the MSWI BA produced, the possible applications vary. MSWI BA fractions between 1 and 32 mm are generally utilised in concrete as coarse or fine aggregates [83]. The performance of the concrete and mortar samples containing MSWI BA aggregates of different size fractions reported by researchers are mentioned in Table 2.2.

Table 2.2: Mechanical properties of concrete and mortar samples containing MSWI BA aggregates

MSWI BA	Treatment	Replacement level (%)	Observation
Fine aggregates 1-2 mm Caprai et al. (2018) [83]	Hydrothermal treatment	100%	At 28 days, the inclusion of MSWI BA in mortars was reported to cause a reduction in compressive strength of approximately 15% and a reduction in flexural strength of approximately 9% compared to the reference samples without MSWI BA. Caprai et al. (2018 [83] explained that the lower mechanical strength observed was attributed to the higher porosity of the MSWI BA aggregates when compared to natural sand. This porosity-related decrease in strength is likely due to the failure of aggregates compared to the interfacial transitional zone (ITZ) where it is generally observed.
Fine aggregate <4 mm Lynn et al. (2016)[84]	Washing and chemical treatment(1 M NaOH solution)	Various replacement levels	Addition of MSWI BA aggregates in all the replacement levels were observed to cause a reduction in strength varying from , 2% to 30% for every 10 % increase in the replacement. However the washing and chemical treatment was reported to improve the strength compared to samples with untreated MSWI BA aggregates. Lynn et al. (2016) [84] reported that the improvement was due to the diminishing organics, salts and metals in the MSWI BA aggregates

Fine aggregates 0-4 mm Kim et al. (2015) [80]	Alkaline pre-treatment (1 M NaOH solution)	10%, 20%, 30% and 50%	Kim et al. (2015) [80] observed that the compressive strength at 28-days decreased rapidly with increasing replacement ratio when fine aggregate was re-placed with untreated bottom ash. The expansion of the concrete due to hydrogen gas release from the metallic aluminium in MSWI BA aggregates was mentioned as the cause for loss in strength. Further, it was reported that with increasing replacement ratio the compressive strength of the specimens with treated bottom ash decreased more gradually than the untreated ash specimens. A large drop in compressive strength was noticed by Kim et al. (2015) for the specimens with 50% replacement of untreated or treated MSWI BA aggregates.
Coarse and fine aggregate <10 mm Lynn et al. (2016) [84]	Alkaline pre-treatment (1 M NaOH solution)	Various replacement levels	Strength reductions of 5% per 25% replacement with MIBA content was observed after 28-days of curing when coarse aggregates were replaced. The lower absorption properties of the MSWI BA coarse aggregates compared to the finer fraction is explained as the cause for the strength reduction by Lynn et al. (2016) [84]. Further, the higher concentration of sulfate and chloride salts and metals lead, aluminium and zinc in the finer fraction of MIBA was also reported as the factors hindering strength development. Tensile strength was shown in the study to be decreasing with increasing MIBA fine and coarse aggregate content components, similar to the compressive strength.

Coarse aggregates <12.5 mm Saad et al. (2019) [85]	Cement solidification	Various replacement levels	The inclusion of MSWI BA (Municipal Solid Waste Incineration Bottom Ash) aggregates as a partial replacement for natural aggregates in concrete caused a decrease in compressive strength. However, Saad et al. (2019) [85] reported that the extent of this strength reduction was influenced by the amount of cement used during the solidification process in the treatment of MSWI BA aggregates. Further, concrete mixes incorporating solidified MSWI BA with a higher cement content exhibited a lower reduction in compressive strength compared to concrete containing natural aggregates.
Coarse aggregates 6-20 mm Van den Heede et al. (2016) [81]	Alkaline pretreatment (1 M NaOH solution)	Various replacement levels	Concrete containing MSWI BA demonstrated a strength performance that was reasonably comparable to the reference concrete. However, the strength gain between 28 days and 56 days of optimal curing was more pronounced in the BA concrete.
Coarse aggregates <22 mm Zhang & Zhao (2014) [76]	Wet grinding	30%, 50% and 70%	The increase in the weight percentage of MSWI BA aggregates in concrete exhibited a significant impact on early strengths. The study determined that the MSWI BA replacement of 50% was acceptable to replace natural aggregates. According to Zhang and Zhao (2014) [76], the decrease in early strength development was attributed to the substandard aggregate quality and delays in cement hydration as the content of MSWI BA is elevated. Furthermore, the study highlighted that MSWI BA demonstrated strength development during the later stages of hydration, which differed from OPC 42.5 R samples. Concrete mixtures with 70% replacement levels of BA exhibited lowest compressive strength. The diminished strength development in the later stages was attributed to the dilution effect, resulting in an insufficient amount of calcium hydroxide available for pozzolanic reactions.

Coarse and fine aggregates <5 mm S. Zhang et al. (2021) [86]	Pyrolysis and magnetic separation	50, 75 & 100%	The data provided in the study revealed a negative correlation between the strength of the concrete and the replacement ratio of the aggregate. The research indicated that the concrete mixture incorporating 50% BA-MSW aggregate exhibited a strength comparable to the reference batch at 1-day and 28-day ages.
Coarse aggregate 2-8 mm and 8-16 mm Keulen et al. (2016) [67]	Weathering, dry separation, wet separation and magnetic separation	40%, 70% and 100%	Increasing replacement levels of 2-8 mm aggregates was reported to enhance the tensile strength of concrete. This improvement was explained by the introduction of rougher and more rectangularly shaped MSWI BA aggregate and improved interfacial bonding compared to the rounder and smoother shape of conventional gravel aggregates. However, a reduction in flexural strength was observed as the replacement levels increased for the 8-16 mm particle size. The author explained this phenomenon as a consequence of reduced hardness, increased smoothness caused by the presence of glass and ceramics, and a lower specific surface area

Based on the findings summarized in Table 2.2, it is evident that incorporating MSWI BA aggregates as coarse or fine aggregates reduces the mechanical performance of concrete or mortar samples. Moreover, the concentration of harmful metals and the specific pre-treatment method employed to mitigate their presence play a significant role in determining the properties of concrete containing MSWI BA aggregates. Among the various pre-treatment techniques, alkaline pre-treatment being simple and cost-effective is frequently employed. Therefore, the selection of replacement levels and pre-treatment processes should be based on the specific requirements of the intended application.

2.7. FREEZE-THAW RESISTANCE OF CONCRETE CONTAINING MSWI BA AGGREGATES

Freeze-thaw resistance of the concrete containing MSWI BA aggregates, as observed by researchers, is explained in this section. The findings are as follows:

- Lynn et al. (2016) [84] conducted the freeze-thaw test on concrete mixes incorporating MSWI BA coarse and fine aggregates. The 20% MSWI BA coarse aggregate in concrete revealed enhanced durability. The study described the higher porosity of

MSWI BA aggregates, which effectively function as air entrainers, increasing the void spaces inside the concrete and, thus, the enhanced freeze-thaw resistance. Further, the study also indicated that the concrete containing 10% MSWI BA as fine aggregate exhibited favourable frost resistance.

- The study conducted by Keulen et al. (2016) [67] on concrete containing MSWI BA coarse aggregates showed promising results to freeze-thaw cycles. Although the resistance was lower compared to concrete containing natural aggregates, the replacement levels of MSWI BA aggregates at 40%, 70% and 100% satisfied the limits specified for the application of the concrete in road pavements.

- Yan et al. (2020) [87] evaluated the performance of concrete containing MSWI BA aggregates of size <20 mm based on the freeze-thaw index (BDR). It was observed that there was higher resistance to freeze-thaw cycles up to 10% replacement, beyond which the resistance was reduced. At lower replacement levels, the pozzolanic reaction of SiO_2 and Al_2O_3 phases in the reactive phases enhanced the cementitious material present, thus leading to a denser matrix and better freeze-thaw resistance. However, at higher replacement levels, the increased water absorption and resulting expansion lead to the poor freeze-thaw performance of concrete.

- Van den Heede et al. (2016) [81] investigated the freeze-thaw resistance of concrete with MSWI BA (2-20 mm) based on ultrasonic testing. The introduction of the treated aggregates in concrete caused no cracking on visual inspection. Further, the ultrasonic pulse velocities were almost equal before and after 14 freeze-thaw cycles. However, the study did not investigate the effects of de-icing salts on the freeze-thaw resistance of concrete.

Hence, to conclude, the freeze-thaw resistance of the concrete containing MSWI BA aggregates were lower than that of the concrete containing natural aggregates. At lower replacement levels, the pores inside the MSWI BA aggregate can accommodate freezable water, thus enhancing the freeze-thaw resistance of the concrete. Further, the reactive phases in MSWI BA aggregates can participate in the chemical reaction, thus making a denser matrix and subsequently improving the freeze-thaw resistance of concrete. However, it was observed that at increasing replacement levels, the favourable impact of the pozzolanic reaction and the presence of pores within the MSWI BA aggregates is outweighed by the higher water absorption capacity of these aggregates. This increased water absorption results in the expansion and failure of the aggregates during freezing conditions. Therefore, the utilization of higher replacement levels of MSWI BA aggregates necessitates careful consideration to avoid potential issues.

2.8. CONCLUSION

MSWI BA aggregates are commonly used in road constructions, particularly in unbound sub-base or base layers. However, their use in the top layers is restricted due to harmful materials in the aggregates, which can negatively impact the performance of concrete when utilised in upper layers. To address this limitation, various pre-treatment methods, such as weathering, solidification, magnetic separation, and alkaline pre-treatment, are employed to enhance the quality of the MSWI BA aggregates by removing pollutants.

Alkaline pre-treatment has proven to effectively eliminate metallic aluminium (Al) and zinc (Zn) from the aggregates. Nonetheless, the reactivity of the pre-treatment process depends on the aggregate size and the alkalinity of the solution utilised. The reaction rate has been reported to be higher in the initial stages but significantly decreases after 7 days. Importantly, larger particles of MSWI BA exhibit lower reactivity during the early stages than the finer fraction. This can be attributed to the embedded nature of metallic Al particles within the MSWI BA aggregates, which makes it challenging to expose them fully for pre-treatment. Consequently, removing harmful materials and achieving the desired aggregate quality for potential applications become more complex.

In summary, MSWI BA aggregates have found practicality in concrete road constructions due to their comparable physical properties to natural aggregates. However, their use in the top layers is limited due to the presence of harmful materials. To improve the quality of these aggregates, a combination of pre-treatment methods, including alkaline pre-treatment, is employed to remove metallic Al and Zn. Despite these efforts, the application of MSWI BA aggregates is currently restricted to Ordinary Portland Cement (OPC) concrete systems. The feasibility of using these aggregates in AAC systems is an area that requires further investigation.

3

MATERIALS AND METHODS

3.1. INTRODUCTION

This chapter presents an overview of the materials employed in this study for the production of concrete samples intended for potential utilisation in pavements. The material proportions and the concrete performance requirements stipulated in the norm are applied to design the concrete and to evaluate the feasibility of utilising the developed concrete in pavements. In addition, the experimental setup for this research is devised based on the norm requirements to evaluate the properties of the concrete. Further, the chapter entails the mix design and sample preparation procedure for producing the concrete samples used in this research.

3.2. MATERIALS

The materials used in the research consist of CEM III/B cement, ground granulated blast furnace slag (GGBFS), sodium hydroxide (NaOH) solution, water glass (Na_2SiO_3) solution, gravel, river sand and municipal solid waste incineration bottom ash (MSWI BA) aggregates as shown in Figure 3.1. Further, Table 3.1 shows the details of these materials.

The MSWI BA aggregates received from the company have undergone preliminary treatment to remove heavy metal and organic pollutants. However, analysis of the harmful substances present in the MSWI BA aggregates was conducted to ensure that the quality of the aggregates complies with the requirements of the standard. This evaluation verifies that the presence of MSWI BA aggregates does not induce detrimental effects on the performance of the AAC incorporating these aggregates.

Table 3.1: Materials used in concrete preparation

Catergory	Material	Size fraction	Source of acquisition
Precursor	GGBFS	-	Eco2cem Benelux B.V.
Activator	Sodium hydroxide solution (50% wt%)	-	Brenntag
	Water glass solution (37.5% wt%) (62.5% wt% water, Modulus=2.0/2.1)	-	PQ Corporation
Aggregates	MSWI BA	4-11 mm	Mineralz B.V.
	Gravel	4-8 mm 8-16 mm	Sibelco Benelux B.V.
	Sand	0-4 mm	Sibelco Benelux B.V.
Cement binder	CEM III/B 42.5 LH	-	ENCI

3.3. REQUIREMENTS FOR ROAD PAVEMENTS

In accordance with NEN 1338 (2003) [25] and NEN 206 (2017) [88], AAC containing MSWI BA aggregates is required to comply with certain mechanical and durability performance requirements prior to their application in pavements. To ensure the performance, the mix proportion requirements outlined in NEN 206 (2017) [25] are utilised for the design of concrete samples. Table 3.2 shows the performance and design requirements set forth by the norms.

3.4. RESEARCH METHODOLOGY

This research aims to develop an alkali-activated concrete (AAC) utilising MSWI aggregates for application in road pavements. Traditionally, pavements are constructed using ordinary Portland cement (OPC) concrete and blended cement concrete (BCC). However, AAC is used in this research as it offers a more sustainable alternative to the other concrete systems, and its feasibility for application in pavements is yet to be fully realised. AAC is designed considering the mechanical and long-term performance that needs to be satisfied by concrete applied in pavements. Since pavements mostly deteriorate when subjected to Freeze-thaw cycles, the resistance of the AAC to this mechanism is the primary long-term effect considered in this research. The concrete is designed to resist severe freeze-thaw conditions under the XF4 environmental exposure class.

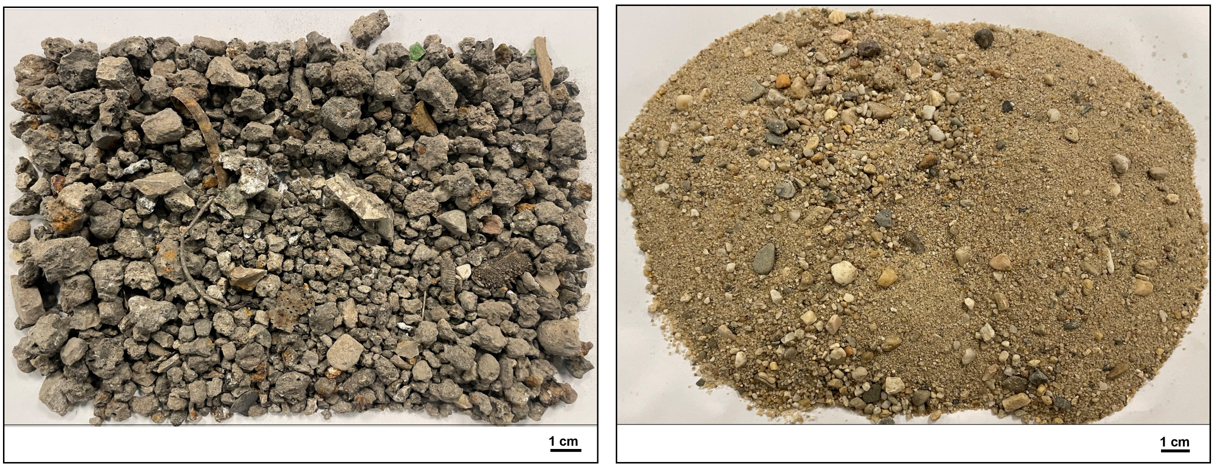

(a) MSWI BA aggregates (4 to 11 mm)

(b) Sand (0 to 4 mm)

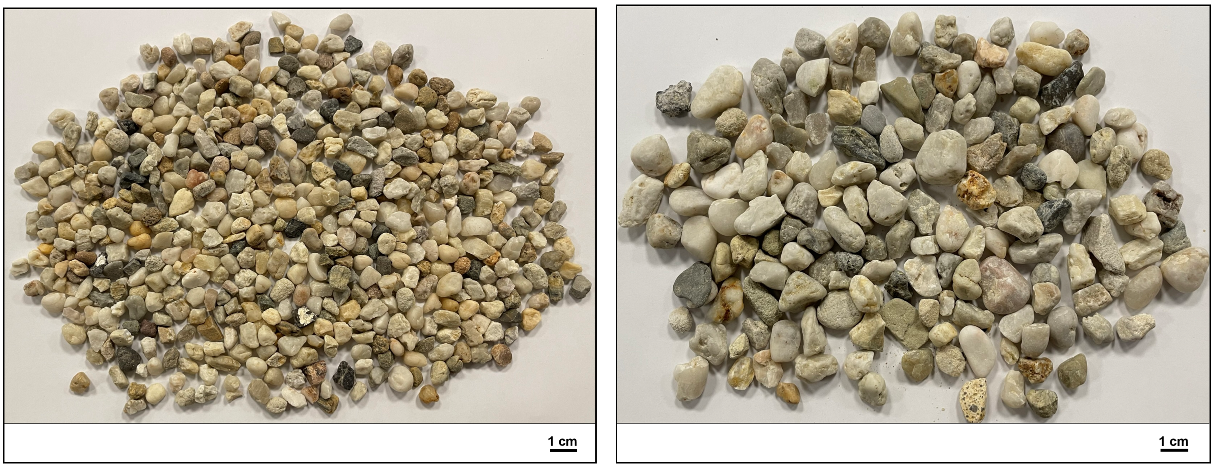

(c) Gravel (4 to 8 mm)

(d) Gravel (8 to 16 mm)

(e) Ground granulated blast furnace slag (GGBFS)

Figure 3.1: Images of materials used in this research

Table 3.2: Design and performance requirements for pavements

Performance parameters	**Requirements**	**Norm**
Freeze thaw resistance	Surface scaling less than 1 kg/m^2 after 28 freeze-thaw cycles	EN 1338 (2003) [25]
Tensile strength	Min 3.6 MPa	
Compressive strength	Min 37 MPa cube compressive strength after 28 days	NEN-EN 206+ NEN 8005 (2017) [88]
Metallic Al	Less than 1%	CUR Recommendation 116 (2017)[89]
Design parameters	**Requirements**	**Norm**
Durability requirement	Freeze-thaw	NEN-EN 206+NEN 8005 (2017) [88]
Environmental exposure class	XF4	
Strength requirement (28-day)	≥C 30/37	
Water-to-cement ratio	≤ 0.45	
Cement content (kg/m^3)	≥ 340	
Slump (mm)	0	

A key challenge with MSWI BA aggregates is the presence of metallic aluminium, which releases hydrogen gas in the presence of alkalis. This release of gas can cause severe cracking and swelling in the AAC and the subsequent decline in its performance. Hence, the norm specifies the maximum amount of metallic Al that can be present in the MSWI BA aggregates to ensure its quality. Thus, alkaline pre-treatment is conducted to reduce the presence of metallic Al in the aggregates before it is introduced in AAC. Further, this research quantifies the content of metallic Al in the pre-treated aggregates.

The gravel in the concrete is then partially replaced with pre-treated MSWI BA aggregates at replacement levels of 30%, 50% and 75%. The effectiveness of the pre-treatment of MSWI BA aggregates and the compressive strength of the AAC containing these aggregates are evaluated to obtain the optimum replacement level. Further, the mechanical properties and durability of the optimum replaced MSWI BA-containing AAC are examined and compared with the pavement requirements.

The effect of the addition of the MSWI BA aggregates on the mechanical properties and durability of the AAC is realised with microstructure analysis. The formation of air voids and subsequent cracking is a major reason for the loss of performance of AAC utilising MSWI BA aggregates. Hence, X-ray computed tomography (CT) is conducted to analyse the air voids and their distribution inside the concrete. Further, scanning electron microscopy (SEM) analysis is used to investigate the morphology of the MSWI BA aggregate, aggregate-matrix bonding and gel formations in the AAC containing MSWI BA aggregates. Further, to evaluate the environmental effects of the addition of MSWI BA aggregates in AAC, life cycle analysis (LCA) assessment is performed. Further, the leaching of heavy metals from the AAC containing MSWI BA aggregates is evaluated and compared with the limits specified in the Soil Quality Decree [90].

3.5. EXPERIMENTAL SETUP

The test plan for the research is developed based on the requirements for pavements, as mentioned in Section 3.3. Characteristics of the aggregate used in the research are analysed to ensure that it meets the norm requirements. Following this, the aggregates are introduced in AAC, and the performance of the concrete is investigated. Finally, Life cycle assessment (LCA) and leaching of the AAC containing MSWI BA aggregates are conducted to study its environmental effects.

3.5.1. TEST ON AGGREGATE

PHYSICAL PROPERTIES OF AGGREGATES

- Particle size distribution: The gradation of aggregates present in the concrete can influence its compaction, workability and performance. Hence, the norm specifies a range within which the aggregates must lie to ensure a good distribution.

- Water absorption: It is a direct indicator of the porosity of the aggregates, and it has a critical influence on the durability of the concrete. Further, the water absorption of the aggregate can influence the water content in the concrete mixture; hence it must be considered while designing the concrete mixtures.

- Density: The toughness of the aggregates is indicated by the density. Less dense aggregates tend to be weaker, thus reducing the strength of the concrete. The results of the aggregate density test are used to determine the quantity of MSWI BA aggregates that will replace the gravel fraction in the concrete.

- Loose bulk density: The packing of aggregates in concrete influences its strength and durability, and this property is influenced by the quality of the aggregate grading. A well-graded aggregate fraction forms lesser pores and denser packing, thus enhancing the concrete performance.

- Los Angeles abrasion: The aggregates used in the pavements must resist wearing from vehicle movement. A strong and dense aggregate tends to be more resistant to wear. Since MSWI BA aggregates are inherently porous, the aggregate's ability to resist wear must be assessed.

METALLIC AL QUANTIFICATION OF MSWI BA AGGREGATES

MSWI BA aggregates contain metallic Al, and their presence can be detrimental to AAC when the aggregates are directly introduced into it. The alkalis present in the AAC can react with metallic Al to release hydrogen gas. Thus, to avoid the cracking induced by this effect, the MSWI BA aggregates are treated before utilising in concrete. Alkaline pre-treatment using NaOH is adopted in this research.

3.5.2. TESTS ON CONCRETE

MECHANICAL PERFORMANCE

- Compressive strength test: Compressive strength is used as the index to compare the performance of the concrete samples. Mix designs are modified based on the 7-day compressive strength. Further, concrete samples used for pavements must satisfy a minimum requirement of C30/37 after 28 days.

- Splitting tensile strength test: Tensile stress development in concrete pavement is a major reason for its cracking, thus compromising its mechanical and long-term performance. Hence, the norm specifies a minimum tensile strength of 3.6 MPa after 28 days for the concrete used for the pavements.

- Flexural strength test: Road pavements are subjected to various loads, including traffic and stress-induced loads, that causes the bending of concrete. Flexural strength indicates the ability of the concrete to resist these loads.

DURABILITY

- Freeze-thaw: Concrete pavements used in cold regions are mostly affected by freeze and thaw cycles. The ability of the concrete specimen to resist these loads needs to be investigated based on the scaling of the material from the surface of the concrete sample. The loss of material from the concrete has to be less than the norm-specified amount of 1 kg/m^2

MICRO-STUDY

- X-ray-computed tomography (CT): Concrete microstructure is investigated to study the effect of introducing MSWI BA aggregates in AAC. X-ray CT scanning is conducted to obtain high-quality images of the concrete sample for microstructure study, specifically air voids. The effectiveness of the pre-treatment in removing metallic Al is investigated based on the porosity and air void distribution in the concrete sample. Further, the effect of the air voids on the mechanical properties and durability of the AAC utilising MSWI BA aggregates is also studied.

- Scanning Electron Microscopy (SEM): MSWI BA aggregates utilised in the AAC contain various phases, including reactive phases, which can influence the gel formations in the concrete and bonding between the MSWI BA aggregates and the matrix. These factors play a pivotal role in determining the mechanical performance and durability of the AAC containing MSWI BA aggregates. Hence, SEM-energy dispersive spectroscopy (EDS) is used to examine the morphology of the MSWI BA aggregates, the gel formation inside the AAC containing MSWI BA aggregates and the MSWI BA aggregate-matrix bonding.

ENVIRONMENTAL IMPACT

- Life cycle assessment (LCA): The life cycle assessment is conducted to assess the environmental impacts of the addition of MSWI BA aggregates in AAC.

- Leaching: The Soil Quality Decree [90] specifies the permissible amounts of leaching of heavy metals into the soil. Since the AAC incorporates MSWI BA aggregates that contain heavy metals, it is necessary to evaluate the potential leaching of these metals from the concrete into the soil, particularly due to its intended application in pavements.

3.6. MIXTURE DESIGN

The research aims to introduce MSWI BA aggregates in AAC to replace ordinary Portland cement (OPC) concrete. Further, the performance of the concrete subjected to freeze-thaw gives the long-term performance under investigation. In the Netherlands, Blended cement concrete (BCC) is used frequently to improve the sustainability of the pavements [26]. NEN 206 (2017) [91] specifies the mixture requirements for conventional concrete and BCC exposed to severe freezing and thawing condition in cold regions. Hence, the first step is to design BCC based on the norm-specified freeze-thaw XF4 exposure class. After obtaining the proportions for the BCC concrete, the second step is to design the Alkali activated concrete (AAC). The aggregate volume in the AAC and BCC mixture is kept constant. BCC and AAC use different mechanisms for microstructure development. Hence, 7-day compressive strength is used as the index to compare the mixtures. The activator content in the AAC is adjusted such that it achieves comparable compressive strength to the BCC mixture after 7-days. Pre-treated MSWI BA aggregates are introduced into the finalised AAC mixture, and their properties are investigated. Figure 3.2 shows the methodology used for designing the mixtures. Table 3.3 gives the nomenclature of all the mixtures that will be used throughout this research.

Table 3.3: Representation of mixtures used in the research

Category	Mixture	Representation	Description
Control sample	Blended cement concrete	100NA-BCC	100% Natural aggregate-BCC
Control sample	Alkali activated concrete	100NA-AAC	100% Natural aggregate-AAC
Test sample	AAC containing 30% MSWI BA aggregate	30BA-70NA-AAC-T20	30% MSWI BA aggregate+70% natural aggregate (4-8 mm)-AAC at 20°C
Test sample	AAC containing 50% MSWI BA aggregate	50BA-50NA-AAC-T20	50% MSWI BA aggregate+50% natural aggregate (4-8 mm)-AAC at 20°C
Test sample	AAC containing 75% MSWI BA aggregate	75BA-25NA-AAC-T20	75% MSWI BA aggregate+25% natural aggregate (4-8 mm)-AAC at 20°C

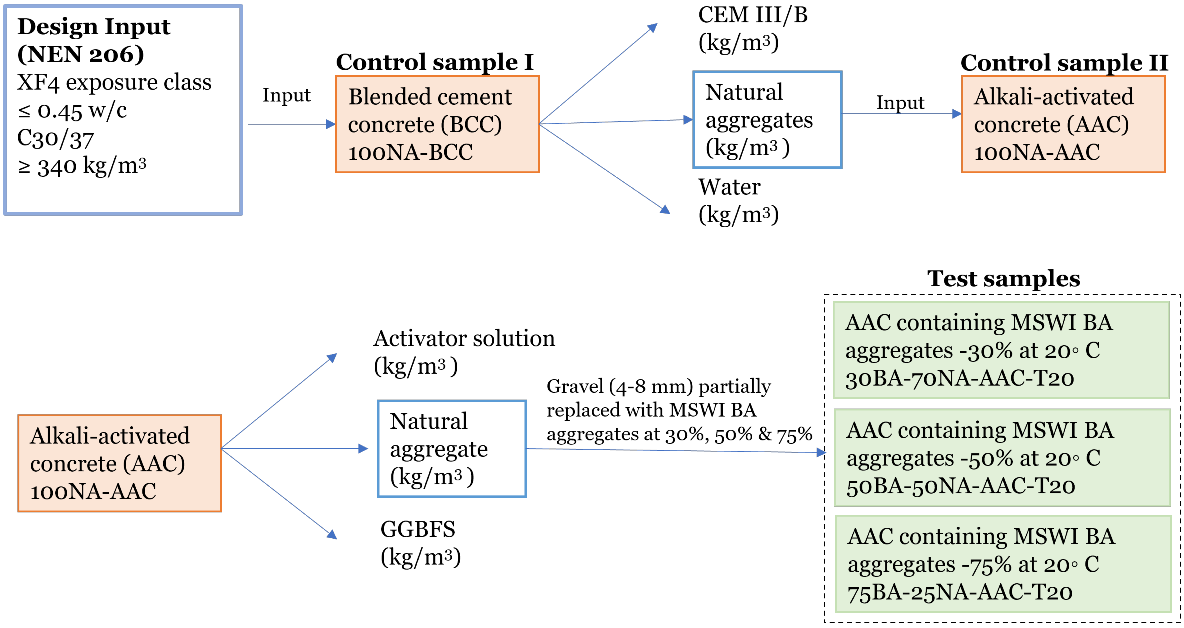

Figure 3.2: Mix design methodology for samples used in the research

Concrete samples used in this research belong to either a control or test group. The control group consists of BCC and AAC mixtures containing natural aggregates. The test group consists of AAC concrete containing pre-treated MSWI BA aggregates. The samples in this group are produced by partially replacing gravel of 4-8 mm fraction with MSWI BA aggregates. The performance of the test samples is compared with the control group samples.

3.6.1. MIXTURE DESIGN FOR BLENDED CEMENT CONCRETE (BCC)

NEN 206 (2017) [91] specifies a maximum water-to-cement ratio (w/c) of 0.45 and a minimum cement content of 340 kg/m^3 for concrete exposed to XF4 environmental exposure class. Further, the concrete used in pavements necessitates a consistency of zero slump. Hence, considering the w/c requirement, two trial batches with w/c=0.4 and w/c=0.45 was prepared. It was observed that with w/c=0.45, the concrete gave a slump of 70 mm, while zero slump was observed with w/c=0.4. An attempt was made with w/c=0.42, which gave a slump of 11 mm. Thus w/c=0.4 with the associated zero slump was chosen for the mixture design of BCC. Further, to ensure a reduced environmental impact of the concrete, the BCC mixture design incorporated the minimum cement content necessary as per the norm requirement. Table 3.4 shows the mixture design used for the preparation of BCC.

3.6.2. MIXTURE DESIGN FOR ALKALI-ACTIVATED CONCRETE (AAC)

The design of AAC control sample having comparable 7-day compressive strength to BCC control sample is the next step in the research. This is achieved by modifying the activator proportions in the concrete. Three trial concrete mixtures were batched with a constant proportion of sodium hydroxide solution (NaOH, 50% w/v) and varying proportions of water glass solution (Na_2SiO_3, 37.5% w/v). Table 3.5 gives the mixture design used for the preparation of AAC. In the design of AAC, the following terminologies are used,

Table 3.4: Mixture design for BCC control sample

Mixture	100NA-BCC	Unit
Water-to- cement ratio (w/c)	0.4	
CEM III/B cement	340	kg/m^3
Sand (0-4 mm)	751	kg/m^3
Gravel (4-8 mm)	557	kg/m^3
Gravel (8-16 mm)	557	kg/m^3
Water	136	kg/m^3

- Modulus of alkaline solution M_S: Ratio of the molar mass of activator ($\frac{SiO_2}{Na_2O}$)
- Water-to-binder ratio: $\frac{\text{Total water}}{\text{solid part of activator+ precursor}}$

Table 3.5: Mixture design for AAC control sample

Mixture	100NA-AAC	Unit
Water-to-binder ratio	0.43	
Ms	0.75	
Ground granulated blast furnace slag	314	kg/m^3
Na_2SiO_3 solution (37.5% w/v)	33.53	kg/m^3
NaOH solution (50% w/v)	25.15	kg/m^3
Sand (0-4 mm)	751	kg/m^3
Gravel (4-8 mm)	557	kg/m^3
Gravel (8-16 mm)	557	kg/m^3
Water	109	kg/m^3

3.6.3. MIXTURE DESIGN FOR AAC CONTAINING MSWI BA AGGREGATES

Concrete test samples were prepared by replacing gravel in the finalized AAC mixture. Pretreated MSWI BA aggregates partially replace gravel fraction of 4-8 mm at 30%, 50% and 75% replacement levels by volume. Table 3.6 shows the mix design for the test samples. This research partially replaces the gravel fraction (4-8 mm) in AAC with MSWI BA aggregates by aggregate volume.

Table 3.6: Mixture design for AAC control containing MSWI BA aggregates

Mixture	**30BA-70NA-AAC-T20**	**50BA-50NA-AAC-T20**	**75BA-25NA-AAC-T20**	**Unit**
Replacement level (%)	30	50	75	
Water-to-binder ratio	0.43	0.43	0.43	
Ms	0.75	0.75	0.75	
GGBFS	314	314	314	kg/m^3
Na_2SiO_3 solution (37.5% w/v)	33.53	33.53	33.53	kg/m^3
NaOH solution (50% w/v)	25.15	25.15	25.15	kg/m^3
Sand (0-4 mm)	751	751	751	kg/m^3
MSWI BA (4-8 mm)	151	252	378	kg/m^3
Gravel (4-8 mm)	399	278.5	139.5	kg/m^3
Gravel (8-16 mm)	557	557	557	kg/m^3
Water	109	109	109	kg/m^3

3.6.4. PARTICLE SIZE DISTRIBUTION OF THE COARSE AGGREGATES IN THE CONCRETE SAMPLES

The coarse aggregate fraction in the test samples used in this study consists of a combination of natural and MSWI BA aggregates. It is crucial to assess whether the aggregate distribution meets the gradation requirements specified in the relevant standard (NEN 933-1 (2012) [92]) for each replacement level. Figure 3.3 illustrates the particle size distribution of the coarse aggregates fraction in concrete mixtures specified in Sections 3.6.1, 3.6.2 and 3.6.3.

According to the particle size distribution depicted in Figure 3.3, the aggregate fraction demonstrates overall compliance with the specified gradation according to the relevant standard, with minor deviations observed primarily at the 2 mm sieve size. However, at the 4 mm sieve size, noticeable variations were observed for the 50% and 75% replacement levels of gravel with MSWI BA aggregates. Despite these observed deviations, the overall distribution of the coarse aggregate fraction indicates marginal variations. Consequently, it can be concluded that the replacement levels of natural aggregates with MSWI BA aggregates in the test samples are acceptable.

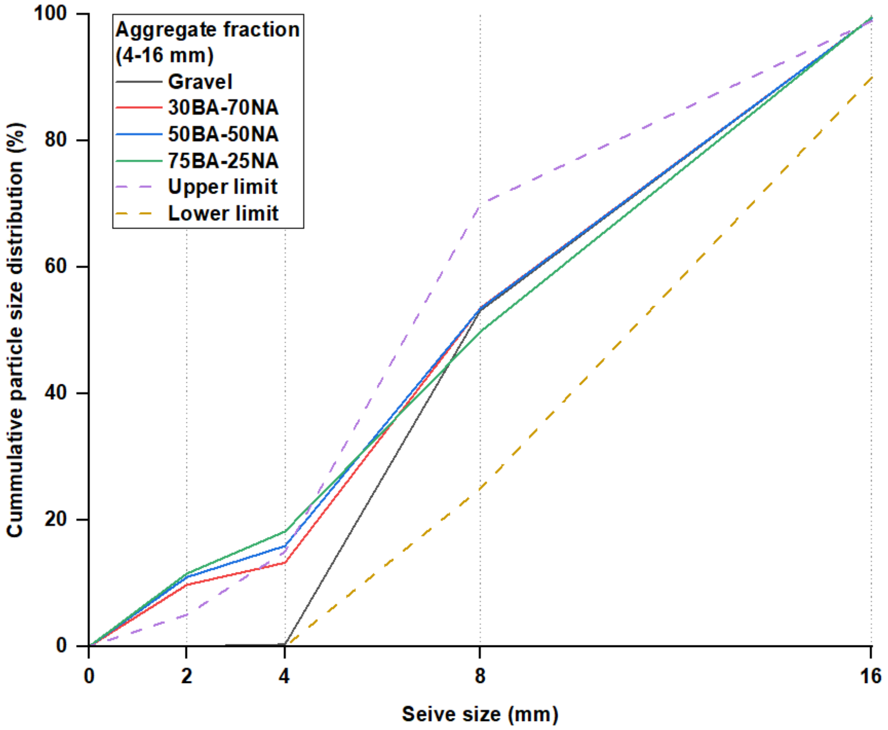

Figure 3.3: Particle size distribution of the coarse aggregate fraction in the concrete control and test samples

3.6.5. CONCRETE SAMPLE PREPARATION

The sample preparation of BCC concrete involves dry mixing the aggregates and CEM III/B cement together in the mixer for about 4 minutes. Later, water is introduced into the mixer. The components are mixed for 3 minutes and then transferred into the moulds. Since the mix is dry (zero slump), the moulds are filled while being vibrated. The samples are left to harden at room temperature (20°C) with a plastic film on top to prevent excessive moisture loss. The sample is de-moulded after 24 hours and placed in the curing chamber (Temperature=20°C & Relative Humidity=99%)

In the preparation of the AAC control sample, the initial step is to prepare the activator solution 24 hours prior to the casting of concrete. The activator solution is prepared by mixing sodium hydroxide solution with water glass solution in the required proportions, followed by the additional water. Subsequently, the activator solution is left to cool since the dissolution process involves heat generation. At the time of production of concrete, ground granulated blast furnace slag (GGBFS) is added to the concrete mixer, followed by the activator solution. They are mixed for 2 minutes, after which aggregates are added. The components are mixed for 3 to 4 minutes, after which they are transferred to the moulds and covered. The sample is de-moulded after 24 hours and wrapped in a plastic film before storing it in the curing chamber.

The AAC test samples are prepared differently from the control AAC sample. A part of the NaOH solution and the additional water is used for the MSWI BA aggregate pre-treatment. Hence, the activator preparation involves mixing the remaining NaOH and water glass solutions 24 hours before casting concrete samples. During the concrete production, the pre-treated MSWI BA aggregates and the pre-treatment solution are added to the mixer. The remaining activator solution is added and mixed for 1 minute. GGBFS is introduced into the concrete mixer, and the components are mixed for 2 to 3 minutes. Later, the aggregates are introduced and mixed for another 2 minutes. The mix is then transferred to the moulds while being vibrated on the vibration table. It was observed that the introduction of MSWI BA aggregates to the AAC caused delayed setting of the concrete. Hence, one test sample is produced by curing at an elevated temperature of 40°C for 24 hours, after which it is de-moulded, wrapped in plastic film and stored in the curing chamber. The other test sample is allowed to cure at an ambient temperature of 20°C. It is then de-moulded after 3 days, wrapped and stored in the curing chamber.

4

CHARACTERISTICS AND PRE-TREATMENT OF MSWI BA AGGREGATES

4.1. INTRODUCTION

The characterisation of the MSWI BA aggregates is discussed in this chapter. The physical properties of the MSWI BA aggregates are quantified and compared to natural aggregates. Moreover, a crucial part of the study involves quantifying metallic aluminium (Al) in the MSWI BA aggregates. The presence of metallic Al deteriorates the quality of the AAC when MSWI BA aggregates are introduced into it. The properties of the aggregates are compared to the norm-specified requirements to ensure that the MSWI BA aggregates satisfy the quality requirements for introducing in concrete for pavement application.

The MSWI BA aggregates are currently applied in ordinary Portland cement (OPC) concrete and blended cement concrete (BCC) systems. Thus, the requirements set forth by the standards are based on the utilisation of the MSWI BA aggregates for these concrete systems. However, this research aims to introduce MSWI BA aggregates in AAC and the presence of alkali activators used in AAC can aggravate the release of hydrogen gas when it reacts with the metallic Al. Hence, the requirement for MSWI BA aggregates is stringent when utilised in AAC. Pre-treatment of MSWI BA aggregates is performed to alleviate the quality and ensure that the performance of the AAC is not compromised when MSWI BA aggregates are introduced in it. This chapter discusses the physical properties of the aggregate, the pre-treatment of the MSWI BA aggregates and the optimum MSWI BA aggregate replacement levels in AAC based on the effectiveness of the pre-treatment.

4.2. TESTING PROCEDURE FOR AGGREGATE CHARACTERISTICS

4.2.1. PARTICLE SIZE DISTRIBUTION

Particle size distribution (PSD) represents the dimensional distribution curve of a granular material. The test for determining PSD was conducted as per NEN 933-1 (2012) [92]. A sample size of 1 kg was used for the test. The MSWI BA aggregates used in this test were not washed as per the norm to prevent the reaction of metallic Al in the aggregates. The material was then transferred to a sieving column that comprised of a number of sieves (16 mm, 11.2 mm, 8 mm, 4mm, and 2 mm) which were fitted together and arranged, from top to bottom, in order of decreasing aperture sizes with the pan and lid. The column was vibrated manually or mechanically, ensuring no material was lost. Material retained on each sieve size was then weighed.

4.2.2. Water absorption

Water absorption of aggregates is calculated as the amount of water that the aggregate particles are capable of absorbing. The test was conducted as per NEN 1097-6 (2022) [93]. A test portion of 2 kg was considered, which was then placed in water for 24 hrs and allowed to drain. An absorbent cloth was used to remove the excess water on the surface of the aggregates (saturated surface dry (SSD) condition). The sample was then weighed (w_1) and dried to a constant mass in an oven at a temperature of (110±5)°C. Further, the test sample was cooled at room temperature and weighed (w_2). The percentage loss in water between the SSD and oven-dried condition is the amount of water absorbed by the aggregate. Water absorption (WA) after immersing the aggregates for 24 hrs was calculated using the formula,

$$\mathrm{WA} = \frac{(\mathrm{W}_1 - \mathrm{W}_2)}{\mathrm{W}_2} \times 100\ \%$$

4.2.3. Apparent density

Apparent particle density refers to the correlation between the mass of aggregates that have been oven-dried and the volume they occupy when immersed in water. The test was conducted as per NEN 1097-6 (2022) [93]. A test portion of a minimum of 2 kg was considered as per the norm. The sample was placed in a pycnometer and filled with water. The whole setup was then kept in a water bath for 24 hrs. Any entrapped air was released before weighing (M_1), and the pycnometer was filled with water until the top of the cover. The pycnometer was later emptied, refilled with water and weighed (M_2). The saturated aggregates were placed in the oven at (110±5)°C and dried till a constant mass was achieved. Subsequently, the weight (M_3) of the oven-dried sample was recorded.
The apparent density (ρ_a) was calculated as per the formula,

$$\rho_a = \rho_w \frac{\mathrm{M}_3}{\mathrm{M}_3 - (\mathrm{M}_1 - \mathrm{M}_2)}\ \mathrm{kg/m^3} \text{ where } \rho_w \text{ is the density of water}$$

4.2.4. Loose bulk density

Loose bulk density is the weight of the aggregates contained in a defined volume. The test was conducted as per NEN 1097-6 (1998) [94]. A test sample of 5 kg was taken for the coarse aggregates and 1 kg for sand as per the standard. They were oven dried at (110 ± 5)°C to a constant mass and then transferred to a spherical container (of mass m_1) without segregation. The top of the aggregates were levelled with a straightedge without compacting the upper surface. The volume of the cylinder (V) and the weight (m_2) of the aggregates were measured. The loose bulk density (ρ_b) is given by the formula,

$\rho_b = \frac{(\mathrm{m_2} - \mathrm{m_1})}{\mathrm{V}}\ \mathrm{kg/m^3}$

4.2.5. LOS ANGELES COEFFICIENT

Los Angeles (LA) coefficient indicates the resistance of the aggregates to abrasion under loading. The test was conducted as per NEN 1097-6 (1998) [95]. A sample of 5 kg was prepared for the test and steel balls that weigh around 400 to 410 grams were used for crushing the aggregates. The number of balls used were 11 for the 8-16 mm size fraction and 8 balls for the 4-8 mm size fraction. The steel balls were first placed in the Los Angeles abrasion machine, followed by the sample. The material along with the balls were then subjected to 500 revolutions at a speed of 31 rev/min to 33 rev/min. At the end of the test, the broken material was transferred into a steel tray attached to the bottom of the machine. The broken material collected in the tray was then sieved through a 1.6 mm sieve. The weight of the material retained on the sieve was noted (m). The Los Angeles (LA) coefficient value is given by the formula,

$\mathrm{LA} = \frac{5000 - \mathrm{m}}{50}$

4.3. AGGREGATE CHARACTERISTIC RESULTS

4.3.1. PARTICLE SIZE DISTRIBUTION

Figure 4.1 shows the particle size distribution for the MSWI BA aggregates used in this research which were compared with the norm limits (NEN 12620 (2002) [96]) prescribed for 4-8 mm size fraction. The as-received bottom ash aggregates were in the size range of 4-11 mm, and the gravel fractions were in the range of 4-8 mm and 8-16 mm. The particle size distribution of the MSWI BA aggregates satisfies the requirement for the size range of 4-8 mm as shown in Figure 4.1, with the deviations at each sieve size being less than 5%. It was observed that the deviations were greater than 10% when the MSWI BA aggregate gradation was compared to the norm limits for the 8-16 mm size range. Sieving and removing bottom ash particles to fit the gradation limits was not an efficient option. Further, the deviations at each sieve size from the norm limits for the 4-8 mm fraction was less than 5%; hence it was safe to consider that the MSWI BA aggregates to be in the size range of 4-8 mm and replace gravel fraction of the similar size.

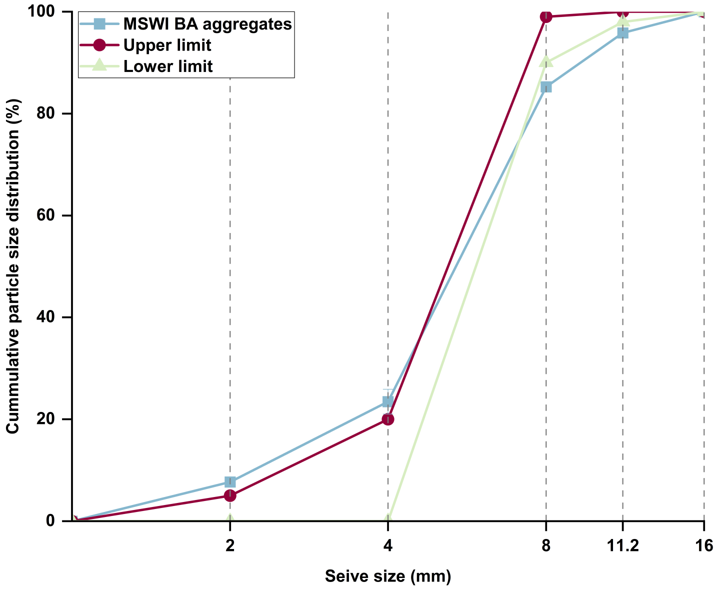

Figure 4.1: Particle size distribution of MSWI BA aggregates

4.3.2. WATER ABSORPTION

Table 4.1 shows the water absorption of the aggregates used in this research. The MSWI BA aggregates showed the highest water absorption of 7%, which was 10 times higher compared to the water absorption of natural aggregates. This indicated that the MSWI BA aggregates were porous compared to the natural aggregates. This result was consistent with the findings of researchers who sourced the aggregates from the Netherlands [67]. The differences in the results reported by different authors [11, 58] can be due to the heterogeneous nature of the MSWI BA aggregates. The composition of MSWI BA aggregates changes were dependent on the waste composition, incineration process and post-incineration treatment [11, 97]. Hence, regional variation must be considered when comparing the results from other studies. Additionally, due to the significantly higher water absorption of MSWI BA aggregates compared to natural aggregate, the concrete mixture design takes into account the water absorption of the MSWI BA aggregates.

Table 4.1: Water absorption of aggregates

Aggregate	Size (mm)	Water absorption(wt %)
MSWI BA	4-11	7.04±0.56
Gravel	8-16	0.57±0.00
Gravel	4-8	0.70±0.08
Sand	0-4	0.10±0.00

4.3.3. APPARENT DENSITY

Table 4.2 shows the density of the aggregates used in this research. The density of the MSWI BA aggregates was observed to be the lowest, which was in conjunction with the results of the water absorption test that indicated that the aggregates were porous and weak. Natural aggregates were comparatively denser, with river sand having the highest density. The results for the density of the aggregates were in coherence with the results obtained by other authors [11, 67, 98].

Table 4.2: Apparent density of aggregates

Aggregate	Size (mm)	Apparent density (kg/m^3)
MSWI BA	4-11	2370±0.01
Gravel	8-16	2610±0.00
Gravel	4-8	2590±0.00
Sand	0-4	2640±0.01

4.3.4. LOOSE BULK DENSITY

Table 4.3 shows the loose bulk density of the aggregates used in this research. The loose bulk density of MSWI BA aggregates was observed to be the lowest. This might be due to the poor gradation of the MSWI BA aggregates compared to natural aggregates. This result was in conjunction with the particle size distribution curve that showed deviations from the norm required gradation. Additionally, it indicated the presence of a larger proportion of coarser fractions compared to finer fractions in the MSWI BA aggregates, allowing more voids between the aggregates and resulting in poor packing. Sand showed the highest loose bulk density since the finer fraction in the sand could fill even the smaller void, thus allowing a denser packing of the aggregates.

Table 4.3: Loose bulk density of aggregates

Aggregate	Size (mm)	Loose bulk density (kg/m^3)
MSWI BA	4-11	1260±0.02
Gravel	8-16	1540±0.00
Gravel	4-8	1580±0.02
Sand	0-4	1750±0.02

4.3.5. LOS ANGELES COEFFICIENT

Table 4.4 shows the Los Angeles (LA) coefficient for the coarse aggregates used in this research. The results show a LA coefficient of 34.34 for MSWI BA aggregates indicating that 34.34% weight of the aggregates was disintegrated under the loading of the steel balls. Additionally, the test results showed that the MSWI BA had poor resistance to abrasion compared to natural aggregates. This might be due to the inherent porosity of MSWI BA aggregates, making them weaker. Further, the gravel particles of size 8-16 mm showed poor performance compared to the 4-8 mm gravel fraction despite having similar density. This could be due to the larger number of steel balls used in the test for the larger sized aggregate fraction causing higher damage to the aggregates.

Table 4.4: Los Angeles coefficient of coarse aggregates

Material	Size(mm)	LA coefficient
MSWI BA	4-11	34.34
Gravel	8-16	30.58
Gravel	4-8	20.36
Sand	0-4	N/A

4.4. PRE-TREATMENT OF MSWI BA AGGREGATES

The MSWI BA aggregates used in this research contain metallic aluminium (Al), which can pose challenges when directly introduced into alkali-activated concrete (AAC). The interaction of alkalis in the AAC activator can react with the metallic Al to release hydrogen gas. This may lead to cracking and loss in the performance of the concrete.

To address the issue of cracking of AAC concrete when MSWI BA aggregates are introduced, pre-treatment of the MSWI BA aggregates was conducted. Alkaline pre-treatment using NaOH solution was used in this study to remove metallic Al in the MSWI BA aggregates. Researchers have already proved the effectiveness of the alkaline pre-treatment procedure [99, 82]. In addition, the treatment process uses economically viable and readily accessible material to remove metallic Al, thus making it an appealing solution. The MSWI BA aggregates are intended to replace gravel particles at 30%, 50% and 75% replacement levels. The optimum MSWI BA aggregate replacement level is chosen based on the effectiveness of the pre-treatment, which was evaluated based on the remaining metallic Al present in the MSWI BA aggregates and the compressive strength of the AAC after introducing the pre-treated MSWI BA aggregates.

This section entails the pre-treatment methodology adopted for removing metallic Al, the quantification of metallic Al after pre-treatment, and the determination of the optimum replacement level of MSWI BA aggregates in the AAC mixture. These investigations aim to verify that the inclusion of MSWI BA aggregates in AAC does not result in the reduced performance of the concrete.

4.4.1. INITIAL TREATMENT OF ACQUIRED MSWI BA MATERIAL

The MSWI BA aggregates were subjected to preliminary plant-scale treatment before they were used in this research. The preliminary material treatment adopted for the MSWI BA aggregates were as follows:

PHASE 1: WEATHERING OF FRESH MSWI BOTTOM ASH

One of the primary concerns associated with MSWI BA aggregates is the potential for heavy metal leaching into the surrounding environment. Weathering of the aggregates is the first step in the treatment. Freshly produced MSWI BA aggregates were stored outdoors for 3 months, during which the material got slowly dried and naturally weathered [100]. This process lowered the pH of the material leading to metal oxidation, thus enabling the MSWI BA to become physically and chemically stable [101, 67]. The leaching potential of heavy metals was drastically reduced by the end of this process.

PHASE 2: DRY SEPARATION AND METAL RECOVERY OF MSWI BA

Mechanical crushing of the MSWI BA aggregates was conducted following the weathering process. The particles were reduced to a size lower than 400 mm and consisted of unburned and metallic materials [67]. These materials were then screened and extracted by passing them through a powerful overhead magnet. Further dry separation in the same screener produced MSWI BA aggregates of size fractions; 0-12 mm and 12-31.5 mm. Additional separation of the 0-12 mm fraction was also conducted, and the finer fraction of 0-2/3 mm was not further treated. The 2-12 mm and 12-31.5 mm fractions underwent further processing using magnets, an eddy current system and fluff extraction to maximise the removal of unburned and metallic metals. Finally, both fractions were mixed to produce an MSWI BA aggregate fraction of size 2-31.5 mm.

PHASE 3: WET SEPARATION AND WASHING TREATMENT

The dry-separated MSWI BA aggregates underwent mobile water separating-cleaning procedure. The input for this process was the 2–31.5 mm fraction of MSWI BA aggregates. A mobile plant designed for water separation and cleaning was utilised, employing a liquid-to-solid (L/S) ratio of 1:2. The washing and scrubbing actions effectively eliminated material disturbances, including fine particles and leachable organic and inorganic contaminants. Consequently, these pollutants were concentrated in the sludge fraction, leading to a cleaner and higher quality coarse aggregate fraction. Among the various aggregate size fractions produced, the 4-11 mm size MSWI BA aggregates was used in this research.

PHASE 4: MAGNETIC SEPARATION

Metals, including aluminium and zinc, in the MSWI BA aggregates must be reduced before they can be used in concrete. Hence, magnetic separator systems were utilised for removing these metals. This ensured better metal recovery and reduced the effect of potential damage to the concrete containing these aggregates.

4.4.2. ALKALINE PRE-TREATMENT

The obtained MSWI BA aggregates underwent preliminary plant-scale treatment, as mentioned in Section 4.4.1. However, the aggregates contained pollutants even after this process. This led to the production of inferior-quality concrete with poor mechanical properties and durability. Excessive cracking and swelling of concrete were observed when the aggregates were directly introduced into AAC as shown in Figure 4.2. Further, delayed setting of AAC concrete was observed when MSWI BA aggregates were introduced into it. The findings of Zhang & Zhao (2014) [76] indicated delayed initial and final setting of mortar samples containing fine fraction of MSWI BA aggregates which is consistent with the observations in this study. Since the aggregates received had negligible amounts of metallic zinc present, the deterioration of the concrete was mainly attributed to the presence of metallic aluminium (Al). Hence, alkaline pre-treatment using NaOH solution was directed towards removing metallic Al in the aggregates.

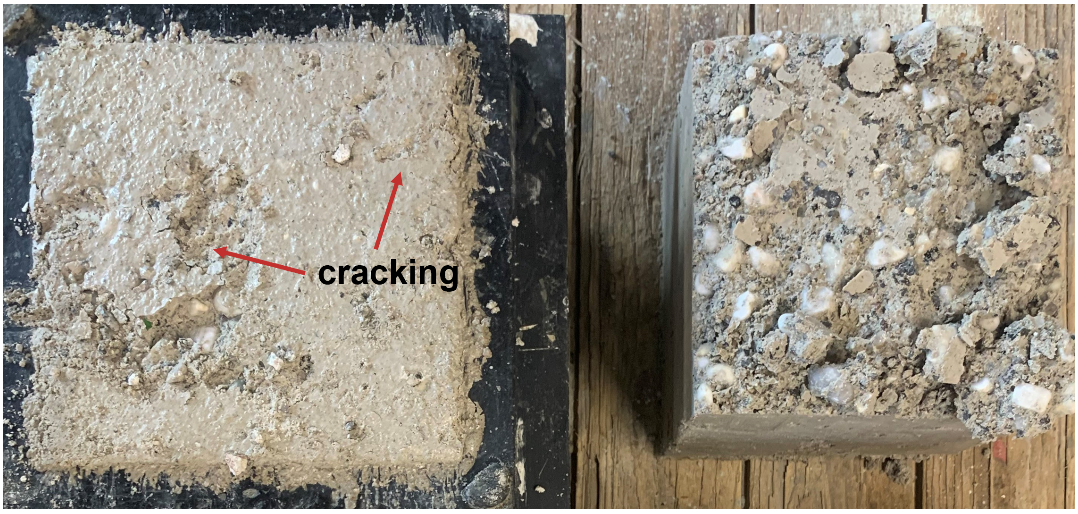

Figure 4.2: Cracking and swelling of AAC containing untreated MSWI BA aggregates after 1-day (100% replacement of gravel (4-8 mm))

The alkaline pre-treatment process involved immersing the MSWI BA aggregates in NaOH solution for a specific duration. During this period, reactive aluminium in the MSWI BA aggregates underwent conversion into a soluble hydroxide, which subsequently got precipitated. Further, the pre-treatment encapsulated the remaining reactive aluminium within a passive layer, making it unable to participate in the chemical reactions. The factors that influenced the effectiveness of the pre-treatment were; the liquid-to-solid ratio, pre-treatment duration, NaOH concentration, temperature, and particle size [99, 82]. This study focuses on identifying the optimal combination of NaOH concentration and treatment duration that achieves the maximum removal of metallic aluminium in the MSWI BA aggregates. Table 4.5 below shows the parameter and trial values chosen to design a suitable pre-treatment procedure.

Table 4.5: Pre-treatment parameters considered

Parameter	Trial
Mass ratio of NaOH solution to MSWI BA aggregates	Constant for different replacement levels
Duration of pre-treatment	5-days, 12-days & 14-days
Molarity of NaOH solution	0.1 M, 0.5 M & 1 M

The effectiveness of the pre-treatment was assessed by quantifying the remaining metallic Al in the treated MSWI BA aggregates using the water displacement technique. Further, the suitable replacement level was determined based on the 7-day and 28-day compressive strength of the AAC containing MSWI BA aggregates.

DURATION OF PRE-TREATMENT

In this study, three pre-treatment durations were investigated; 5-days, 12-days and 14-days. Based on the literature, 15 days of immersion in 1 M NaOH solution is reported to fully remove the Metallic Al present in the aggregates [102]. However, to minimize the time required for pre-treatment, a preliminary attempt was made with a duration of 5-days and a concentration of 1 M NaOH. A significant delay in setting was observed, and the concrete exhibited cracking once it hardened. Similar delayed setting and cracking issues were observed in the concrete with MSWI BA aggregates treated for 12-days; although, the effects were much lower compared to 5-days of pre-treatment. The concrete containing 14-days of pre-treated MSWI BA aggregates showed promising results with no visible cracks in the hardened concrete. However, the issue of delayed setting persisted, and the concrete was observed to harden after 3-days. In order to address this challenge, thermal curing at 40°C for 24 hours was adopted to increase the reactivity of the precursor and, thus the hardening of the concrete. Curing at higher temperatures (greater than 40°C) may drastically increase the reaction of metallic Al with the alkali, thus elevating the release of hydrogen gas and subsequent cracking of concrete. Mary Joseph et al. (2020) [56] demonstrated the increased reactivity of metallic Al in bottom ash with NaOH solution at elevated temperatures. Consequently, a 14-day duration was opted for the pre-treatment of the MSWI BA aggregates.

CONCENTRATION OF NAOH

NaOH concentrations of 0.1 M, 0.5 M and 1 M were chosen for the pre-treatment of MSWI BA aggregates. A minimum concentration of 0.1 M was selected based on the literature [82]. Since the alkalis used had detrimental effects on the environment, the research tried to optimise the pre-treatment process. The approach utilised a part of the NaOH in the AAC activator for the pre-treatment of MSWI BA aggregates, ensuring that no additional NaOH was consumed after the pre-treatment. The maximum concentration of 1 M was opted since the NaOH used was obtained from the AAC activator. Hence, higher concentrations of NaOH solution for pre-treatment resulted in reduced quality of NaOH solution for the polymerisation reaction of the AAC precursor, which can affect the properties of the concrete. Trial concrete batches prepared using 0.1 M and 0.5 M NaOH solution showed delayed setting and extreme cracking after 14-days of pre-treatment. Conversely, the 1 M NaOH yielded better results after 14-days of pre-treatment; however, delayed setting of concrete was still observed.

Table 4.6 shows the ratio of MSWI BA aggregates to the NaOH solution and the percentage of NaOH taken from the activator for the replacement levels of 30%, 50% and 75%. Based on the results of the trial batches, 1 M NaOH was chosen as the optimum concentration for pre-treatment.

Table 4.6: NaOH concentrations considered for pre-treatment

NaOH Molarity	Mass ratio of NaOH solution to MSWI BA aggregate	NaOH taken from AAC activator (wt %)
	0.85	40
1M	0.54	42
	0.38	45

4.4.3. METALLIC ALUMINIUM QUANTIFICATION IN MSWI BA AGGREGATES

The optimum pre-treatment procedure for the MSWI BA aggregates involved immersing the aggregates in a 1 M NaOH solution for a duration of 14-days. However, the effectiveness of the pre-treatment could be assessed based on the metallic Al remaining in the treated MSWI BA aggregates at various replacement levels. This section explores the alumina quantification procedure, including the set-up employed for the quantification.

PRE-TREATMENT SETUP

Figure 4.3 shows the experimental set-up made for quantifying the metallic aluminium in the MSWI BA aggregates. About 5 g of MSWI BA aggregates were placed in a plastic container which was connected to a tube. The tube is passed through a water bath into a graduated cylinder which was supported on a clamp stand. The bottle was placed on a magnetic stirrer to ensure continuous mixing of the NaOH solution with the bottom ash aggregates. The metallic Al in the bottom ash aggregates reacted with the NaOH solution to release hydrogen gas which was transferred through the silicon tube into the graduation cylinder. To prevent the leakage of hydrogen gas, it was important to have airtight connections and joints. This was achieved by applying epoxy to the joints and connections. The entire apparatus was placed in a fuming cupboard to ensure that the hydrogen gas released did not pose any safety concerns.

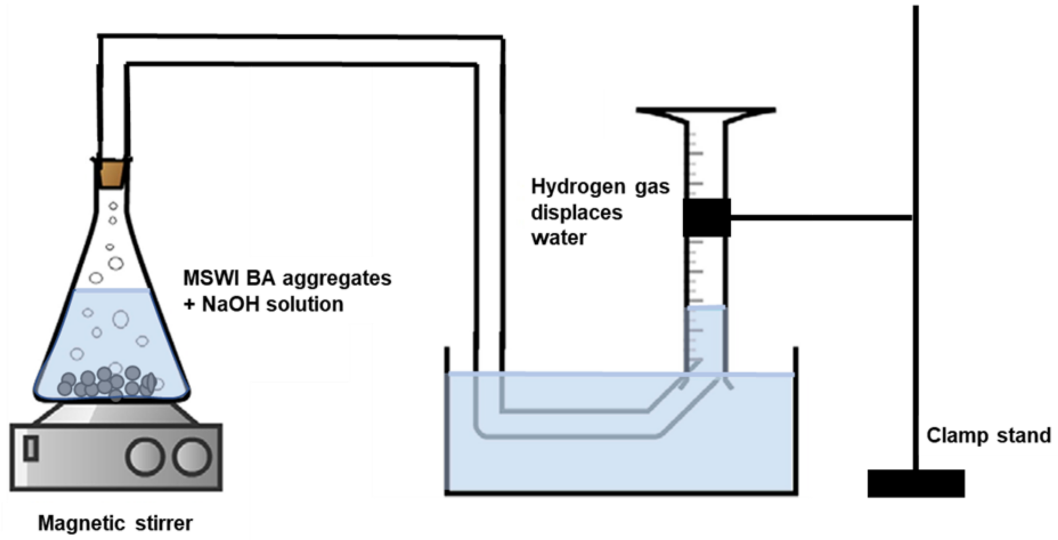

Figure 4.3: Experimental set-up for metallic aluminium quantification, redrawn from [56]

METALLIC AL AFTER PRE-TREATMENT

The metallic Al present in the MSWI BA aggregates after 7-days and 14-days of pre-treatment is shown in Table 4.7. The untreated MSWI BA aggregates have a metallic Al content of 2% which was obtained based on the water displacement procedure using the set-up made. It was observed that for a constant NaOH concentration of 1 M, the pre-treatment yielded better results for a higher mass ratio of NaOH solution to MSWI BA aggregates compared to a lower mass ratio. Further, the metallic Al in the aggregates was observed to reduce with increasing pre-treatment duration.

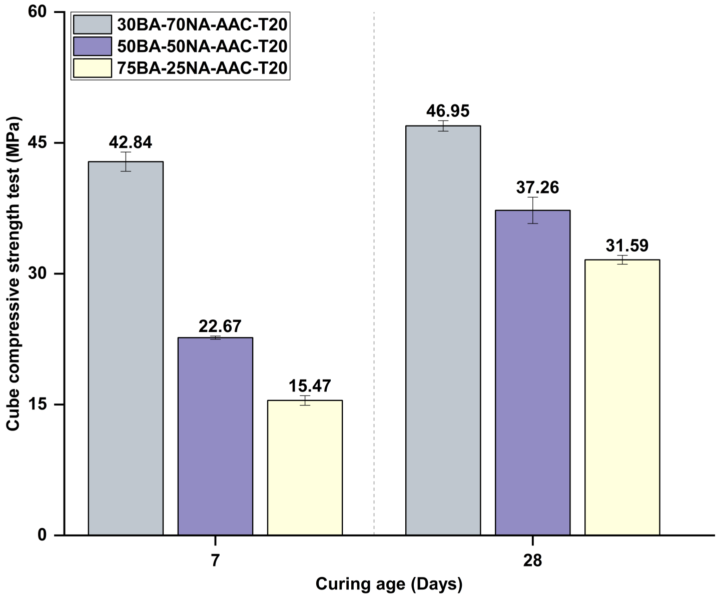

Figure 4.4: Compressive strength of concrete with 30%, 50% and 75% replacement levels

The effect of pre-treatment duration was more prominent for the higher replacement levels than for the lower levels. To fully understand the effect of the pre-treatment, AAC concrete with MSWI BA aggregates was prepared with different replacement levels. Figure 4.4 shows the 7-day and 28-day cube compressive strength of AAC containing different replacement levels of MSWI BA aggregates. The 30% replacement (30BA-70NA-AAC-T20) level showed the highest compressive strength after 7-days and 28-days of curing. The 75% replacement (75BA-25NA-AAC-T20) level showed the least compressive strength, which was approximately 36% and 67% of the 30BA-70NA-AAC-T20, after 7-days and 28-days, respectively. However, a pronounced strength development was observed in the 75BA-25NA-AAC-T20 sample compared to 30% and 50% replacement levels. It was also observed that the sample with 50% replacement (50BA-50NA-AAC-T20) satisfied the strength requirement for pavement. However, the strength was insufficient to ensure that the sample will meet all the performance requirements for pavement application. Thus, in this study, 30% replacement was chosen as the optimum replacement level. Further investigation needs to be conducted to ensure that the sample satisfies the requirements for pavements. The persistent issue of delayed setting observed in all the replacement levels was solved using thermal treatment at 40°C for 24 hours after casting. The performance of the thermally treated 30% replacement sample (30BA-70NA-AAC-**T40**) was also investigated in this research.

Table 4.7: Metallic Aluminium after pre-treatment for various NaOH solution to MSWI BA aggregates

Mass ratio of NaOH solution to MSWI BA aggregate	Metallic Al remaining after 7-days of pre-treatment (wt%)	Metallic Al remaining after 14-days of pre-treatment (wt%)
0.85	0.77	0.53
0.54	1.48	1.02
0.38	2.04	1.67

4.5. CONCLUSION

The results of the physical characteristics of the aggregates show that MSWI BA aggregates have good properties and can be compared to natural aggregates. Hence it can be used to replace natural gravel (4-8 mm) in AAC. The water absorption of the MSWI BA aggregates is a factor that needs to be considered while performing the pre-treatment of aggregates. An effective pre-treatment procedure was designed based on the removal of metallic Al from the aggregates. A concentration of 1 M NaOH was considered based on requirements for the mix design. Casting using 0.1 M and 0.5 M NaOH did not show promising results. The release of hydrogen gas was noticed even after 24 hours. Hence higher percentage of NaOH was preferred. Also, the threshold for the maximum preferred concentration of NaOH was based on the setting of the concrete. The higher the alkali used for the pre-treatment, the lower the NaOH used in the activator to react with the precursor and the delayed setting as a result. The casting of concrete showed delayed setting and excessive hydrogen gas release after introducing 5 days and 12 days of pre-treated MSWI BA aggregates. Hence 14 days of pre-treatment was preferred and it showed promising results with minor surface cracking. Thus, in this research, a 1 M NaOH solution and a 14-day immersion period was chosen as the optimum pre-treatment procedure. Following the selection of the pre-treatment parameters, aluminium remaining in the aggregate after pre-treatment was quantified with the 30% replacement showing promising results.

5

MECHANICAL PROPERTIES & DURABILITY OF CONCRETE CONTAINING MSWI BA AGGREGATES

5.1. INTRODUCTION

The AAC containing MSWI BA aggregates are intended for their application in pavements and the suitability for the application is assessed based on the key mechanical and durability performance parameters

The ability of the AAC containing MSWI aggregates to withstand the applied loads without structural failure is assessed based on the mechanical properties. The properties evaluated are compressive strength, splitting tensile strength and flexural strength. Further, concrete pavements in cold regions are exposed to severe environmental conditions throughout their service life, with freeze-thaw cycles being a significant factor that compromises their durability. The cyclic transition between freezing and thawing temperatures induces internal stresses within the concrete, leading to its deterioration. Additionally, the application of de-icing salts to prevent ice formation on the pavement surface can cause spalling of the concrete. Therefore, it is crucial to design concrete mixtures that meet the mechanical strength requirements and exhibit the ability to withstand the aggressive in-service conditions of freeze-thaw cycles for pavement application.

In this chapter, the properties of the AAC containing MSWI BA aggregates including compressive strength, splitting tensile strength, flexural strength and freeze-thaw resistance are studied.

5.2. TESTING PROCEDURE

5.2.1. COMPRESSIVE STRENGTH TEST

The test was conducted in a two-column universal compression testing machine as per NEN 12390-3 (2019) [103]. For the test, 3 cubes of size 150x150x150 mm^3 were used as per the testing standard. The test was done within 10 hours after removing the samples from the curing room(T=20°C & RH=99%). The surface of the cubes were wiped to remove excess water and any loosely adhering material. The sample was then placed on the compression testing machine with the casting side facing one of the columns of the machine. This was to ensure that the sides in contact with the loading plates were flat to avoid eccentric loading.

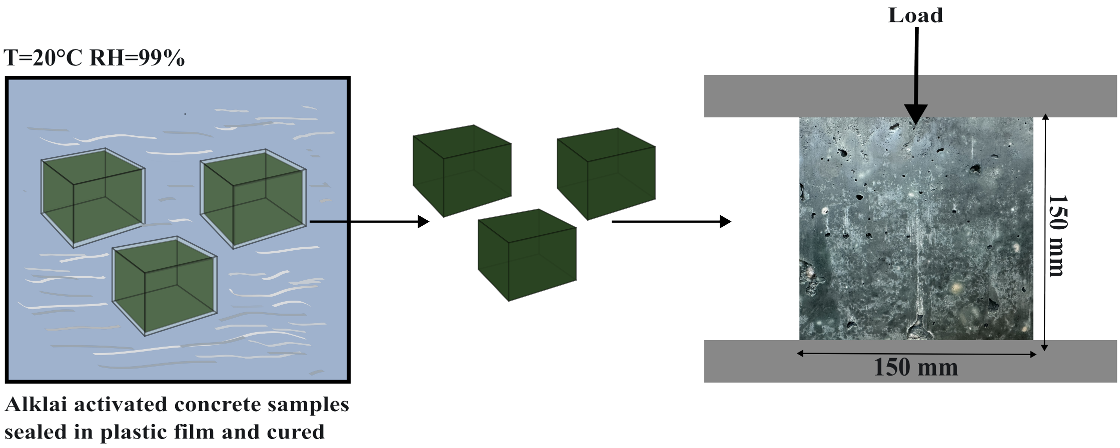

Figure 5.1: Schematic representation of the compressive strength test

An initial load of approximately 30% of the failure load was applied on the cubic specimen. The load was gradually increased at a constant rate of 13.5 kN/s until failure. The compressive strength is calculated as per the formula, $f_c = \frac{\text{(Failure load)}}{\text{(Surface are)}}$ N/mm^2 or MPa. The average strength of the 3 samples is reported as the compressive strength. The testing was conducted after 1-day, 3-days, 7-days and 28-days from the day of casting the samples. Figure 5.1 shows the schematic representation of the test.

5.2.2. SPLITTING TENSILE STRENGTH

The splitting tensile test is an indirect method to determine the tensile strength of concrete. The test was conducted on a two-column universal compression testing machine as per NEN 12390-6-Annex A (2009) [104]. For the test, 8 cubes of size 150x150x150 mm^3 were prepared. The samples were removed from the curing room and wiped to remove excess water and additional material on the surface. The sample was then placed on the compression testing machine. Hardboard packing strips were placed on top and bottom of the surfaces along the loading plane. The strips were then adjusted using a jig.

An initial load that did not exceed 20% of the failure load was applied. The load was then gradually increased at a constant rate of 2.12 kN/s until failure. The tensile strength is given by the formula $f_{ct}=\frac{2\text{ Failure load}}{\pi \text{L d}}$. The average of the 8 samples is reported as the tensile strength. The testing of the samples were conducted 28 days from the day of casting. Figure 5.2 shows the schematic representation of the test.

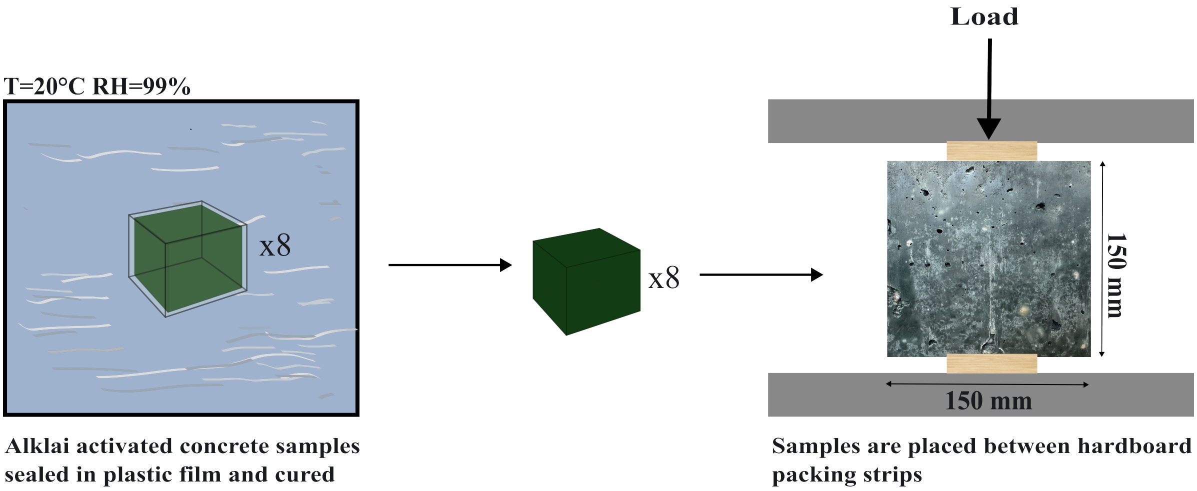

Figure 5.2: Schematic representation of the Splitting tensile strength test

5.2.3. FLEXURAL STRENGTH TEST

The flexural strength test is an indirect method to determine the tensile strength of concrete. The test was conducted as per NEN 14651+A1(2005) [105]. In this research, the flexural strength of concrete was determined by a 3-point bending test on the INSTRON Univeral testing system, which has a maximum load capacity of 10 kN. Concrete prisms of size 400(L)x100(B)x100(H) mm^3 were prepared for the test. A notch of 2.5 mm was made at the centre of the casting surface along the width, a day before the test. The testing was done as per the testing standard, except the size of the prisms were smaller than the size mentioned in the norm.

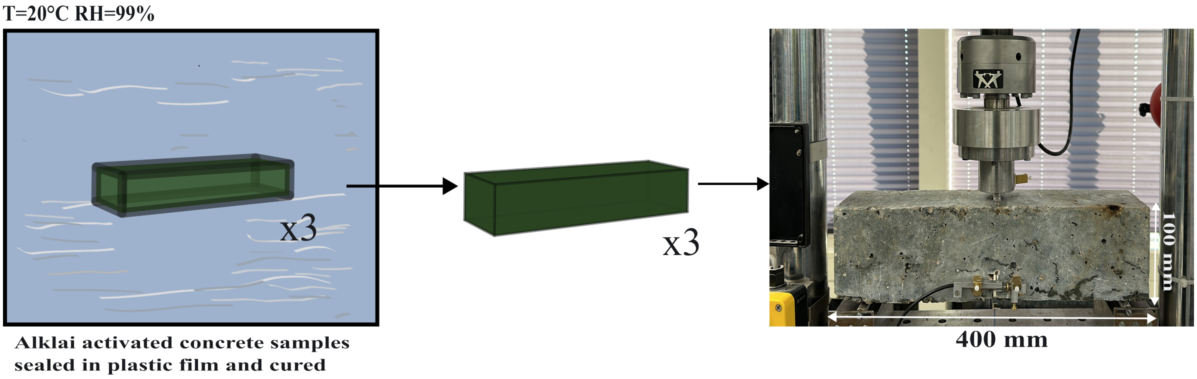

Figure 5.3: Schematic representation of the Splitting tensile strength test

Before the start of the test, concrete prisms were removed from the curing room and allowed to dry for at least 2 hours. Strain gauges were glued at a spacing of 5 cm from the middle of the notch on both sides of the prism. An initial speed of 0.5 microns/second was applied until the first crack appeared; later, the speed was increased to 1 micron. For this test, 700 microns was mentioned as the maximum crack mouth opening displacement. Figure 5.3 shows the schematic representation of the test.

5.2.4. FREEZE-THAW RESISTANCE

Freeze-thaw resistance of the concrete was conducted as per NVN-CEN/TS 12390-9(2016) [106]. Cube moulds of size 150x150x150 mm are taken, and a polytetrafluoroethylene (PTFE) plate was placed in between. The surface touching the PTFE plate was the testing surface and had approximately a size of 150x140 mm^2 and must not be lubricated. The plates can also be placed at the end of the cubes; however, since the concrete mix was dry with very low workability, the plates were preferred to be placed in the middle.

Once the samples were cast, they were covered with a plastic sheet for 24 hours to prevent the loss of moisture. The demoulded samples were then wrapped in a plastic film and stored in the curing room for 2 weeks. Following this, the plastic film was removed, and the samples were placed in a climate chamber (T=20°C, RH=50%) for 2 weeks. Butyl tape was used to cover the lateral surfaces of the concrete sample before the start of the test. This was to ensure that the lateral surfaces did not participate in the reaction.

Following the 2 weeks of drying, the samples were placed on top of spacers of height 5 mm in steel test containers, with the testing surface facing downwards. The samples were then allowed to saturate in a 3% NaCl solution for 7 days. The solution was filled up to 1 cm height from the bottom of the container, ensuring that the solution did not wet the top surface. Following this capillary suction phase, the containers were removed from the temperature-controlled chest and placed in an ultrasound bath for 3 minutes. The solution comprising the loosely adhering particles were filtered using filter paper. Subsequently, the filter paper was dried in an oven at 110±10°C for 24 hours. Before weighing the material, the filter paper was allowed to cool to room temperature.

During the test, the samples went through freeze-thaw cycles of 12 hours each. In each cycle, the temperature fluctuated between -20°C to +20°C. After every testing cycle; the containers were placed in an ultrasound bath for 3 minutes. The solution with the material was filtered, and the filter paper was allowed to dry at 110 ±10°C for 24 hours. The solution in the container was refilled after testing cycles 4, 6, 14 and 28.

5.3. RESULTS & INTERPRETATION

5.3.1. COMPRESSIVE STRENGTH

Compressive strength is used as the index to evaluate the performance of the concrete samples. The concrete mixtures are designed for a minimum compressive strength of C30/37 after 28 days as per the requirement for XF4 exposure class (NEN 206 [88]). The strength after 1-day, 3-days, 7-days and 28-days were measured. The early age strength is emphasised since it is a primary factor in the decision to allow constructed roads for public use. This aspect becomes even more critical in densely populated areas where traffic congestion and mobility are major concerns. Further, analysing the early age strength development ensures that the pavements are not loaded pre-maturely, which can cause its subsequent failure. The cube compressive strength at various testing periods is shown in Figure 5.4

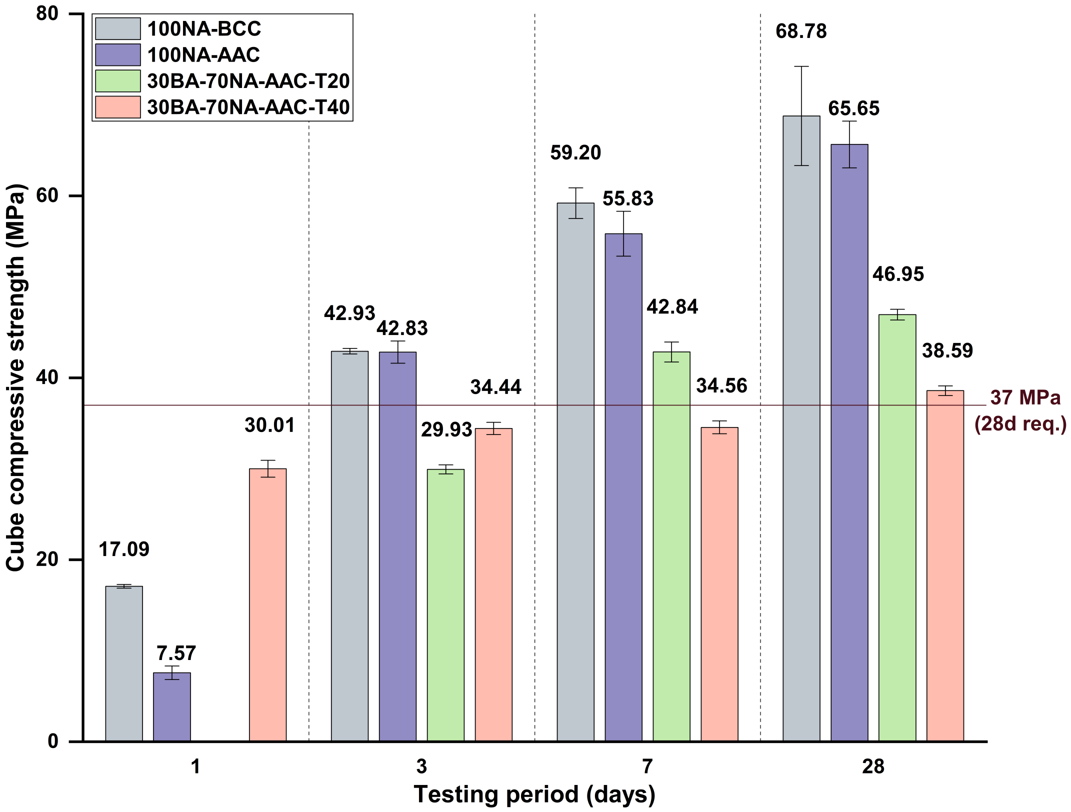

Figure 5.4: Cube compressive strength of concrete samples at different curing ages

- CURING AGE OF 1 DAY

Thermally treated test sample (30BA-70NA-AAC-T40) showed the highest strength of 30.01 MPa among the concrete samples. The improved strength of the 30BA-70NA-AAC-T40 can be due to the higher polymerisation degree and increased formation of reaction products at elevated temperature curing [107]. This is comparable to the trend observed by other researchers [107, 108, 109].

The ambient temperature cured test sample (30BA-70NA-AAC-T20) did not harden after 1 day. This can be partly due to a portion of the NaOH from the activator being used in the pre-treatment of the MSWI BA aggregates. The Na_2O ion plays a key role in the dissolution of the aluminosilicates and in the formation of the microstructure [110]. Hence the reduced availability of the ions can directly affect the geopolymerisation reaction and hence the delayed setting and strength development. The other reason can be the participation of the reactive phases in the fine MSWI BA fraction in the geopolymerisation reaction which further reduces the activator solution available for the reaction with GGBFS [111]. Further, the rate of pozzolanic reactivity is less for MSWI BA ashes [112, 113]. Hence, the reduced availability of the activator solution and the decreased rate of reactivity of MSWI BA ashes can collectively contribute to the increased setting time of the concrete. Among the control samples, alkali-activated concrete(100NA-AAC) indicated the lowest strength of 7.57 MPa.

- CURING AGE OF 3 DAYS

Blended cement concrete (100NA-BCC) and AAC (100NA-AAC) control samples attained equal strength of 42 MPa after 3 days of curing. This increased strength development of 100NA-AAC can be attributed to the higher reactivity of GGBFS that releases reactive calcium into the matrix. This enables the development of C-(A)-S-H gel, making the matrix homogeneous and dense [114]. The 30BA-70NA-AAC-T40 sample had a marginal increase of 15% compared to its 1-day strength. However, it was observed that the strength attained corresponded to 81% of the strength of the control samples. The 30BA-70NA-AAC-T20 sample set after three days and the strength attained indicated 70% of the strength of the control samples.

- CURING AGE OF 7 DAYS

The 30BA-70NA-AAC-T40 sample had negligible strength gain from its 3-day strength as shown in Figure 5.4. This may be due to the slight modifications in the matrix as the majority of the polymerisation products were already formed by the increased temperature curing [109]. In contrast, the 30BA-70NA-AAC-T20 sample demonstrated a notable strength gain of 43% from its 3-day strength. This enhancement can be attributed to the ongoing geopolymerisation reaction in the concrete sample. The 100NA-AAC control sample is designed to have comparable strength to the 100NA-BCC sample after 7-days of curing. Figure 5.4 shows that the control samples had attained comparable strength with a minimal deviation of 3 MPa after 7-days of curing.

- CURING AGE OF 28 DAYS

  The control and test samples satisfied the minimum strength requirement of 37 MPa after 28 days required for pavements. Among the concrete samples, 100NA-BCC showed the highest strength of 68.8 MPa after 28 days of curing. The 100NA-AAC control attained similar strength to the BCC control with a marginal difference of 3 MPa. The 30BA-70NA-AAC-T20 sample indicated a strength of 47 MPa, about 70% of the strength of control samples. In comparison, the 30BA-70NA-AAC-T40 sample exhibited only 50% of the strength of the control samples. This reduced strength of the test samples compared to the control samples can be attributed to the fundamental porosity of the MSWI BA aggregates [115], making it weaker compared to gravel and the air voids formed inside the concrete as a result of the reaction between metallic Al and alkalis. Further, the observed loss in performance of 30BA-70NA-AAC-T40 compared to 30BA-70NA-AAC-T20 can be due to the following reasons:

  - At higher curing temperatures, the reaction of the metallic Al with the alkali is enhanced, leading to the accelerated release of hydrogen gas inside the concrete while it is hardening [116]. This results in the formation of air voids inside the concrete sample and subsequent cracking of the hardened matrix.
  - At elevated temperature curing, it is reported that alkali activated slag concrete (AASC) samples indicated lower later age strength development compared to ambient temperature cured AASC samples [43]. Bakharev et al. (2000) [117] reported that the reduced later age strength observed in the elevated temperature cured AASC sample is due to inhomogeneity of the microstructure, localisation of hydration product near slag grains, and resulting coarse pore structure.
  - C-(A)-S-H gel is the major binding phase when GGBFS reacts with the alkaline solution [118]. Aliabdo et al. (2019)[119] reported that the C-(A)-S-H gel formation is affected by the loss of moisture at elevated temperature curing, hence resulting in reduced compressive strength of the AAC containing GGBFS.

    Thus, the reduced strength of the 30BA-70NA-AAC-T40 sample can be attributed to cracking and air void formation due to hydrogen gas release inside the concrete, inhomogeneity of the matrix and reduced gel formation due to loss of moisture.

5.3.2. SPLITTING TENSILE STRENGTH TEST

The tensile strength affects the durability and serviceability of the concrete used in road pavements. The propagation and formation of cracks are related to the tensile strength of the concrete [120]. NEN 1338 (2003) [25] requires that the concrete used for pavements have a minimum tensile strength of 3.6 MPa after 28 days. The tensile strength of the concrete samples (control and test) after 28-days of curing is indicated in Figure 5.5 The test result showed that all the concrete samples except the thermally treated test sample (30BA-70NA-AAC-T40) satisfy the requirement for pavements. The 30BA-70NA-AAC-T40 indicated a tensile strength of 3.15 MPa after 28 days which was lower than the norm requirement of 3.6 MPa. The loss in performance of the 30BA-70NA-AAC-T40 sample compared to the 30BA-70NA-AAC-T20 can be due to the effects of the elevated temperature curing discussed in Section 5.3.1. Further, the test samples indicated a strength lower than the control group. This can be due to the application of weaker MSWI BA aggregates replacing denser gravel particles in the test sample as well as the air void formation resulting from the formation of hydrogen gas inside the AAC concrete containing MSWI BA aggregates. Among the concrete samples, the highest tensile strength of 5.08 MPa was exhibited by the BCC control sample.

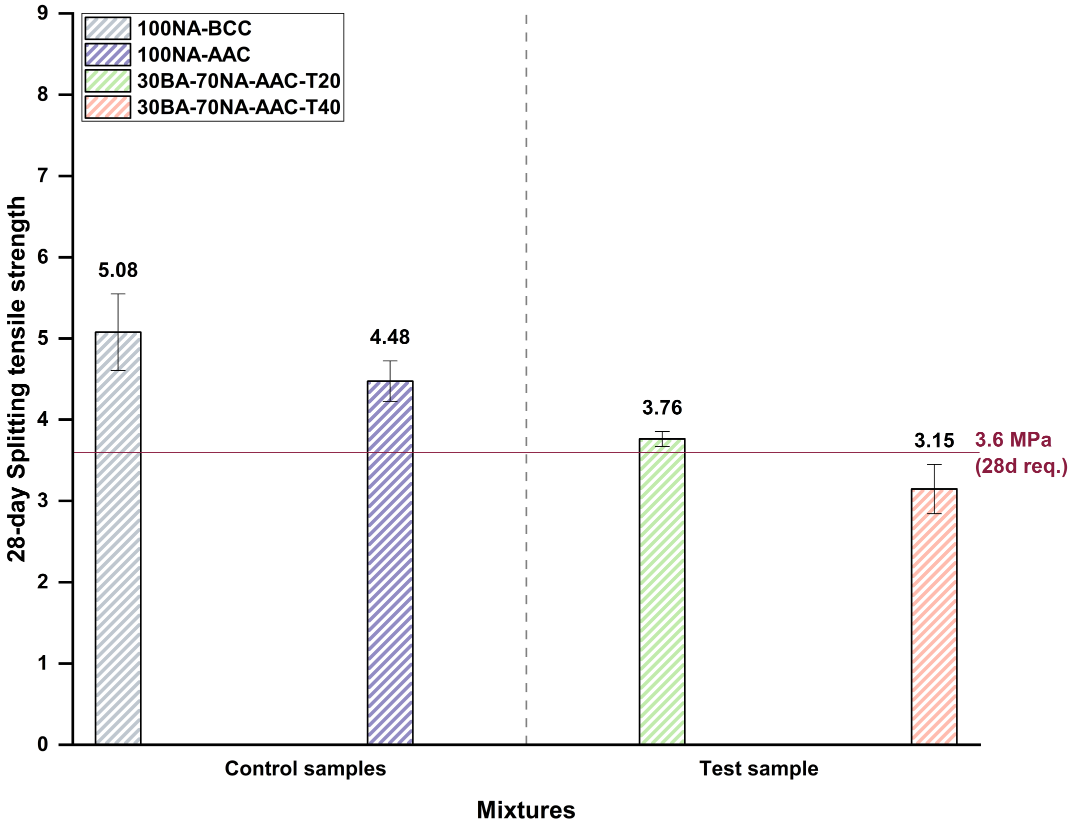

Figure 5.5: Splitting tensile strength of concrete specimens at 28-day curing age

5.3.3. FLEXURAL STRENGTH TEST

The flexural strength of concrete samples after 28 days of curing is shown in Figure 5.6. The flexural strength test of the concrete samples indicated a similar trend to that of the splitting tensile strength. The thermally cured test sample (30BA-70NA-AAC-T40) showed the lowest strength of 4.1 MPa after 28 days. This was in conjunction with the tensile strength results that showed the lowest value for the thermally cured test sample. The reason for the reduced strength is discussed in Section 5.3.1. The test samples showed lower flexural strength compared to the control mixes. The highest flexural strength of 8.07 MPa was shown by the blended cement concrete control (100NA-BCC). Flexural strength results are influenced by various factors, including notching the sample, curing, loading and fabricating [121]. Since the test results are sensitive to numerous factors, conclusive results are obtained when combined with the results of the split tensile strength.

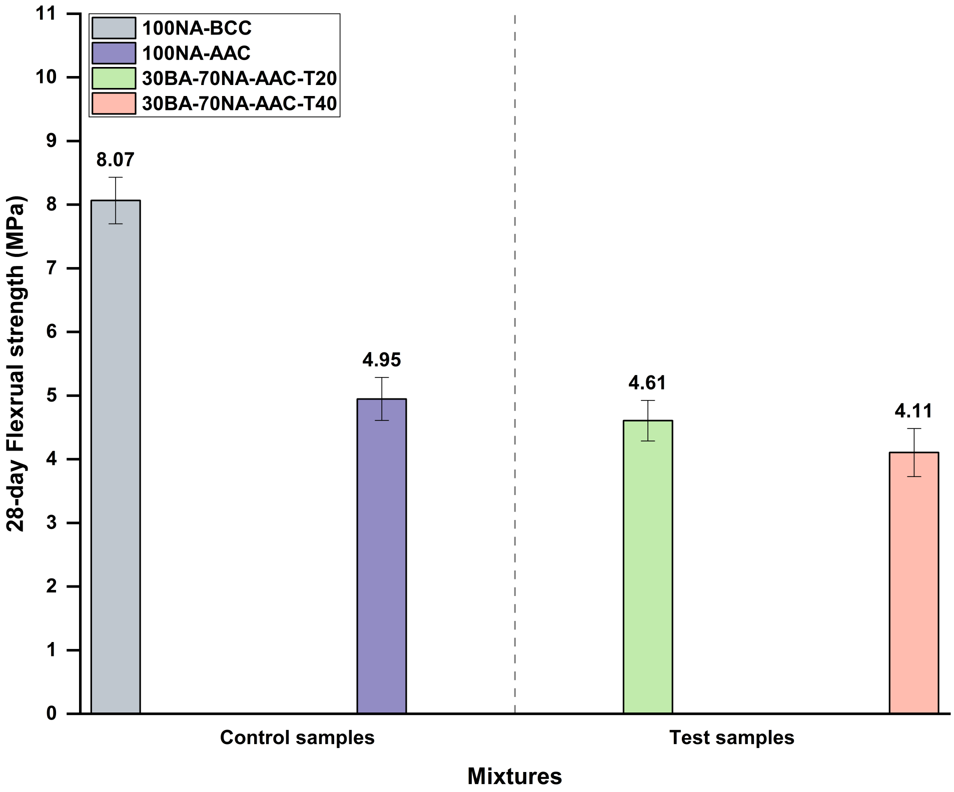

Figure 5.6: Flexural strength of concrete specimens at 28-day curing age

5.3.4. FREEZE-THAW RESISTANCE

Capillary suction of **D**eicing chemicals and **F**reeze-thaw (CDF) test was used to evaluate the freeze-thaw performance of the concrete samples. It is calculated as the mass loss or mass scaled from the concrete samples when subjected to 28 freeze-thaw cycles. The maximum scaling of material after 28 cycles must not exceed 1 kg/m^2, as per the requirement of NEN 1338(2017) [88] for pavements. The scaling of the material was quantified after 4, 6, 14 and 28 testing cycles. Table 5.1 shows the total material loss after 28 cycles for the concrete samples (control and test). The total mass of the scaled material after every testing cycle is depicted in Figure 5.7

Table 5.1: Total scaled material from concrete samples after 28 testing cycles

Mixture	**Total scaled material after 28 cycles (kg/m^3)**
100NA-BCC	2.43
100NA-AAC	4.52
30BA-70NA-AAC-T20	5.23
30BA-70NA-AAC-T40	5.53

Figure 5.7 shows the surface scaling of concrete samples after 4, 6, 14 and 28 testing cycles of the CDF test. The loss of material in all the samples was much higher than the norm requirement of 1 kg/m^2. This research does not introduce air-entraining admixtures that provide entrained air voids for accommodating freezable water. The air voids present

in the concrete samples are large entrapped air void that are formed as a consequence of mixing and insufficient vibration [122]. Details on the effect of air voids on the freeze-thaw resistance is discussed in Chapter 6. During freezing, water from the smaller pores migrates to the larger air voids, which are only partially filled, thus reducing the internal pressure and related damage to the concrete sample [123, 124]. The absence of entrained air voids in the concrete samples can explain the poor resistance of the concrete samples to the freeze-thaw cycles.

Blended cement concrete control (100NA-BCC) sample showed the highest resistance to freeze-thaw cycles among the concrete samples with a total surface scaling of 2.43 kg/m^2. On the contrary, AAC control sample (100NA-AAC) showed lower resistance with a total material loss of 4.52 kg/m^2 as indicated in Table 5.1. The poor freeze-thaw resistance of the 100NA-AAC concrete can be explained by its dense microstructure with small capillary pores and trapped impermeability, making it difficult for the freezable water to migrate to the air voids, thus introducing stress and related cracking in the concrete [123].

Both the test samples showed higher surface scaling compared to the control mixes, as shown in Figure 5.7. In general, the larger pores inside the MSWI BA aggregate can act as expansion chambers where the pressure resulting from water freezing can be released. However, it is essential to ensure that the pores are not saturated, which can otherwise cause detrimental effects on the concrete [125, 126]. The saturated aggregates can cause expansion near the surface of the specimen and consequently cause the disintegration of the surrounding cement or failure of the aggregates due to expansion while freezing [125]. The MSWI BA aggregates used in the test sample were saturated in the process of two weeks of pre-treatment. This may be the reason for the further deterioration of the test samples compared to the 100NA-AAC control sample.

Amongst the test samples, the ambient temperature cured sample (30BA-70NA-AAC-T20) showed higher resistance compared to the thermally cured (30BA-70NA-AAC-T40) sample. 30BA-70NA-AAC-T40 sample was observed to have small amounts of visible surface cracks. This can be due to drying cracks due to the loss of moisture during oven curing or the cracks formed as a result of increased reactivity of remaining aluminium in the MSWI BA aggregates, as discussed in Section 5.3.1. However, cracking in concrete is reported to have adverse effects on its freeze-thaw resistance [127]. This is in conjunction with the results obtained as indicated in Table 5.1 that showed a higher material loss for the 30BA-70NA-AAC-T40 sample compared to 30BA-70NA-AAC-T20. The cracks inside the concrete sample allow for further penetration of external water into the concrete sample through the cracks, thus filling the internal pores, which can lead to expansion of the concrete during freezing and subsequent spalling [127].

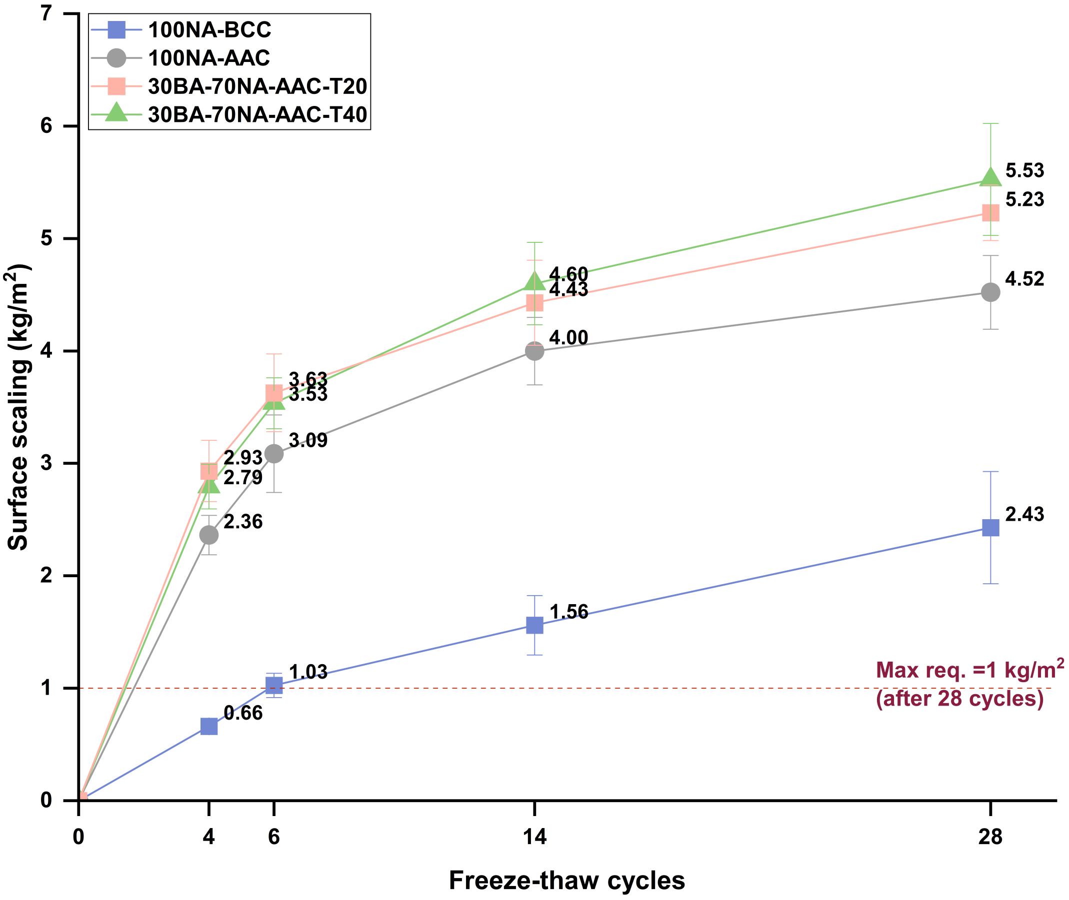

Figure 5.7: Surface scaling of concrete after 4, 6, 14 and 28 freeze-thaw testing cycles

5.4. CONCLUSION

Ambient temperature-cured AAC containing MSWI BA aggregates(30BA-70NA-AAC-T20) satisfied all the mechanical performance requirements for application in the pavements. On the contrary, the thermally cured sample (30BA-70NA-AAC-T40) did not satisfy the tensile strength requirement. The observed loss in performance may be attributed to the higher cracking and lower gel formations at higher temperatures. Further, the compressive strength results indicated more significant strength development over time for the 30BA-70NA-AAC-T20 sample compared to the 30BA-70NA-AAC-T40 sample. However, the compressive strength, splitting tensile strength and flexural strength of the test samples were observed to be much lower compared to the control samples (100NA-AAC and 100NA-BCC). The lower performance of the concrete containing MSWI BA aggregates was mainly attributed to the high porosity of the MSWI BA aggregate, thus making it weaker than the dense gravel particles.

The freeze-thaw resistance of the test samples did not meet the norm requirement. The deterioration of the samples can be attributed to the saturation of the aggregates and the additional cracking observed in the thermally cured test sample. The saturation of porous MSWI BA aggregates during the pre-treatment process can cause expansion during freezing and subsequent failure of the aggregate. Further, the saturation of aggregates contributed to spalling of the concrete due to surface expansion. The presence of cracking in the thermally cured test sample also facilitated water penetration and volume expansion during freezing, further compromising the resistance to freeze-thaw cycles. The control samples also showed lower resistance to freeze-thaw cycles which can be attributed to the absence of air-entraining admixtures in the concrete to provide sufficient air voids for freezable water.

6

MICROSTRUCTURE STUDY OF CONCRETE CONTAINING MSWI BA AGGREGATES

6.1. INTRODUCTION

This chapter focuses on the microstructure formation of AAC (alkali-activated concrete) containing MSWI BA (municipal solid waste incineration bottom ash) aggregates. Specifically, the porosity, morphology, and matrix- MSWI BA aggregate bonding are examined. Further, considering the inferior mechanical performance and durability of the thermally cured test sample (30BA-70NA-AAC-T40) in comparison to the ambient cured sample (30BA-70NA-AAC-T20), the focus of the study henceforth will be solely directed towards the analysis of the 30BA-70NA-AAC-T40 test sample.

Hardened concrete has numerous voids within its hydrated matrix, primarily formed during mixing, compaction, and hardening [128]. These voids can be categorized based on their size as gel pores, capillary pores, and air voids. The properties of these pores, such as the pore size distribution, the pore shape or the total void volume in the concrete, play a significant role in influencing the mechanical characteristic and durability of hardened concrete [129, 128]. Analyzing the characteristics of these voids is crucial for comprehending the overall performance and behaviour of concrete in its hardened state.

Air voids within concrete can be classified as entrapped or entrained air voids[130]. Entrained air voids are deliberately introduced in concrete using admixtures, while entrapped air voids are formed during concrete mixing [122]. Generally, air voids are incorporated in concrete to improve its resistance to freeze-thaw cycles by providing adequate space for water migration from smaller capillary pores to the air voids during freezing [131]. The presence of metallic aluminium in the MSWI BA aggregates can introduce air voids in the AAC as a result of hydrogen gas release [82]. Hence, analysis on the properties of the air voids formed was investigated using X-ray computed tomography (CT), with a focus on the effects of air voids on the mechanical properties and durability of the AAC containing MSWI BA aggregates.

Scanning Electron Microscopy (SEM) was used to explore the morphology of the MSWI BA aggregates, gel formations inside AAC containing MSWI BA aggregates and the MSWI BA aggregate-matrix bonding. This enables a deeper understanding of the microstructural characteristics and their impact on the mechanical properties and long-term behaviour of AAC containing MSWI BA aggregates.

6.2. TESTING PROCEDURE

6.2.1. X-RAY COMPUTED TOMOGRAPHY

X-ray computed tomography (X-ray CT) is an effective and non-destructive technique for the exploration of the three-dimensional microstructure of materials [132]. In this research, high-resolution X-ray CT scans, obtained using TESCAN CoreTOM, are employed to analyze the air voids present in AAC incorporating MSWI BA aggregates. For optimal scan quality, cylindrical core specimens with dimensions of 50 mm (diameter) and 150 mm (height) were extracted from a 28-day cured cubic specimen. The selection of 50 mm diameter ensured that a representative portion of the concrete was captured while ensuring a high-quality scan. Prior to testing, the specimen was subjected to a 24 hour drying period inside a desiccator. The sample for the test is shown in Figure 6.1(b).

The sample was wrapped in a plastic film and fixed on a rotating table for scanning during testing, as shown in Figure 6.1(a). The sample is scanned in three sections which were then merged to produce a complete scan. A resolution of 60 µm per pixel was used for air void characterisation. The scan produced approximately 3000 slices, with small variations in the number of slices depending on the resolution and merging of individual scan sections. The test was conducted on both the control group (100NA-BCC and 100NA-AAC) and the ambient temperature-cured test sample (30BA-70NA-AAC-T20). The scanned slices were reconstructed and analysed using Dragonfly ORS software.

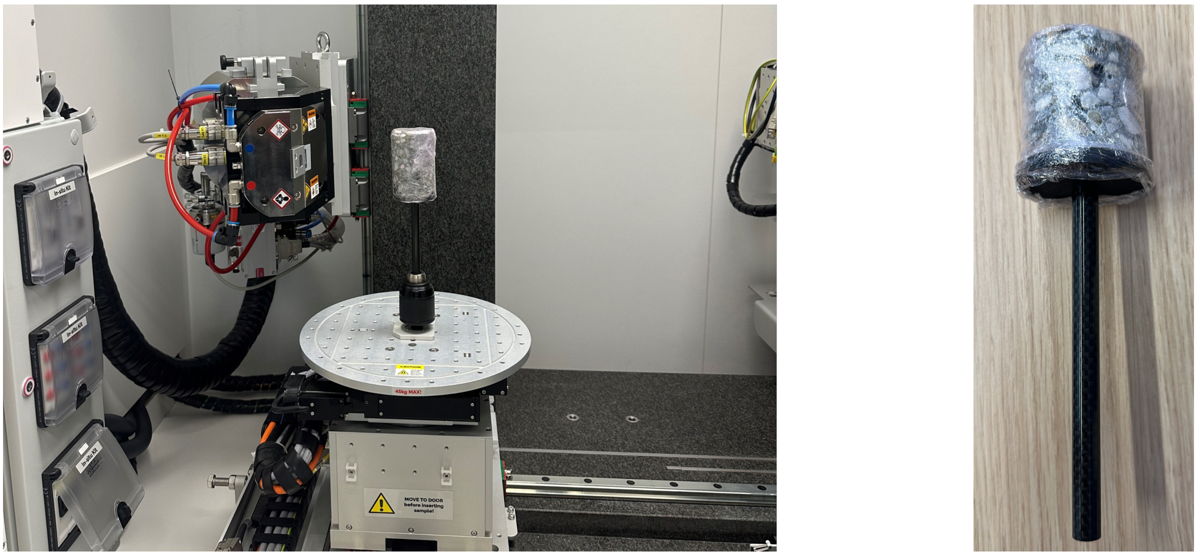

(a) Concrete sample on rotating table for CT scan

(b) Sample for CT scan

Figure 6.1: Scanning of concrete sample using X-Ray CT

IMAGE SEGMENTATION OF CONCRETE

The Dragonfly ORS software was utilised for the analysis of the air voids present in the concrete samples. To extract the necessary information from the region of interest, it is crucial to identify the appropriate greyscale value. The greyscale values of the matrix, aggregates, and air voids differ, and an effective thresholding method can facilitate the extraction of air void information. In the conducted research, the Otsu thresholding method was employed to distinguish air voids from background information by dynamically calculating the optimal grey threshold [133]. This method considers each pixel in the image and determines the region to which it belongs, the target or background area, resulting in the generation of a corresponding binarized image [134]. The air voids inside a concrete section after the segmentation is shown in Figure 6.2.

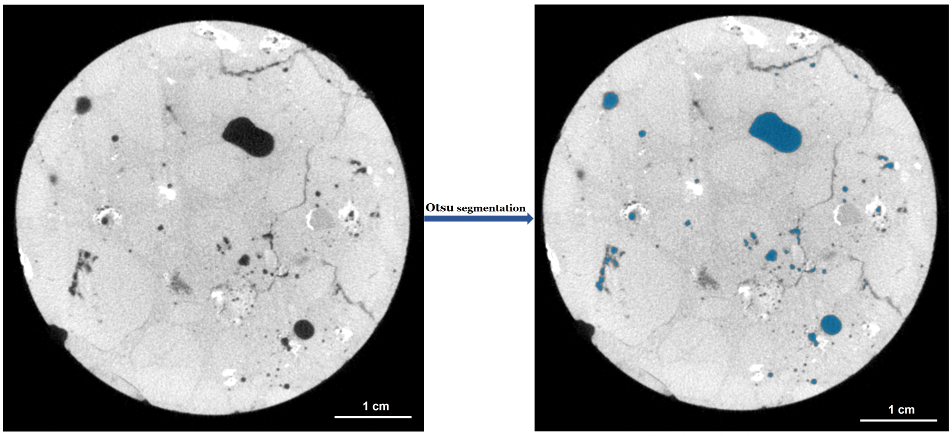

30BA-70NA-AAC-T20 section obtained from X-ray CT

30BA-70NA-AAC-T20 section after Otsu segmentation

Figure 6.2: Air voids inside a concrete section before and after image segmentation

6.2.2. SCANNING ELECTRON MICROSCOPY

A scanning electron microscope is an optical microscope that uses electron beams to provide information on the sample's chemical composition, morphology and phase distribution. To further enhance the features of the microscope, energy dispersive spectrometer (EDS) is mounted on SEM. This allows to simultaneously analyse and provide qualitative information on the elements on the surface investigated and the analysis is termed as energy dispersive X-ray spectroscopy (EDX). To fully realise the factors affecting the performance of the AAC containing MSWI BA aggregates, EDX analysis was conducted. Since air voids in the concrete sample was analysed using X-ray CT, SEM-EDX is used to investigate further; the morphology of the MSWI BA aggregates, the nature of the MSWI BA aggregate-matrix bonding and the gel formations inside the concrete containing MSWI BA aggregates.

To conduct the scanning electron microscopy (SEM) test, a concrete block measuring 40 (Length) x 35 (Width) x 30 (Height) mm^3 was prepared from a 28-day cured concrete sample. An object glass was glued to the surface of the block, which was then cut to the desired size of 40 (Length) x 35 (Width) x 1 (Height) mm^3 using a thin section machine. This ensured that the surface of the sliced sample was straight to avoid undercuts during the grinding and polishing stages. Following this, the sample was impregnated with epoxy to fill the pores in the concrete section by placing it in a vacuum impregnator for 1.5 hours as shown in Figure 6.3(a). After impregnation, the sample was allowed to dry for a day after which the epoxy on the surface of the sample was removed using silicon carbide sandpaper in decreasing grit sizes in the order of 800, 1200 and 2000. Each grit size was applied to the sample for approximately 1 to 2 minutes at 300 rpm. It is important to maintain the same thickness of the sample before impregnation and after removing the surface epoxy as shown in Figure 6.3(b). Care must be taken during grinding to avoid scratches on the sample surface. Additionally, excessive grinding can damage the concrete matrix.

Following the grinding process, the sample was polished at 250 rpm with polishing cloths containing diamond compounds of 6 µm, 3 µm, 1 µm, and ¼ µm for durations of 5 minutes, 3 minutes, 2 minutes, and 1 minute, respectively. The sample was immersed in ethanol and placed in an ultrasound bath for a minute between each polishing size to remove any excess diamond compound on the surface of the sample.

An hour prior to the test, the sample was carbon-coated to enhance the conductivity of the sample as shown in Figure 6.3 (c). Following this, the sample was mounted on copper stubs using carbon tapes and the test is conducted using FEI Quanta 650 FEG-SEM.

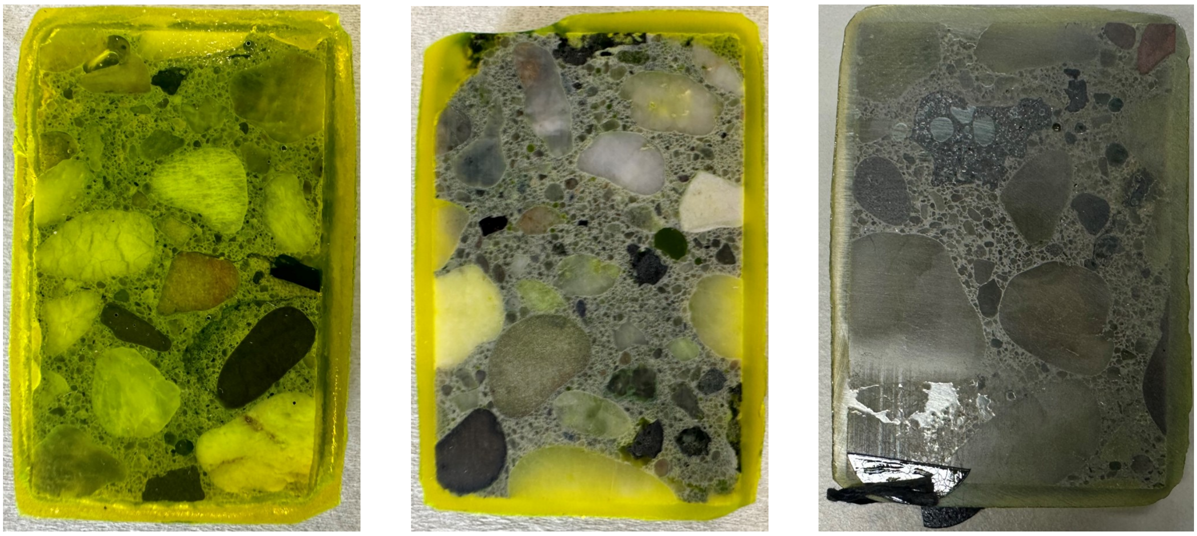

(a) Epoxy impregnated sample **(b)** Sample without surface layer epoxy **(c)** Carbon coated sample

Figure 6.3: Sample preparation for SEM analysis

6.3. RESULTS AND DISCUSSION

6.3.1. AIR VOID ANALYSIS

The investigation of air voids in the concrete section focused on analysing the porosity and air void distribution. X-ray CT was employed to obtain scanned sections of the concrete for air void analysis. Figure 6.5 and 6.6 illustrates the air void distribution in the control samples (100NA-BCC and 100NA-AAC) and the test sample (30BA-70NA-AAC-T20).

The smallest air void detected in all the concrete samples after thresholding was 80 µm, which largely depended on the resolution of the scan. The thresholding technique also contributes to the size of the air void detected. Higher-resolution scanning allows for clearer differentiation between pores (region of interest) and the background. Figure 6.6(a) demonstrates that the control sample 100NA-AAC exhibits a denser microstructure with smaller air voids compared to the control sample 100NA-BCC shown in Figure 6.6(b). The larger air voids observed in the control samples are entrapped air voids since no entraining admixtures were introduced in the concrete samples. The maximum size of air voids detected in the control samples was approximately 6 mm, which is close to findings by other researchers [135]. The introduction of MSWI BA aggregates in the AAC resulted in the presence of air voids as large as 9.67 mm, as indicated in Figure 6.5. These large air voids in the 30BA-70NA-AAC-T20 test sample can be attributed to the release of hydrogen gas in the concrete due to the reaction of metallic Al with the alkali activator. Further, these air voids follow the contours of the MSWI BA aggregate as shown in Figure 6.4. This observation aligns with the result reported by Müller & Rübner (2006) [70].

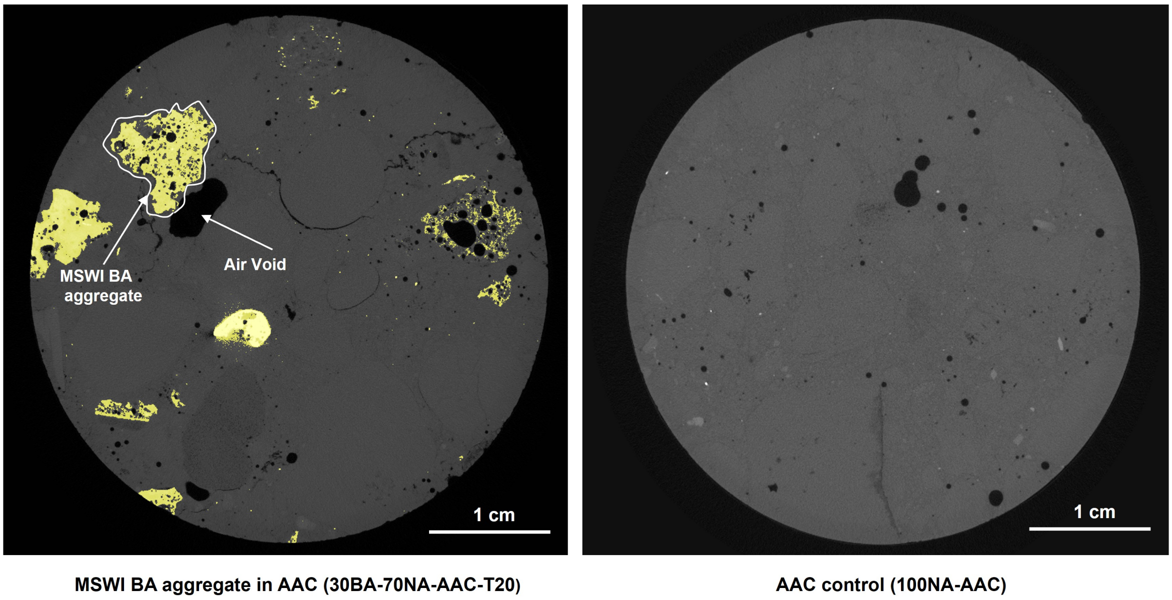

Figure 6.4: X-ray CT image of a section of 30BA-70NA-AAC-T20 and 100NA-AAC

Figure 6.7(b) presents the normalized frequency distribution of air voids in the concrete samples, which in this research is categorized into five groups based on their equivalent spherical diameter. As anticipated from the visualized air void distribution in Figures 6.5 and 6.6, the AAC control sample predominantly contains smaller pores with sizes below 250 µm, occupying 80% of the void space. It was also noted that the 30BA-70NA-AAC-T20 test sample exhibited a similar air void size distribution to the 100NA-BCC control sample, which demonstrated superior mechanical performance and freeze-thaw resistance among the concrete samples. In contrast, the test sample exhibited a higher number of larger diameter pores within the category of air voids exceeding 1 mm when compared to the 100NA-BCC sample. Consequently, although the distribution of air voids larger than 1 mm was similar, the presence of these larger pores in the test sample could contribute to the difference in the observed performance of the control and test sample.

To gain a comprehensive understanding, it is necessary to quantify the total porosity within the samples. Figure 6.7(a) presents the total porosity in the concrete samples, with the MSWI BA test samples indicating the highest porosity of 2.34%, while the AAC control sample showed the lowest porosity of 1.19%. The higher porosity in the 30BA-70NA-AAC-T20 test sample compared to the control samples further supports the claim of hydrogen gas release in the concrete and subsequent air void formation. The effects of these air voids on the mechanical properties and durability of AAC containing MSWI BA aggregates will be explored in the subsequent sections.

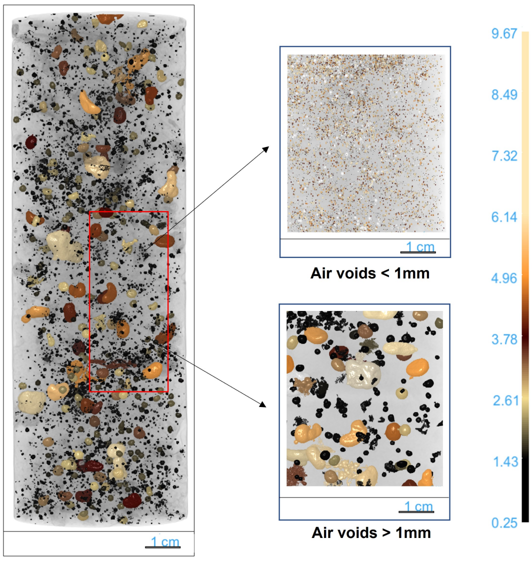

Figure 6.5: Air void distribution in AAC containing MSWI BA aggregates (30BA-70NA-AAC-T20)

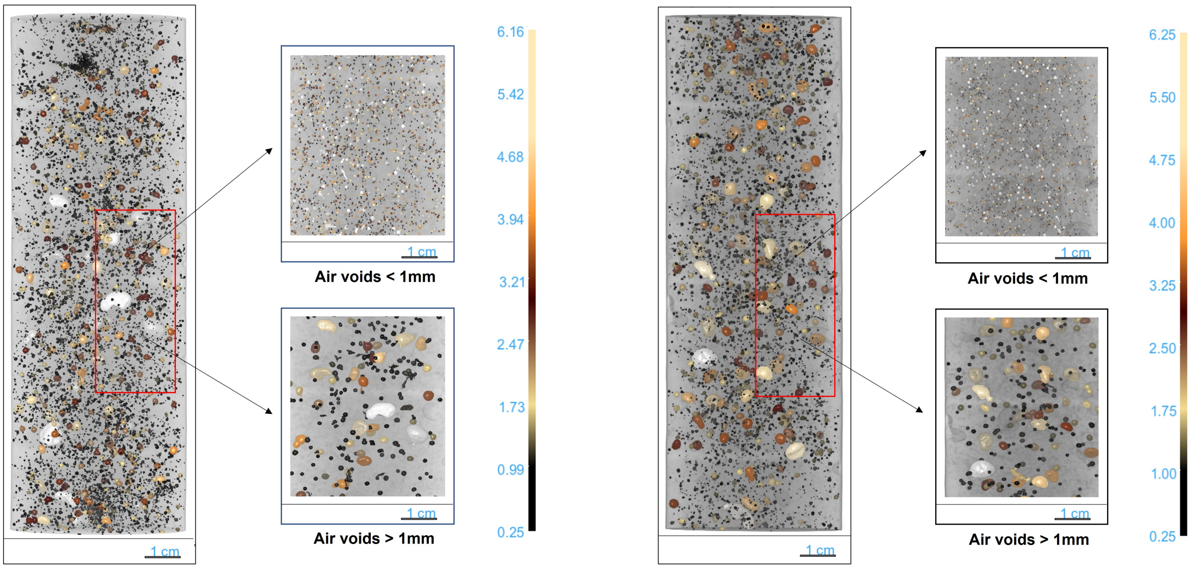

(a) Air void distribution in AAC control sample (100NA-AAC)

(b) Air void distribution in BCC control sample (100NA-BCC)

Figure 6.6: Air void distribution in AAC and BCC control sample

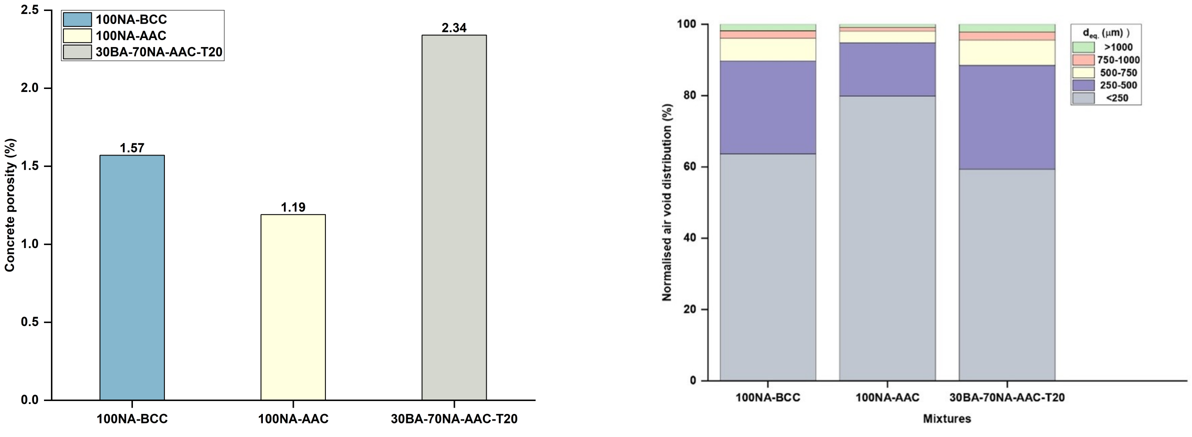

(a) Total porosity in the concrete sample

(b) Normalised frequency distribution of air voids in concrete samples

Figure 6.7: Frequency distribution of air voids and total porosity in concrete samples

6.3.2. EFFECT OF AIR VOIDS ON THE MECHANICAL PROPERTIES OF AAC CONTAINING MSWI BA AGGREGATES

The presence of air voids has a negative impact on the mechanical properties of concrete. Researchers have reported a 4–6% decrease in compressive strength for every 1% increase in air content [136, 137]. Consistent loss in performance exhibited by the 30BA-70NA-AAC-T20 sample compared to the control samples in all the mechanical tests can be attributed to the higher porosity in the sample as shown in Figure 6.7(a). Further, the inherent porosity of the aggregate makes it more vulnerable to damage and failure.

The air voids in the test sample show higher diameter air voids with a maximum size of 9.67 mm compared to the control samples that had a maximum size of 6 mm, as shown in Figure 6.5 and 6.6. This indicates hydrogen gas release inside the concrete, and subsequent cracking that can cause deterioration of the concrete sample. Despite the higher porosity indicated by the MSWI BA aggregate, the pre-treatment can still be considered effective since the 30BA-70NA-AAC-T20 sample satisfied all the mechanical performance requirements for pavements. Hence the reduction in the mechanical properties of the 30BA-70NA-AAC-T20 compared to the control samples can be attributed to the combined influence of aggregate porosity, higher air voids compared to concrete with natural aggregates and possible cracking as a consequence of hydrogen gas release in the concrete.

6.3.3. EFFECT OF AIR VOIDS ON THE FREEZE-THAW RESISTANCE OF AAC CONTAINING MSWI BA AGGREGATES

The freeze-thaw resistance of concrete is influenced by various factors such as air void size, spacing between air voids, air void distribution, and total porosity of the sample [124, 138]. The air void distribution of the 30BA-70NA-AAC-T20 test sample exhibited an even distribution, as depicted in Figure 6.7(b). Similar air void size distribution was observed in the 100NA-BCC control sample. However, the 100NA-AAC control sample displayed poor air void distribution, with approximately 80% of the pores occurring in the range of very small air voids. Existing literature indicates that an even distribution of air voids contributes to the enhanced freeze-thaw performance of concrete [124]. Thus, the absence of well-distributed air void distribution in the AAC control sample could be a contributing factor to its deterioration when subjected to freeze-thaw cycles.

Further analysis of air void sizes revealed that the 30BA-70NA-AAC-T20 test sample exhibited large-sized air voids, ranging around 9 mm, with a high frequency above 1 mm. In contrast, the control samples had air voids in the size range of 6 mm, with a lower frequency of air voids above 1 mm compared to the control samples. Air voids smaller than 1 mm in size are known to enhance the resistance of concrete to freeze-thaw cycles [139]. Hence, despite the well-distributed air voids in the 30BA-70NA-AAC-T20 sample, the presence of larger air voids may contribute to its poor freeze-thaw resistance, as illustrated in Figure 5.7.

Furthermore, the porosity of the samples were examined, revealing that the 30BA-70NA-AAC sample had the highest porosity with a percentage of 2.34%, while the 100NA-AAC control sample exhibited the lowest porosity of 1.19% as shown in Figure 6.7(a). A total porosity within the range of 3-6% is known to enhance the performance of concrete in freeze-thaw cycles [138]. The combined effect of lower porosity and larger-sized air voids in the 30BA-70NA-AAC-T20 sample compared to the control samples could account for its poor freeze-thaw resistance.

Additionally, the spacing of air voids also affects the freeze-thaw resistance of concrete, which was not investigated in this research. A comprehensive analysis incorporating this additional information could provide more insights into the effect of air void on the freeze-thaw resistance of the AAC containing MSWI BA aggregates.

6.3.4. MORPHOLOGY OF AAC WITH MSWI BA AGGREGATE

Polished sections of 30BA-70NA-AAC-T20 are used to observe the morphology of MSWI BA aggregates. Figure 6.8(a) shows an MSWI BA aggregate embedded in the analysed concrete section. The MSWI BA aggregate was observed to have an irregular shape, rough surface texture and porous microstructure. These pores inside the MSWI BA aggregate are visible as black regions due to the dominant oxygen and carbon content in the epoxy filling them. The microstructure of the MSWI BA aggregate was in accordance with the aggregate characteristic tests that indicated lower density and higher water absorption due to its porous nature. These pores, formed as a result of the rapid quenching process during the MSWI BA aggregate production, was a leading cause for the loss of performance in the concrete containing these aggregates [140, 141]. Further, the pores inside the MSWI BA aggregate were observed to be filled with various products, which are magnified and shown in Figure 6.8(b) and (d). Chemical analysis using SEM-EDX spot analysis of these regions are shown in Figure 6.8(c), and it indicated the presence of iron oxide, reaction products, sand, glass and oxidised aluminium. Similar observations were reported by other researchers [142, 77].

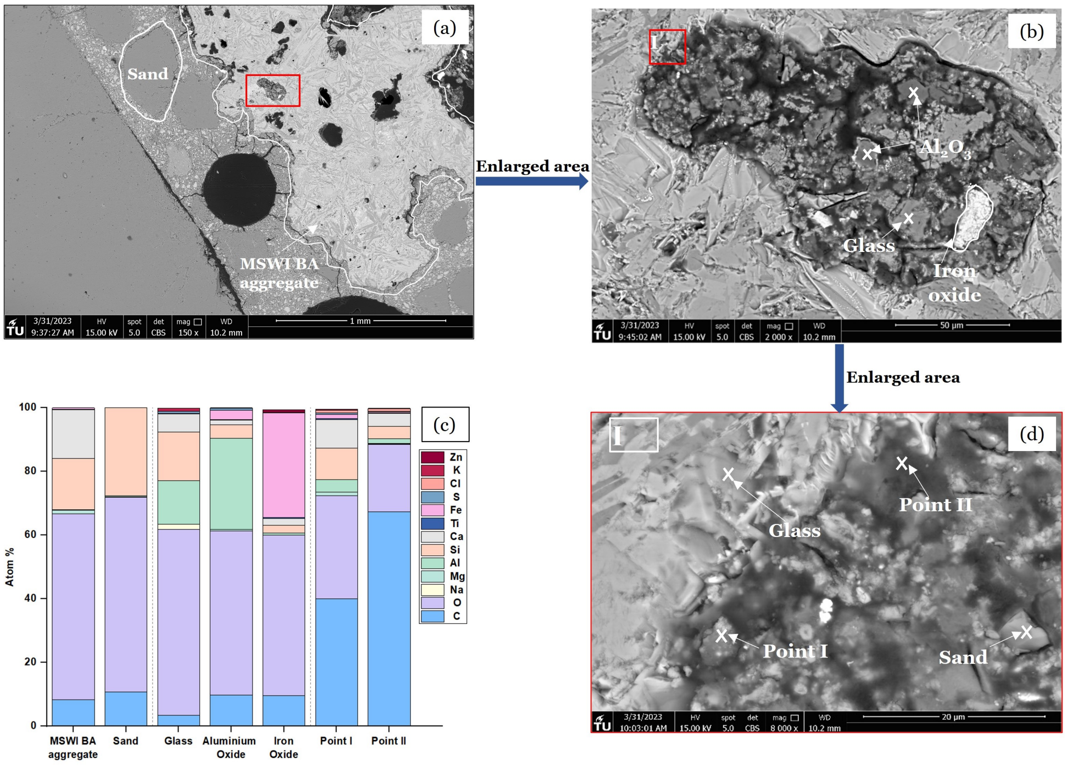

Figure 6.8: (a)Section of the concrete sample containing MSWI BA aggregate (b)enlarged section of the MSWI BA aggregate (c)chemical analysis of the phases inside the MSWI BA aggregate (d)enlarged section under investigation inside the MSWI BA aggregate

A closer examination of the components of the MSWI BA aggregates is shown in Figure 6.8(d). The MSWI BA aggregates mainly consist of glass, constituting over 50% by weight of the aggregate and are mainly of two kinds; primary and secondary glass [142]. The primary glass is derived from packing glass and is reported to have the same composition as soda-lime glass [142]. These glass particles remain unchanged after the combustion of municipal solid waste. Further, the primary glass is reported to be the major component in the larger bottom ash fractions (4-16mm) [142]. Additionally, secondary glass is newly formed at high temperatures during the combustion process in the furnace [143, 144]. It contains large amounts of gas bubbles, vesicles and cracks [145].

Figure 6.8(c) shows the chemical composition of the glass particles detected in the MSWI BA, and it mainly consists of SiO_2, Na_2O and CaO. This observation was consistent with the results obtained by other researchers [146, 147]. Further, the particles were noticed to be without pores and cracks, thus indicating the presence of primary glass particles in the MSWI BA aggregate.

Additionally, upon examining the enlarged section (I) of the MSWI BA aggregate, as depicted in Figure 6.8(d), it was observed that the section consisted of two distinct phases with different compositions. The chemical analysis of Point I using EDX, as shown in Figure 6.8(c), revealed the presence of predominantly Si, along with other elements such as Al, Ca, and Fe. This composition resembled the amorphous reactive phases found in MSWI BA aggregates [11, 148, 111].

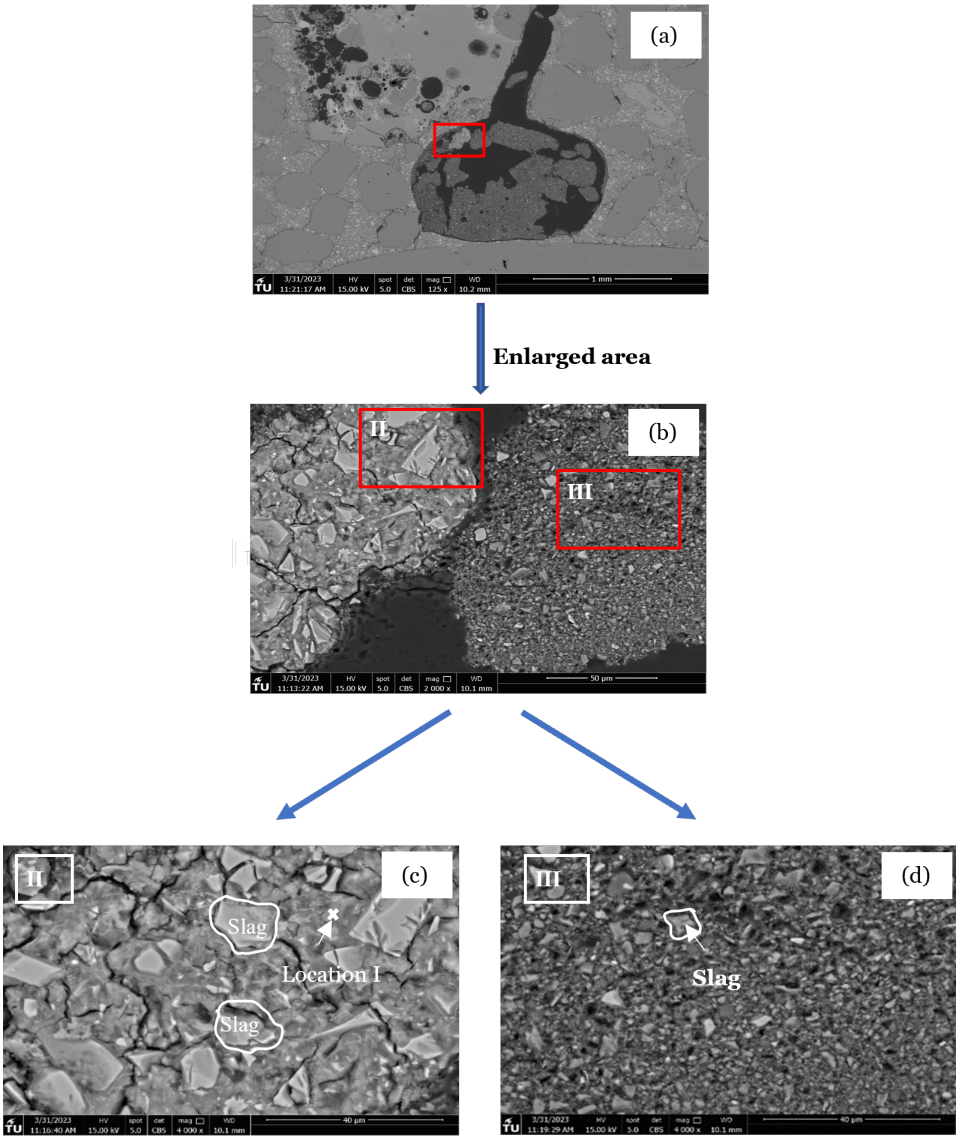

Figure 6.9: (a) Air void inside the concrete sample (b)enlarged section of the phases inside the air void (c)thick gel formations observed inside the air void (d)thin gel formations observed inside the air void

The concrete sample was observed to have air voids filled with gel formations, as shown in Figure 6.9(a). The gel formations were observed to be of broadly two types; a thick, dense formation and a thin porous formation, as shown in the enlarged sections (II) and (III) in Figure 6.9(c) and (d). The chemical composition of the enlarged images as shown in Figure 6.10 indicated the presence of unreacted slag particles in both the thin and thick gel formation, while the chemical composition of Location I represented gel phase (C-(A)-S-H gel). The composition of GGBFS is given in Appendix D

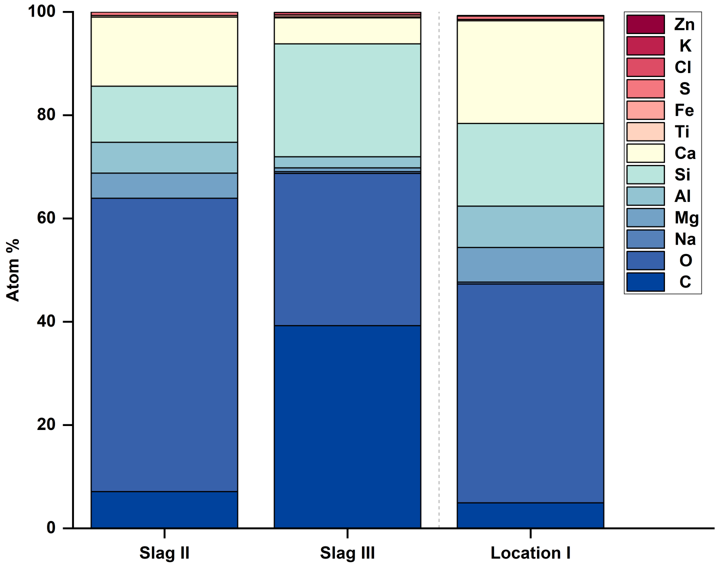

Figure 6.10: Chemical composition of the formations in the air voids inside the concrete sample

6.3.5. MSWI BA AGGREGATE BONDING

The bonding between the bottom ash aggregates and the matrix is investigated in this section. The finer fraction exhibited good bonding with the matrix, displaying a lack of cracks in the interfacial transition zone (ITZ), similar to the natural aggregates as depicted in Figure 6.11. However, the enlarged section of fine MSWI BA aggregates, as shown in Figure 6.11, was observed to have a less distinct boundary between the bulk paste matrix and ITZ compared to the natural aggregates. Additionally, the bulk matrix appeared to stretch to the aggregate boundary without a clear distinction between the matrix and the aggregates. The heterogeneity of MSWI BA aggregates, coupled with the presence of different reactive phases within them, can account for these observations.

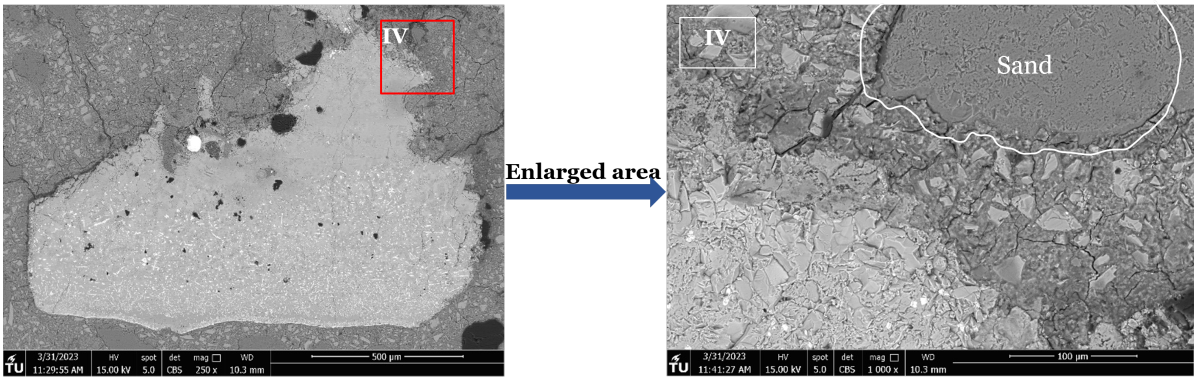

Figure 6.11: Aggregate-matrix bonding of the fine MSWI BA aggregates in the concrete sample

Conversely, the larger-sized MSWI BA aggregates demonstrate poor bonding with the matrix with minor cracks in the ITZ as indicated in Figure 6.12. This may be due to the loosely and physically held raw materials within the aggregate, irregular particle shape and porous structure and hinder the satisfactory bonding of the MSWI BA aggregates and the matrix[59, 148]. The poor MSWI BA aggregate-matrix bonding, in addition to the weaker physical properties of the aggregates and the higher air voids in the concrete, can account for the poor mechanical performance displayed by the 30BA-70NA-AAC-T20 test sample compared to the control samples.

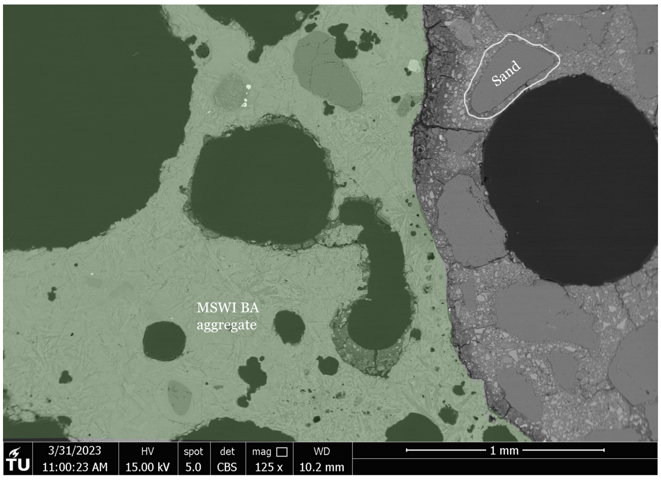

Figure 6.12: Aggregate-matrix bonding of coarse MSWI BA aggregates in the concrete sample

6.4. CONCLUSION

The microstructure formation of AAC containing MSWI BA aggregates was investigated in this chapter. The analysis focused on the porosity, cracking, morphology, and matrix-aggregate bonding of AAC with MSWI BA aggregates using X-ray-CT scans and scanning electron microscopy (SEM). The following key findings were observed:

- **Air void distribution and porosity:** The AAC utilising MSWI BA aggregates exhibited larger air voids and higher porosity compared to the control samples, which was attributed to the hydrogen gas release in the 30BA-70NA-AAC-T20 sample. Although, a good air void distribution was observed in the 30BA-70NA-AAC-T20 comparable to the 100NA-BCC sample that demonstrated the best performance among the concrete samples.

- **Effect of air voids on mechanical properties and durability**: The presence of larger-sized air voids compared to the control samples, possible cracking as a result of hydrogen gas release and the inherent porosity of the MSWI BA aggregates, resulted in the decreased mechanical performance and durability of the AAC containing MSWI BA aggregates.

- **Morphology of MSWI BA aggregates:** The MSWI BA aggregates exhibited an irregular shape, rough surface texture, and porous microstructure. Further, the presence of primary and secondary glass particles, along with various reaction products, were observed within the MSWI BA aggregates.

- **Bonding between MSWI BA aggregates and matrix:** The finer fraction of MSWI BA aggregates showed better bonding with the matrix compared to the larger-sized fraction. The heterogeneity of the MSWI BA aggregates and the reactive phases present in them contributed to the bonding characteristics.

In summary, the microstructure study revealed that the incorporation of MSWI BA aggregates in AAC resulted in larger air voids, increased porosity, reduced mechanical properties, and lower freeze-thaw resistance. The morphology of MSWI BA aggregates and the bonding between aggregates and the matrix were also influenced by the characteristics of the MSWI BA aggregates.

7

ENVIRONMENTAL IMPACT OF CONCRETE CONTAINING MSWI BA AGGREGATES

7.1. INTRODUCTION

Life cycle assessment (LCA) is a tool that is used to study the environmental impacts of a product or process during its entire life cycle [149]. It uses impact categories to capture the effect of the product or process on various aspects of the environment. Since the research aimed to replace ordinary Portland cement (OPC) concrete pavements with AAC containing MSWI BA aggregates, its environmental effects are quantified using LCA. Further, each impact category has an equivalent cost needed to reduce its harmful environmental effects. The cost of a product or process in each environmental category is termed shadow cost. In the Netherlands, the environmental cost indicator (ECI) or the total environmental cost of a product, needs to be calculated using the SBK method. The method specifies calculating the ECI of a product using 11 environmental impact categories that include the effect on global warming, abiotic resource depletion, ozone layer depletion, photochemical ozone creation, acidification, eutrophication, human toxicity, and ecotoxicity. In this chapter, the environmental effects of AAC containing MSWI BA aggregates are quantified and compared with OPC concrete and AAC systems from literature, having similar performance. The LCA analysis is conducted using SBK method and considers all the 11 impact categories. Additionally, the leaching of heavy metals from the AAC containing MSWI BA aggregates are evaluated to ensure that it is within the limits specified by the Soil Quality Decree [90].

7.2. METHODOLOGY

7.2.1. LIFE CYCLE ASSESSMENT

The LCA is conducted based on the method described in ISO 14040 [150]. The process involves four distinct phases as shown in Figure 7.1: the goal and scope of the study, life cycle inventory (LCI) formation and analysis, life cycle impact assessment (LCIA) and result interpretation. The data for the inventory analysis are acquired majorly from NIBE database [151]. The impact assessment is based on Dutch SBK method, which considers 11 impact categories for the LCA analysis as shown in Table 7.1. Additionally, the concrete mixtures used for comparison are taken from the literature.

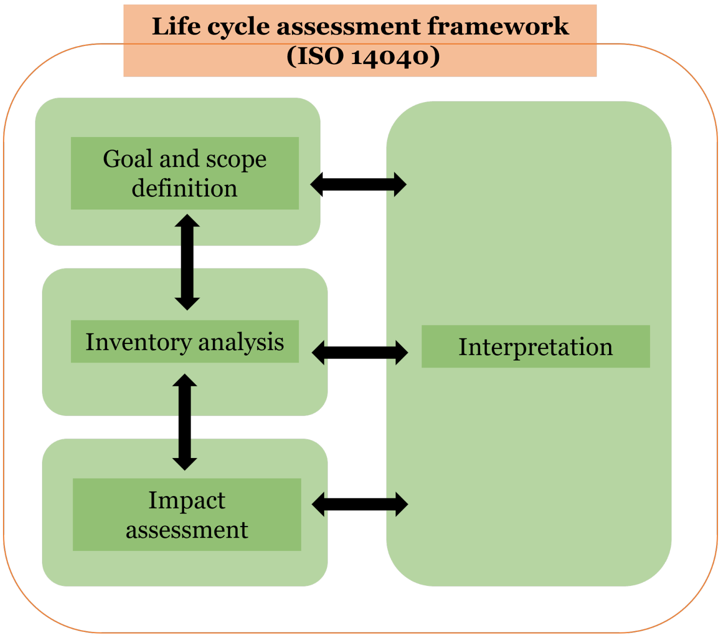

Figure 7.1: LCA framework as per ISO 14040 [150]

Table 7.1: Impact categories and their respective shadow cost

Environmental impact category	**Abbreviation**	**Unit**	**Shadow cost (€) per kg equivalents**
Global warming potential	GWP-100	kg CO2 equivalent	€ 0.05
Abiotic depletion non-fuel	ADP-non fuel	kg Sb equivalent	€ 0.16
Abiotic depletion fuel	ADP-fuel	kg Sb equivalent	€ 0.16
Ozone layer depletion	ODP	kg CFC-11 equivalent	€ 30.00
Photochemical oxidation	POCP	kg Ethene equivalent	€ 2.00
Acidification	AP	kg SO2 equivalent	€ 4.00
Eutrophication	EP	kg PO43- equivalent	€ 9.00
Human toxicity	HTP	kg 1,4-dichloro benzene equivalent	€ 0.09
Fresh water aquatic ecotoxicity	FAETP	kg 1,4-dichloro benzene equivalent	€ 0.03
Marine aquatic ecotoxicity	MAETP	kg 1,4-dichloro benzene equivalent	€ 0.00
Terrestrial ecotoxicity	TAETP	kg 1,4-dichloro benzene equivalent	€ 0.06

7.2.2. COLUMM LEACHING TEST

The leaching analysis, is conducted by column leaching test described in NEN 7375 (2004). The test was conducted on 28-day concrete sample of size 100 x 100 x 100 mm^3 which was crushed to a particle size of less than 4 mm before testing. This test measured the leaching as a function of the liquid-to-solid (L/S) ratio through the percolation of the MSWI BA. The cumulative emission at an L/S ratio of 10 L/kg was measured as a single cumulative eluate fraction. Leachate samples obtained from the leaching tests were chemically analysed using inductively coupled plasma atomic emission spectroscopy (ICP-AES). Ion chromatography (IC) was employed to analyse chloride (Cl), bromide (Br), and sulfate (SO_4), while fluoride was analysed using flow injection analysis with spectroscopic detection.

7.3. LCA GOAL AND SCOPE

- **Goal**
  The goals of the LCA analysis are the following:

  1. To compare the AAC containing MSWI BA aggregates with other concrete systems (AAC with gravel & conventional cement concrete).
  2. To assess the concrete components that have adverse environmental impacts and the environmental categories they affect.
  3. To quantify and compare the total shadow cost of the AAC containing MSWI BA aggregates with other concrete systems.

- **Functional unit definition**
  The definition of the functional unit used for the LCA study is an essential parameter in defining the scope. It defines the intended function of the product or process. Further, it allows for a meaningful comparison between different products and processes of equal performance [152]. The functional unit used in the study was,
  "1 m^3 of concrete (alkali-activated concrete & conventional cement concrete) that has equal 28-day compressive strength"

- **Scope**
  The scope of the LCA study is defined using system boundaries [153]. Every system (products and processes), as per NEN 15804 [154], is categorised into 4 stages: product stage, construction process stage, use stage and end-of-life stage. Raw material supply (A1), transportation (A2) and manufacturing (A3) are the processes involved in the product stage. Since the study compares concrete systems constituting various raw materials, the focus will be on the raw material supply(A1) in the product stage. Additionally, the concrete mixtures used in the LCA analysis are taken from the literature; thus, details on the transportation and manufacturing process are lacking.

7.4. LIFE CYCLE INVENTORY ANALYSIS

The materials used in the research are the constituents of concrete (AAC and conventional cement concrete). They consist of GGBFS, Portland cement (CEM I 42.5N), NaOH pellet, sodium hydroxide (50% wt% solid) solution, water glass solution (100% wt% solid), river sand, gravel and crushed limestone. The environmental impact data for GGBFS, and Portland cement are taken from the environmental product declaration (EPD) provided by the suppliers, Eco2cem Benelux B.V and ENCI, respectively. The data for NaOH pellets, sodium hydroxide solution, water glass solution, sand, gravel and limestone are taken from NIBE database [151]. MSWI BA aggregates used in the research are obtained from municipal solid waste; hence, they are considered free of environmental burden. Further, the NaOH solution utilised for the pre-treatment of MSWI BA aggregates was obtained from the activator for the AAC. This approach eliminated the need for additional NaOH consumption and incurred no additional costs for the treatment of the MSWI BA aggregates. Water is a natural resource; hence it has no negative environmental impact. Further, a few assumptions are made regarding the materials in the LCA analysis, and they are as follows,

1. All fractions of gravel are considered to have the same environmental impact.
2. The raw materials utilized in the mixtures from the literature are assumed to be sourced from the same suppliers as the raw materials used in the test sample concrete (30BA-70NA-AAC-T20).

7.5. LIFE CYCLE INVENTORY IMPACT ASSESSMENT

The Dutch SBK method is used to quantify the environmental impact and cost of 1 m^3 of concrete. The total environmental impact (F_{total}) is calculated as $F_{total} = \Sigma F_i M_i$, where F_i is the environmental impact multiplier, and M_i is the mass of each constituent that is needed to produce 1 m^3 of concrete. Similarly, the environmental cost indicator (ECI) is calculated by multiplying the mass of raw material in 1 m^3 of concrete with the shadow cost (ECI_i) of each indicator; $ECI = \Sigma ECI_i M_i$.

Table 7.3 shows the weight of the raw materials of different mixtures used to prepare 1 m^3 of concrete for the LCA analysis and mixture comparison. The proportion of the solid part of the NaOH solution and water glass solution of the concrete mixtures are used for ease of calculation as presented in Table 7.3. Water does not contribute to the environmental impact; hence it is not shown in the components of the concrete mixture.

Table 7.2: Literature's from which mixtures for the LCA analysis are obtained

Mixtures	**Literature**
30BA-70NA-AAC-T20	This research
AAC I	[155]
AAC II	[119]
AAC III	[119]
OPC I	[156]
OPC II	[157]

Table 7.3: Concrete mix design for LCA analysis

Mixture	Concrete system	GGBFS	CEM I 42.5N	NaOH pellet	Water glass [100 wt% solid]	Sand	Gravel	Crushed limestone	MSWI BA Aggregate
30BA-70NA-AAC-T20	AAC	314	-	12.57	12.57	751	956	-	151
AAC I	AAC	400	-	22.4	37.044	650	1208	-	-
AAC II	AAC	400	-	29.41	57.27	858	-	858	-
AAC III	AAC	400		16.92	68.82	858	-	858	-
OPC I	OPC-concrete	-	641	-	-	547	1013	-	-
OPC II	OPC-concrete	-	400	-	-	665	1107	-	-

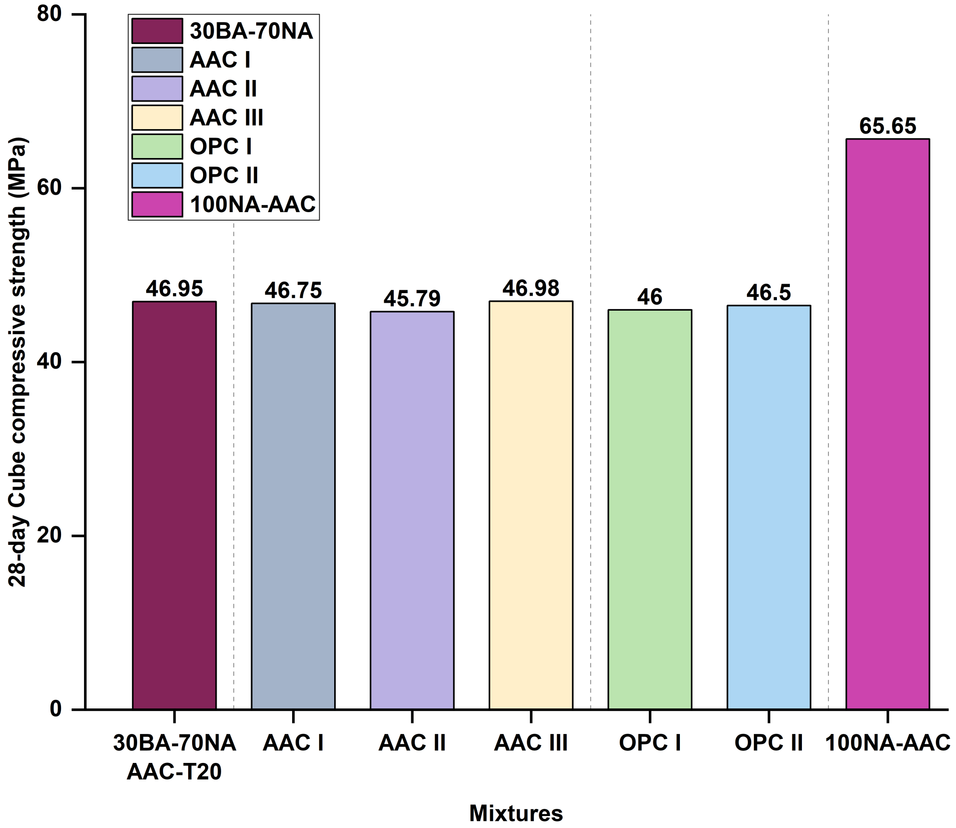

Figure 7.2: 28-day compressive strength of mixtures used for the LCA analysis

The LCA comparison can be conducted only if the concrete mixtures have similar performance. AAC containing MSWI BA aggregates showed 47 MPa 28-day compressive strength.

Hence, in this study, mixtures with similar 28-day compressive strength of about 47 MPa were chosen from the literature given in Table 7.2. Figure 7.2 shows the compressive strengths of the mixtures used for the comparison. Additionally, Figure 7.2 also shows the compressive strength of the 100NA-AAC control sample containing natural aggregates, which is only used for understanding the environmental impact of the mixtures designed in this research. This information is not used in the LCA analysis comparison owing to the difference in the strength of the control and test samples. Detailed calculations of the LCA analysis performed can be found in Appendix A and C.

7.6. RESULTS & INTERPRETATION

7.6.1. LCA ANALYSIS

Figure 7.5 illustrates the environmental impacts associated with various concrete mixtures having similar 28-day compressive strength. The environmental effects are primarily determined by the type and proportion of raw materials used in the concrete. Among the concrete systems, AAC (I, II and III) shows the highest impact in the environmental impact categories except for global warming (GWP-100), abiotic depletion-fuel (ADP-fuel), eutrophication (EP) and terrestrial ecotoxicity (TAETP) potential. Conversely, OPC concrete (I and II) demonstrates the highest impact in the category of GWP-100, ADP-fuel, EP and TAETP.

The sodium hydroxide solution and sodium silicate solution used in the AAC activator is the major contributor to the environmental categories while cement is the largest contributor to these categories in the OPC concrete. Cement concrete mixtures have the largest contribution to the global warming potential, primarily related to the carbon dioxide emissions during cement production. In comparison, AAC mixtures, which lack cement binder, exhibit a favourable effect on the global warming potential. However, the addition of alkalis in AAC mixtures introduces negative effects on the environment which is reflected in other environmental categories.

Aggregates used in the concrete mixtures have minimal effect on the environment compared to other components of the concrete since it is a natural resource. Their negative impact on the environment is associated with the mining from the quarries and this effect is more pronounced in the photochemical oxidation (POCP), acidification (AP), and eutrophication potential (EP). Among the natural aggregates used in the analysis, gravel has the least environmental impact, although this trend may depend on the source from which the gravel is obtained.

Among the cement concrete mixtures, OPC I exhibits the highest negative impact on the environment, while among the AAC mixtures, AAC II has the highest impact. The detrimental effects of OPC I can be attributed to its higher cement content in the concrete, while for AAC II, the presence of a larger proportion of alkalis contributed to the negative impact. AAC mixture containing MSWI BA aggregates (30BA-70NA-AAC) demonstrates superior performance across the 11 impact categories compared to other mixtures in the LCA analysis. This may be due to the limited use of alkalis and precursors in the mixture and the absence of environmental burdens associated with the use of MSWI BA aggregates.

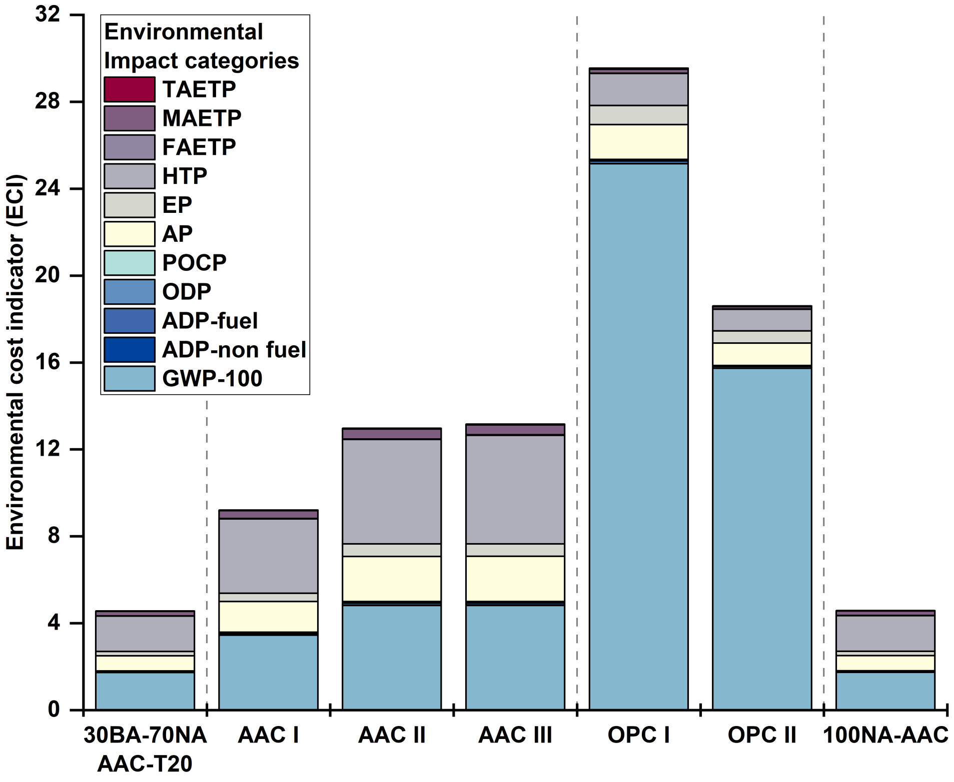

Figure 7.3: Contribution of the environmental impact indicators to the total ECI value

Table 7.4: ECI for each concrete mix

Mixture	ECI (€)
30BA-70NA-AAC-T20	€ 4.56
100NA-AAC	€ 4.58
AAC I	€ 9.21
AAC II	€ 12.97
AAC III	€ 13.15
OPC I	€ 29.55
OPC II	€ 18.61

Each impact indicator has a specific shadow cost, representing the monetary amount required to mitigate its negative environmental effects. The overall effect of the concrete mixtures can be studied by considering their total ECI (Environmental Cost Indicator) values. Figure 7.3 displays the contribution of each impact indicator to the ECI values of the concrete mixtures, and Table 7.3 presents the ECI values (in €) for the concrete mixtures. It was observed that the global warming potential has the greatest impact on the mixtures followed by the acidification potential. The effect of these indicators is more pronounced in cement concrete mixtures. OPC I, with the largest cement content, has the highest ECI value of €29.55. The 30BA-70NA-AAC-T20 indicated the lowest ECI value of €4.56, which can be attributed to the reduced alkali content and higher utilisation of aggregates, specifically MSWI BA aggregates in the concrete. The increased cost of other AAC mixtures (AAC I, AAC II and AAC III) compared to the MSWI BA sample is primarily due to the higher proportion of alkalis (NaOH and Na_2SiO_3).

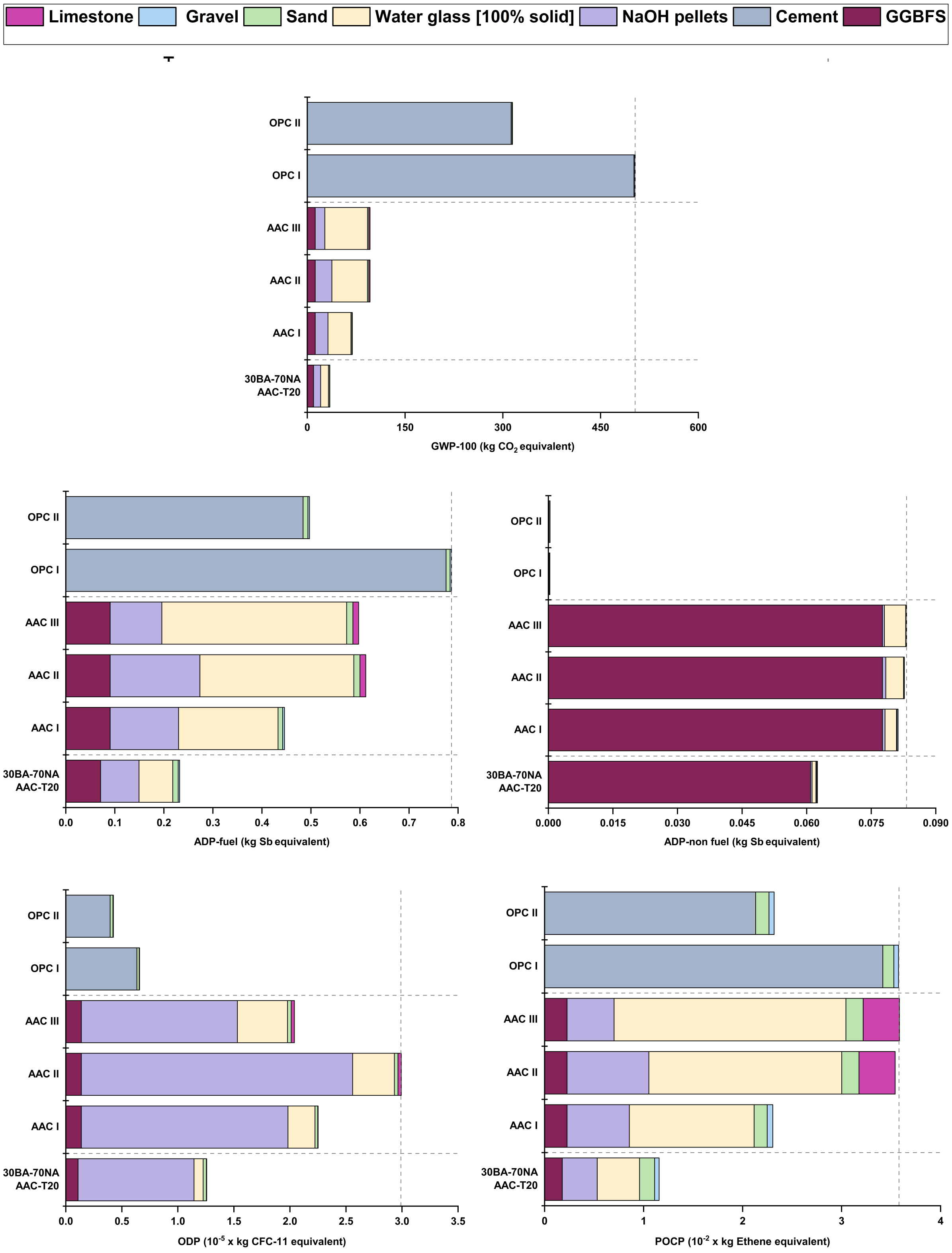
Limestone
Gravel
Sand
Water glass [100% solid]
NaOH pellets
Cement
GGBFS
OPC II
OPC I
AAC III
AAC II
AAC I
30BA-70NA AAC-T20
0
150
300
450
600
GWP-100 (kg CO_2 equivalent)
0.0
0.1
0.2
0.3
0.4
0.5
0.6
0.7
0.8
ADP-fuel (kg Sb equivalent)
0.000
0.015
0.030
0.045
0.060
0.075
0.090
ADP-non fuel (kg Sb equivalent)
0.0
0.5
1.0
1.5
2.0
2.5
3.0
3.5
ODP (10^{-5} x kg CFC-11 equivalent)
0
1
2
3
4
POCP (10^{-2} x kg Ethene equivalent)

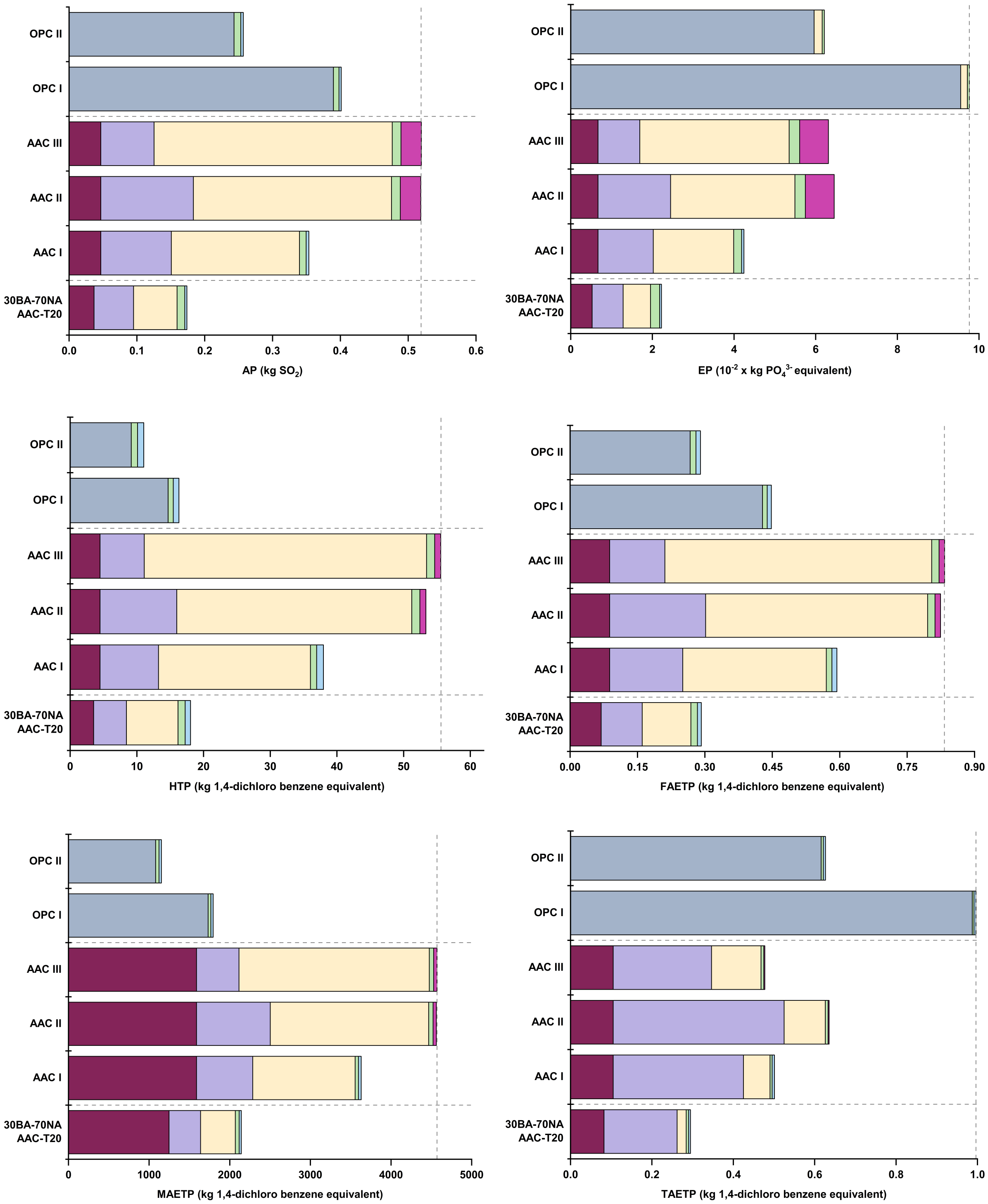

Figure 7.5: Effect of concrete mixtures on the environmental impact indicators

7.6.2. LEACHING OF HEAVY METALS

The heavy metal leaching from the MSWI BA aggregates utilised in AAC were quantified according to NEN 7375 (2004) [158] as indicated in Table 7.5. The outcomes of the leaching test demonstrated that the AAC incorporating MSWI BA aggregates successfully met the criteria outlined in the Soil Quality Decree [90] for open application. The incorporation of a combination of dry and wet separation techniques, along with the additional alkaline pretreatment process, can effectively minimise the release of heavy metals, thus resulting in the reduced release of heavy metals and ions. Furthermore, the test results suggested that any surplus of heavy metal in the MSWI BA aggregates can be contained within the alkali-activated concrete, thus enabling the application of MSWI BA aggregates in pavements.

Table 7.5: Total element emission from AAC containing MSWI BA aggregates obtained with column test

Element	**MSWI BA (4-11 mm)**	**Limit granular material**	**Unit**
Number of samples	1	N/A	
pH	10.3	N/A	
EC	2100	N/A	
Antimony	0.11	0.16	mg/kg db
Arsenic	0.5	0.9	mg/kg db
Barium	<0.1	22	mg/kg db
Cadmium	<0.007	0.04	mg/kg db
Chrome	<0.05	0.63	mg/kg db
Cobalt	<0.05	0.54	mg/kg db
Copper	<0.05	0.9	mg/kg db
Lead	<0.01	2.3	mg/kg db
Mercury	0.0023	0.02	mg/kg db
Molybdenum	0.22	1	mg/kg db
Nickel	<0.01	0.44	mg/kg db
Selenium	0.11	0.15	mg/kg db
Tin	0.03	0.4	mg/kg db
Vanadium	0.47	1.8	mg/kg db
Zinc	<0.2	4.5	mg/kg db
Fluoride	5.5	18	mg/kg db
Bromide	<0.8	20	mg/kg db
Chloride	69	616	mg/kg db
Sulphate	450	2430	mg/kg db

7.7. CONCLUSION

The study aimed to assess and compare the environmental impact of AAC containing MSWI BA aggregates with OPC concrete and other AAC systems from the literature, considering similar performance criteria. The life cycle assessment (LCA) methodology, employing the Dutch SBK method and encompassing 11 impact categories, was utilized for this purpose. The LCA results indicated that the 30BA-70NA-AAC-T20 sample, incorporating MSWI BA aggregates, exhibited favourable environmental performance compared to other concrete systems in the literature. This can be mainly attributed to the lower alkali content and higher aggregate proportion in the mixture.

The analysis revealed that cement concrete mixtures significantly contributed to the global warming potential, while AAC mixtures demonstrated improved performance in this category due to the absence of cement binder. However, the introduction of alkalis in AAC mixtures had a negative impact on other environmental categories

To quantify the environmental effects of each concrete mixture, the environmental cost indicator (ECI) was utilized, representing the monetary amount required to negate the environmental impacts. The findings highlighted that global warming potential had the most significant influence on the overall impact, particularly in cement concrete systems. Among the examined mixtures, OPC I, characterized by a larger cement proportion, exhibited the highest ECI value. Conversely, the 30BA-70NA-AAC-T20 sample displayed the lowest ECI value due to its reduced alkali content and the incorporation of alternative aggregates instead of natural aggregates. Additionally, the leaching of heavy metals from the AAC containing MSWI BA aggregates satisfies the requirement for open application criteria according to the Soil Quality Decree [90].

In conclusion, the study provides insights into the environmental performance and cost implications of AAC containing MSWI BA aggregates. These findings support the potential adoption of this sustainable material in construction practices, specifically for pavements, considering its favourable environmental attributes and cost.

8

DISCUSSION, CONCLUSION AND RECOMMENDATIONS

8.1. DISCUSSION

8.1.1. RESULT OVERVIEW

The main findings of the research are summarised and discussed in this section, together with the limitations. Table 8.1 gives the main findings of this research.

Table 8.1: Summary of results

MSWI BA aggregate characteristics	
Particle size distribution	The particle size distribution for the MSWI BA aggregates marginally deviated from the norm-specified range for 4-8 mm aggregates. Regardless, these deviations were less than 5% from the required percentages of aggregate that should pass through each sieve.
Water absorption	MSWI BA aggregates indicated a very high water absorption of 7% due to their inherent porosity.
Apparent density	The density of the MSWI BA aggregates was observed to be lower than that of the natural aggregates.
Loose bulk density	The loose bulk density of MSWI BA aggregates indicated a lower value compared to the natural aggregates.

Los Angeles (LA) coefficient	The LA coefficient of the MSWI BA aggregates was observed to be higher (LA 35) than that of 4-8 mm natural aggregates (LA 20), which it aimed to replace in the concrete. However, the LA coefficient was close to the norm preferred value of LA 30, indicating that the MSWI BA aggregated can still be used in pavements.
Pre-treated MSWI BA aggregates	
Metallic Al quantification	The metallic Aluminium present in untreated MSWI BA aggregate was approximately 2%, which was reduced to 0.53% after pre-treatment. This is less than the norm specified 1% for the application in concrete pavements.
AAC containing MSWI BA aggregates	
Mechanical properties	
Compressive strength	AAC utilising MSWI BA aggregates showed a consistent reduction in the 3-day, 7-day and 28-day compressive strength compared to the control AAC and BCC. Despite the aggregates being fundamentally porous compared to the natural aggregates, the 28-day compressive strength of 30BA-70NA-AAC-T20 showed 70% strength of the control samples. The delayed setting of the concrete with the introduction of the MSWI BA aggregates was solved with thermal curing at 40°C for 24 hrs. The thermally cured BA sample 30BA-70NA-AAC-T40 gave 50% of the strength of the test sample. Both samples exceeded the norm-specified requirement for 28-day compressive strength.
Splitting tensile strength	AAC concrete containing MSWI BA aggregate showed lower performance in comparison to the control samples. However, the test sample 30BA-70NA-AAC-T20 satisfied the norm requirement, while 30BA-70NA-AAC-T40 did not satisfy the norm requirement.
Flexural strength	The flexural strength of the AAC test samples containing MSWI BA aggregates indicated lower values than the control samples. However, the 30BA-70NA-AAC-T20 sample showed comparable results to the AAC control sample.
Durability	
Freeze-thaw resistance	The freeze-thaw resistance of the test concrete containing MSWI BA aggregates showed poor performance when subjected to freeze-thaw cycles, with higher damage to the 30BA-70NA-AAC-T40 sample. The AAC control mix also exhibited poor freeze-thaw resistance. All the samples (control and test) deviated from the maximum value stipulated by the norm.

Microstructure study	
Micro-CT	The porosity of the concrete sample investigated through micro-CT showed that the 30BA-70NA-AAC-T20 had higher porosity compared to the control samples. However, the air void size distribution of 30BA-70NA-AAC-T20 was comparable to that of the BCC control sample, which showed the best mechanical properties and freeze-thaw resistance.
SEM-EDX	The morphology, aggregate-matrix bonding and gel formations were observed using SEM-EDX. Various reactive phases and pores were observed in the MSWI BA aggregate. The bonding between the finer particle of MSWI BA aggregate and the matrix showed better bonding compared to the coarser particles. Further, thick and thin gel formations were observed inside the concrete sample. The study also showed that the air voids inside the concrete sample indicated the presence of reaction products.
LCA analysis	The environmental impact of the AAC containing MSWI BA aggregate was observed to be much better compared to OPC concrete and AAC mixtures of similar 28-day compressive strength obtained from the literature. Further, the ECI value of the 30BA-70NA-AAC-T20 mix indicated lower costs to negate the harmful impacts of the concrete.
Leaching of heavy metals	The leaching of heavy metals was well below the norm-specified limits indicating the potential of the MSWI BA aggregates to replace natural coarse aggregates in AAC.

The AAC containing MSWI BA aggregates showed promising results that indicate the possibility of its application in pavements. Table 8.2 summarises the pavement norm requirements that need to be satisfied by the concrete. The table shows green for the properties that satisfy the requirements and red for the conditions that are not met. It indicated that the test sample with MSWI BA aggregates, 30BA-70NA-AAC-T20, has satisfied all the norm requirements except for the condition on the resistance to freeze-thaw cycles. It was observed that the environmental impact of the 30BA-70NA-AAC-T20 was much lower compared to the mixtures from the literature. Additionally, the test sample also showed much lower environmental cost, indicating a sustainable alternative to the cement concrete pavements with natural aggregates.

Table 8.2: Properties of AAC containing MSWI BA aggregates compared to pavement norm requirements

Property	**Observed value**	**Required value**	**Requirement check**
Compressive strength	46 MPa	37 MPa	🟩
Splitting tensile strength	3.76 MPa	3.6 MPa	🟩
Flexural strength	4.61 MPa		🟩
Freeze-thaw resistance	5.23 kg/m^2	1 kg/m^2	🟥
ECI value	€ 4.56		🟩

8.1.2. LIMITATIONS OF THE RESEARCH

The limitations of the research are the following:

- The pre-treatment of MSWI BA aggregates used a nominal amount of NaOH solution. This prevented the utilisation of higher proportion of MSWI BA aggregates in concrete.

- The flexural strength test was conducted by notching the sample. However, the test is highly sensitive to many factors, including the notch properties and loading rate, which can result in anomalies and variations in the results.

- The sand used in the preparation of the mix was obtained by drying. The presence of moisture can influence the water content in the final mix.

- The MSWI BA aggregates obtained from the industry were in the size range of 4-11 mm. Since the project aimed to replace the 4-8 mm gravel fraction, the particle size distribution of the aggregates had slight deviations from the norm specifications. In this research, the nominal deviations were neglected; however, sieving and producing aggregates that meet the requirements allows for better performance.

- Within the scope of the research, no air-entraining admixtures were utilised. The freeze-thaw resistance of the samples showed high deterioration, including the blended cement concrete sample. Introducing air-entraining admixtures can allow better freeze-thaw performance.

- Life cycle analysis considered the raw material acquisition phase for the production of the concrete samples. Considering the full cycle of the AAC containing MSWI BA aggregates allows for a better comparison with the OPC concrete samples.

- In the LCA analysis, the comparison was made with similar performance mixtures from the literature. The mixtures used a higher proportion of alkali that has the maximum contribution to the environmental impact of AAC. Thus, comparing the control specimen used in the research with the test sample would allow a better understanding of the influence of MSWI BA aggregates in the concrete. To achieve this, the aggregate proportion in the control samples can be varied to obtain similar performance compared to the test samples.

8.1.3. DISCUSSION OF RESULTS

The results obtained in the research indicated the possibility of applying MSWI BA aggregates in AAC, as summarized in Section 8.1.1. Further, the comparison of the results with the pavement requirements further substantiates the potential of the MSWI BA aggregates in concrete for pavement application. Currently, the utilisation of MSWI BA aggregates is mostly limited to OPC concrete and blended concrete systems due to the higher reactivity of the metallic Al in the MSWI BA aggregate with the alkali in the AAC. However, the physical characteristics of the aggregates and the mechanical and durability properties of the AAC containing MSWI BA aggregates can be compared with the results from the literature to observe the difference in the addition of the MSWI BA aggregates in the two different concrete systems (OPC or BCC and AAC).

Characteristics of MSWI BA aggregates compared with the results obtained from literature

The MSWI BA aggregates were observed to have higher water absorption, lower density and lower abrasion resistance compared to natural aggregates. This indicated the porous nature of the MSWI BA aggregates, thus making them weaker compared to the dense natural aggregates. Similar trends were observed by other researchers. However, the reported physical properties of the MSWI BA aggregates in the literature highly varied. This can be attributed to the heterogeneous nature of the MSWI BA aggregates influenced by factors such as the type of waste material, the production process and the post-production treatment process of the aggregates. To obtain a more reliable comparison with existing literature, the aggregates sourced from the same country can be utilised for the comparison. The obtained results on the physical properties of these aggregates align with findings from the study conducted by Keulen et al. (2016) [67] using MSWI BA aggregates from the Netherlands. Despite the relatively lower physical properties of MSWI BA aggregates compared to natural aggregates, the performance of concrete incorporating these aggregates has shown promising results in the literature when partially replacing natural aggregates. Forteza et al. (2004) [68] reported that incorporating MSWI BA aggregates with natural aggregates can improve particle size distribution, abrasion resistance, and overall concrete performance. Building upon these findings, this research aimed to replace natural aggregates with MSWI BA aggregates in alkali-activated concrete.

Metallic aluminium quantification in MSWI BA aggregates

The presence of metallic aluminium (Al) poses a significant challenge when incorporating MSWI BA aggregates into concrete. These aggregates contain approximately 2% metallic Al by weight, which can lead to expansion and swelling when utilised in AAC. To mitigate the adverse effects on AAC performance, pre-treatment of MSWI BA aggregates is necessary. In this study, alkaline pre-treatment using NaOH was employed. NaOH is commonly chosen due to its effectiveness, cost-efficiency, and easy availability. The pre-treatment involved immersing the aggregates in a 1 M NaOH solution for a duration of 14 days to reduce the metallic Al content.

Previous literature reports variations in the proportion of metallic Al present in MSWI BA aggregates. This can be attributed to the inherent heterogeneity of the MSWI BA aggregates. Xuan and Poon (2018) [82] utilised 1 M NaOH solution with a liquid-to-solid (L/S) ratio of 10 for a duration of 3 hours and achieved 90% removal of metallic Al from the MSWI BA aggregates. Additionally, Pera et al. (1997) [102] observed that immersing MSWI BA aggregates in a NaOH solution for 15 days completely eliminated the metallic Al content. Considering that the NaOH used in this research was obtained from the AAC activator, a high L/S ratio was not preferred, and a concentration of 1 M was employed for pre-treatment. Therefore, a duration of 14 days was chosen in this study, following the findings of Pera et al. (1997) [102] to address the reduced reactivity caused by a lower L/S ratio.

Optimum replacement level chosen in this research compared to the optimum levels chosen in the literature

The effectiveness of the pre-treatment in removing metallic Al in MSWI BA aggregates and the compressive strength of the AAC containing pre-treated MSWI BA aggregates is assessed to determine the optimum replacement level of MSWI BA aggregates in AAC. The results reveal that, for a fixed concentration of 1 M NaOH solution, lower quantities of MSWI BA aggregates result in reduced metallic aluminium content. Additionally, a pre-treatment duration of 14 days demonstrates higher removal of metallic aluminium compared to 7-day duration. When the aggregates are incorporated into AAC, the compressive strength was found to be higher for a 30% replacement of gravel with MSWI BA aggregates compared to 50% and 75% replacement levels. The inherent porosity of the MSWI BA aggregates can also contribute to the reduced strength of AAC. Thus, in this research, 30% replacement of gravel with MSWI BA aggregates was chosen as the optimum replacement level. Other studies have also investigated the replacement levels of natural aggregates with MSWI BA aggregates. Khatib et al. (2021) [159] reported an optimum replacement level of natural aggregates with MSWI BA aggregates of 20%, beyond which a reduction in strength was observed. Yan et al. (2020) [87] replaced natural aggregates (fine and coarse) up to 30% satisfying the requirements for road base layer application. It was also observed that higher replacement levels were introduced by researchers owing to the lower metallic Al in the aggregates and the Portland cement concrete systems into which the MSWI BA aggregates are introduced.

Evaluation of the mechanical properties of the AAC containing MSWI BA aggregates

The investigation of the mechanical properties of the AAC concrete containing MSWI BA aggregates was conducted following aggregate characterisation, pre-treatment and selection of optimum replacement level. It was observed that the compressive strength of AAC decreased with the increasing replacement of natural aggregates with MSWI BA aggregates. This reduction in compressive strength can primarily be attributed to the lower density of MSWI BA aggregates compared to natural aggregates. The splitting tensile strength and flexural strength of the AAC also exhibited a decrease when MSWI BA aggregates were used as a substitute for gravel. This observation aligned with the result reported by (Zhang & Zhao (2014) [76] who noticed a reduction in the early age strength of concrete with increasing replacement. Similar trend in the reduction of the mechanical properties with higher

MSWI BA replacement was reported by Yan et al. (2020) [87].

This research further investigated the effect of thermal curing of the AAC containing MSWI BA aggregates on the mechanical properties of concrete. The utilization of MSWI BA aggregates was observed to introduce delayed setting in AAC concrete, which was resolved by increasing the reactivity of GGBFS by elevated temperature (40°C) curing for 24 hours. Conversely, higher temperature curing (above 40°C) can increase the reactivity of the remaining metallic Al in the MSWI BA aggregates while the concrete is hardening. Mary Joseph et al. (2020) [56] observed the increase in the reactivity of metallic Al with alkalis at 80°C. However, in this research, even at a temperature of 40°C curing, increased cracking and subsequent loss in mechanical performance was observed when compared to the AAC containing MSWI BA aggregates cured at ambient temperature (20°C)

Moreover, the remaining metallic Al in the MSWI BA aggregates can react with the alkali in the AAC to release hydrogen gas and subsequent formation of air voids. The investigation of porosity and air void distribution in the concrete provides insights into the presence of air voids resulting from hydrogen gas release. Further, higher porosity was observed in the AAC sample containing MSWI BA aggregates compared to AAC sample with natural aggregates. Additionally, the air void distribution indicated the presence of large air voids compared to AAC concrete containing natural aggregates. These large air voids and higher porosity can adversely affect the mechanical performance of the concrete, which aligns with the research findings indicating lower mechanical properties for AAC containing MSWI BA aggregates.

Evaluation of the durability of AAC containing MSWI BA aggregates
Freeze-thaw resistance of the concrete is the long-term performance investigated in the research. Generally, it was observed that the freeze-thaw resistance of AAC containing MSWI BA aggregates was lower compared to AAC containing natural aggregates. The deterioration of the concrete can be attributed to the presence of saturated MSWI BA aggregates, which can lead to spalling and aggregate failure due to expansion during freezing. Zhu et al.(2017) [126] reported a reduction in freeze-thaw resistance with increasing saturation degree of aggregates. Most researchers introduced MSWI BA aggregates that were not saturated, resulting in higher freeze-thaw resistance compared to the results obtained in this research. However, it was consistently reported that the resistance of concrete containing MSWI BA aggregates was lower than that of concrete containing natural aggregates. This is supported by the findings of Yan et al. (2020) [87], who demonstrated a decrease in freeze-thaw resistance compared to natural aggregates due to the higher water absorption of MSWI BA aggregates and subsequent expansion during freezing. The thermally cured AAC concrete containing MSWI BA aggregates showed lower freeze-thaw resistance compared to the ambient cured AAC sample containing MSWI BA aggregates. Higher cracking in the thermally cured MSWI BA concrete sample allows freezable water to penetrate the concrete, which can lead to expansion and subsequent deterioration of concrete.

The air voids and larger pores inside the aggregates having size lower than 1 mm can support the resistance of the concrete to freeze-thaw. However, since the aggregates used in the concrete were saturated, higher material loss was observed due to aggregate expansion and spalling of concrete during freezing. Additionally, the distribution of pores within the AAC containing MSWI BA aggregates was observed to be favourable for resisting freeze-thaw cycles. Despite the better distribution of air voids, the larger size of air voids within the concrete can have a negative impact on its resistance to freeze-thaw cycles, as indicated by the higher material loss. Therefore, the combined effect of saturated aggregates, cracking, and larger air voids contributes to the deterioration of the concrete. To provide a comprehensive analysis of the effect of air voids on the freeze-thaw resistance of concrete, further exploration of the air void spacing can be considered.

Environmental impact of AAC containing MSWI BA aggregates
To study the environmental impact of the AAC containing MSWI BA aggregates, LCA analysis were conducted. The results indicated a lower environmental impact of the AAC utilising MSWI BA aggregates compared to the similar performing mixtures obtained from the literature for this analysis. The reduced levels of alkali and the use of environmentally burden-free aggregates allowed for the better environmental impact. However, the effect of reduced alkali activator content was observed to have a prominent effect on the environment compared to the introduction of MSWI BA aggregates. The alkali activator and precursor content in the mixtures from the literature was higher compared to the AAC mixture used in this research. This contributed to the negative impact of the mixtures and similar observation was made by Bianco et al. (2021). This study focused on the LCA analysis in the raw material supply phase in the product stage. However, a full life cycle analysis can be conducted to obtain a comprehensive understanding of the addition of MSWI BA aggregates in AAC. Additionally, the MSWI BA aggregates utilised in the AAC had heavy metals present inside, which can contaminate the surrounding soil and water when introduced in the pavements. The study determined that the heavy metal content leaching is well below the limits specified in the Standard (Soil Quality Decree), thus enabling the utilisation of MSWI BA aggregates for pavement applications.

8.2. CONCLUSION

The research aimed to develop AAC mixture utilising MSWI BA aggregates for application in road pavements in the Netherlands. The research questions were formulated to achieve this objective and their conclusions are as follows:

1. **To find the optimum replacement level of natural gravel with bottom ash aggregates in AAC with a minimum compressive strength of C30/37 after 28 days**
    - *To find a suitable pre-treatment procedure for removing metallic Aluminium in the MSWI BA aggregates*
      Metallic Al in the MSWI BA aggregates must be removed to prevent AAC concrete cracking when introduced into it. To achieve this, alkaline pre-treatment using NaOH solution was used, which was obtained from the AAC activator solution. This allows the entire process to be sustainable since using additional NaOH negatively impacts the environment. Further, the pre-treatment utilised a readily available material, thus allowing a cost-effective solution to remove metallic Al. The final developed sample satisfied nearly all the requirements stated by the norm, thus indicating that the pre-treatment is effective.

- *To study the effect of replacement levels of treated MSWI BA aggregates on the strength of AAC*
  The pre-treated MSWI BA aimed to replace gravel at 30%, 50% and 75% replacement levels. Since, the NaOH solution was obtained from the activator solution, a maximum concentration of 1 M was utilised in this study. The compressive strength test after 7-days and 28-days indicated loss in performance with increasing replacement of natural aggregates with MSWI BA aggregates. This suggested that the pre-treatment was not very effective at higher replacement levels. The NaOH pre-treatment solution was able to only wet the surface of the MSWI BA aggregates at higher replacements. Additionally, the concentration of 1 M is not reactive enough to remove the metallic Al by merely wetting the surface. However, the pre-treatment was observed to be effective at lower replacement levels. At 30% replacement, the aggregates were fully immersed in the solution, which can explain the higher performance compared to 50% and 75% replacement levels.

2. **To investigate the mechanical properties (Compressive strength, splitting tensile strength and Flexural strength) and durability (Freeze-thaw resistance) of AAC after introducing MSWI BA aggregates. Further, evaluate the results against the norm requirements**
   AAC containing MSWI BA aggregates exhibited good mechanical performance that satisfied the requirement mentioned in the standard. However, the sample showed poor freeze-thaw resistance, which can be attributed to the combined effects of the absence of air-entraining admixtures, saturation of aggregates and the release of hydrogen gas inside the concrete.

3. **To investigate the porosity and features of the concrete after introducing MSWI BA aggregates**
   Microstructure analysis were conducted to explain the mechanical performance and durability exhibited by the concrete. The porosity of the MSWI BA aggregates was observed to be higher, which explains the loss in mechanical performance. Regardless, an even air void distribution was observed compared to the control AAC sample. The SEM analysis indicated reactive phases inside the MSWI BA aggregates, various gel formations in the AAC concrete sample containing these aggregates and good aggregate-matrix bonding in the finer fraction compared to the coarser MSWI BA fraction.

4. **To analyse the environmental impacts of using the AAC concrete containing MSWI BA aggregates**
   The AAC containing MSWI BA aggregates showed better environmental effects compared to mixtures of similar 28-day compressive strength from literature. The ECI value also highlighted a lower environmental cost which was attributed to the use of a nominal amount of activator solution and precursor content in AAC. Further, the leaching of heavy metals from the AAC containing MSWI BA aggregates was within limits specified in the Soil Quality Decree. Thus, the AAC containing MSWI BA aggregates used in this research allows for a sustainable alternative to the conventional concrete used in pavements.

8.3. RECOMMENDATIONS

8.3.1. FUTURE RESEARCH

- **Mix Design**
  The study used a nominal amount of activator solution to achieve the norm requirements. This research focused on the performance of the concrete containing MSWI BA aggregates. The study on the mix design influence factors, including activator solution moduli and different types of precursors, further allows to optimise the mixture based on the application.

- **Delayed setting of AAC containing MSWI BA aggregates**
  The introduction of MSWI BA aggregates in AAC was observed to have delayed setting and subsequently the concrete did not harden after 24 hours. In this research, thermal curing at 40°C was adopted to solve the delayed setting and hardening of concrete. Another alternative would be to use admixtures to accelerate the setting. The influence of the admixtures on the performance of the AAC containing MSWI BA aggregates can be explored.

- **Presence of metallic Al**
  The alkaline pre-treatment used in the research reduced the metallic Al below the norm requirements for pavements. However, the presence of metallic Al is much more stringent for applications in building construction. The metallic Al must be completely removed to expand the possibility of applying AAC-containing MSWI BA aggregates in other applications. The effect of using higher NaOH concentrations and its effectiveness in removing metallic Al is recommended.

- **Freeze-thaw resistance**
  Air-entraining admixtures improve the performance of concrete against freeze-thaw cycles, which was beyond the scope of this research. The effect of the addition of air-entraining admixtures on the freeze-thaw resistance of the concrete containing MSWI BA aggregate is an area to investigate.

- **LCA analysis**
  The LCA conducted in this thesis mainly focused on the environmental effects of the raw materials used for the preparation of the concrete. A full life cycle analysis from cradle to cradle can give extensive information on the effect of the addition and the stages in the LCA that needs attention.

- **Fatigue resistance of concrete**
  Pavement concrete finds extensive application in various structures, including airfield runways, road surfaces and bridge decks. These structures experience repetitive cyclic loads throughout their service lives due to vehicle traffic. Fatigue cracking is recognized as a significant structural distress and a primary mode of failure in concrete pavements that occurs when the concrete structure fails to sustain the designed load after being subjected to a large number of stress cycles. This leads to the initiation and propagation of cracks and subsequent failure. Consequently, the investigation of fatigue failure represents a crucial parameter in the up-scaling process of AAC concrete incorporating MSWI BA aggregates.

- **Cracking of concrete**
  The occurrence of cracking in pavements represents a significant area of concern for pavement usage and maintenance. These cracks, both micro and macro in nature, can lead to a loss of serviceability and dangerous driving conditions. This phenomenon primarily stems from the brittle behaviour of cement concrete, coupled with its low resistance to fatigue and limited toughness. As AAC containing MSWI BA aggregates exhibits a certain degree of cracking due to the release of hydrogen gas within the concrete, a comprehensive investigation of the concrete cracking becomes imperative. High-resolution micro-CT scanning can be employed to observe the formation of cracks within the concrete. Further, the analysis should also focus on the deterioration of these cracks and the potential development of new cracks. These evaluations are crucial prerequisites before utilising the concrete for pavement applications.

- **Polishing stone value of MSWI BA aggregates**
  Skid resistance is a critical factor that pertains to the frictional interaction between tires and the surface of a pavement. It is primarily influenced by the surface texture and the composition of materials utilised. The degradation of road surfaces caused by traffic and environmental conditions can lead to a reduction in skid resistance, thereby compromising the safety of road users. Currently, the long-term skid resistance is evaluated by assessing the polishing resistance of coarse aggregates, a parameter that can be quantified through standardized laboratory tests. Considering the intended application of MSWI BA aggregates in pavement blocks, it is essential to investigate the polishing stone value of these aggregates to assess their ability to maintain adequate skid resistance.

8.3.2. PAVEMENT APPLICATION: UPSCALING

Previously, MSWI BA aggregates were utilized as unbound granular material in the lower layers of road pavements. However, the potential leaching of heavy metals into the surrounding soil posed environmental concerns, discouraging their use as unbound aggregates. Consequently, this research aimed to investigate the feasibility of employing MSWI BA aggregates for the surface layer of road pavements. Promising results were obtained from this research, thus indicating the potential of applying AAC containing MSWI BA aggregates in pavements. However, further tests need to be conducted to fully realise the suitability of incorporating concrete utilising MSWI BA aggregates in pavement structures. The upscaling process is approached with the consideration for additional structural requirements, functional requirements, and maintenance.

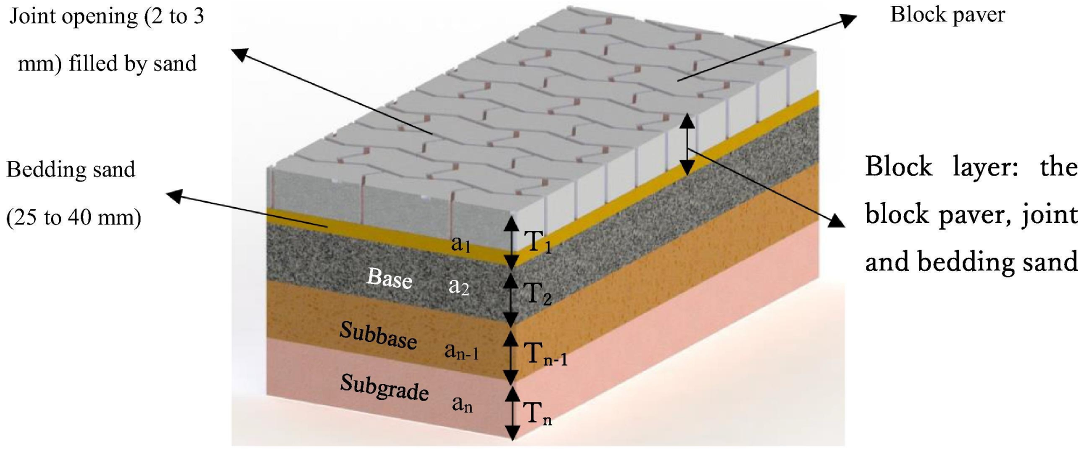

Figure 8.1: Section of concrete block pavement [160]

Concrete block pavements consist of individual solid blocks closely arranged to form a surface for pavement. Generally, these blocks are placed on a thin bed of sand overlying a sub-base, incorporating a variety of shapes and patterns. During the installation process, the spaces between the blocks are filled with sand, ensuring a suitable grading. Figure 8.1 shows the section of the road pavement and AAC containing MSWI BA aggregates are intended to be introduced in the top layer. Figure 8.2 shows the types of pavement blocks that are currently produced.

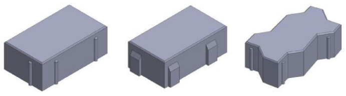

(a) Traditional blocks with spacer nibs standardized by JIPEA (2017)[123]

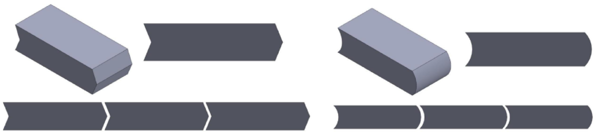

(b) Block paver with lateral anchored sniper developed by Takeyama (2000) [280]

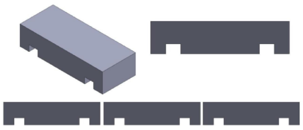

(c) Block paver with vertical dents developed by Tamaki et al. (2000) [277]

(d) A type of double layer or composite block paver developed by Kurotaki et al. (1992) [163] and Sano et al. (1988)[245].

Figure 8.2: Types of concrete pavement blocks [160]

To ensure the suitability of pavement blocks, several factors must be considered during the upscaling process. These factors encompass various aspects such as the shape of the blocks and laying patterns, structural performance, functional performance, safety, and maintenance requirements.

Firstly, the shape of the blocks and the arrangement of their laying patterns should be taken into account to facilitate interlocking and allow for adequate space for expansion. This consideration is essential to promote stability and durability within the pavement system.

Secondly, the structural performance of the pavement blocks should be thoroughly assessed. This evaluation entails examining the load-bearing capacity of the blocks, resistance to deformation under traffic loads, and ability to distribute stresses evenly. By ensuring optimal structural performance, the pavement blocks can effectively withstand the anticipated traffic demands and environmental conditions.

Moreover, functional performance is a crucial aspect to address, particularly in areas with residential proximity to highways and arterial roads. Constructing low-noise pavement is integral to urban design, management, and public health. Therefore, when upscaling the pavement blocks, it is essential to consider their ability to mitigate noise pollution and provide a more favourable acoustic environment in densely populated areas.

Furthermore, prioritising safety is of utmost importance. Regular evaluation of the surface texture of the block pavers is necessary to ensure an appropriate level of roughness. This characteristic promotes increased friction between the tire and the pavement surface, thereby enhancing safety by minimizing the risk of skidding or loss of vehicle control.

Lastly, maintenance procedures should be implemented to prevent surface or functional failures of the pavement blocks. This consists of addressing issues including block cracking, spalling, chipping and abrasion wear. Additionally, the application of AAC containing MSWI BA aggregates poses the challenge of leaching of heavy metals. Thus, regular inspection and timely maintenance activities are crucial to preserve the integrity and functionality of the pavement system.

A

LCA DATA

Table A.1: Environmental indicator equivalents for binder used in the analysis

Indicator	**Abbrevation**	**Binder**		
		BFS	**CEM III/B**	**CEM I**
Global warming potential	GWP-100	3.03E-02	3.71E-08	7.82E-01
Abiotic depletion non-fuel	ADP-non fuel	1.94E-04	7.62E-04	6.80E-08
Abiotic depletion fuel	ADP-fuel	2.26E-04	2.70E-01	1.21E-03
Ozone layer depletion	ODP	3.47E-09	8.10E-09	9.89E-09
Photochemical oxidation	POCP	5.68E-06	3.56E-05	5.33E-05
Acidification	AP	1.17E-04	4.02E-04	6.08E-04
Eutrophication	EP	1.67E-05	6.93E-05	1.49E-04
Human toxicity	HTP	1.12E-02	1.40E-02	2.29E-02
Fresh water aquatic ecotoxicity	FAETP	2.20E-04	3.03E-04	6.68E-04
Marine aquatic ecotoxicity	MAETP	3.97E+00	1.15E+00	2.70E+00
Terrestrial ecotoxicity	TAETP	2.62E-04	3.58E-04	1.54E-03

Table A.2: Environmental indicator equivalents for activator used in the analysis

Indicator	Abbrevation	Activator			
		NaOH (Pellet)	NaOH (50% wt%)	Water Glass (100% wt%)	Water Glass (37.5% wt%)
Global warming potential	GWP-100	8.73E-01	4.36E-01	9.53E-01	3.57E-01
Abiotic depletion non-fuel	ADP-non fuel	2.66E-05	1.33E-05	7.20E-05	2.70E-05
Abiotic depletion fuel	ADP-fuel	6.23E-03	3.11E-03	5.48E-03	2.05E-03
Ozone layer depletion	ODP	8.23E-07	4.12E-07	6.50E-08	2.44E-08
Photochemical oxidation	POCP	2.81E-04	1.40E-04	3.40E-04	1.28E-04
Acidification	AP	4.64E-03	2.32E-03	5.10E-03	1.91E-03
Eutrophication	EP	6.04E-04	3.02E-04	5.32E-04	1.99E-04
Human toxicity	HTP	3.91E-01	1.96E-01	6.15E-01	2.31E-01
Fresh water aquatic ecotoxicity	FAETP	7.26E-03	3.63E-03	8.63E-03	3.23E-03
Marine aquatic ecotoxicity	MAETP	3.11E+01	1.56E+01	3.43E+01	1.29E+01
Terrestrial ecotoxicity	TAETP	1.43E-02	7.14E-03	1.77E-03	6.63E-04

Table A.3: Environmental indicator equivalents for aggregates used in the analysis

Indicator	Abbrevation	Aggregates			
		MSWI BA aggregate	Gravel (4-8 mm &8-16 mm)	Limestone (crushed)	Sand (0-4mm)
Global warming potential	GWP-100	0	4.79E-04	2.23E-03	2.26E-03
Abiotic depletion non-fuel	ADP-non fuel	0	1.99E-07	2.02E-08	2.03E-07
Abiotic depletion fuel	ADP-fuel	0	2.94E-06	1.38E-05	1.48E-05
Ozone layer depletion	ODP	0	3.09E-11	3.38E-10	3.79E-10
Photochemical oxidation	POCP	0	4.72E-07	4.27E-06	2.03E-06
Acidification	AP	0	3.32E-06	3.51E-05	1.51E-05
Eutrophication	EP	0	4.69E-07	8.23E-06	2.99E-06
Human toxicity	HTP	0	8.47E-04	1.05E-03	1.42E-03
Fresh water aquatic ecotoxicity	FAETP	0	9.09E-06	1.43E-05	1.92E-05
Marine aquatic ecotoxicity	MAETP	0	2.76E-02	4.83E-02	6.34E-02
Terrestrial ecotoxicity	TAETP	0	4.82E-06	2.82E-06	7.94E-06

B

OPTIMISED MIXTURES FOR 30BA-70NA-AAC-T40

The MSWI BA test sample (30BA-70NA-AAC-T40) gave promising results for application in pavements. However, the delayed setting as a result of the addition of the MSWI BA aggregates was solved using thermal treatment. The samples were placed in the oven at 40°C for 24 hours. To prevent loss of moisture and subsequent drying cracks as a result, the samples are wrapped and placed in the oven.

The mechanical and durability performance of this sample is observed to be much lower than the sample cured at room temperature. Increased reactivity of metallic Al at increased temperature may be the reason. To solve this problem, the samples were placed in the oven for 1 hour to 6 hour. Following this, the compressive strength of the samples after 1-day and 28-day was tested. The results of the tests are shown in Figure B.1 and B.2.

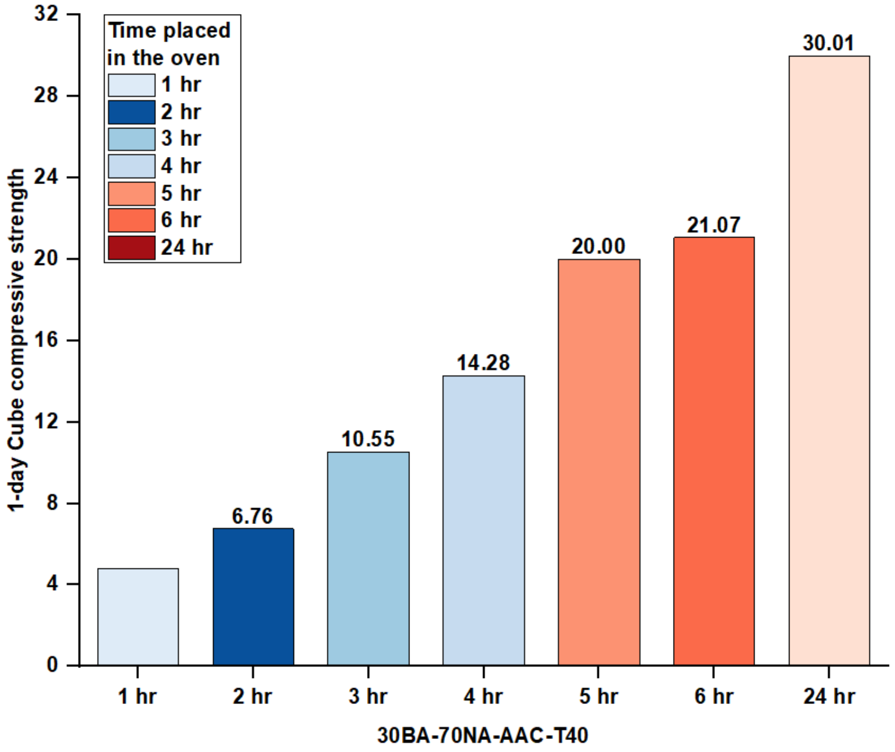

Figure B.1: 1-day cube compressive strength of sample 30BA-70NA-AAC-T40 at different duration's placed inside the oven

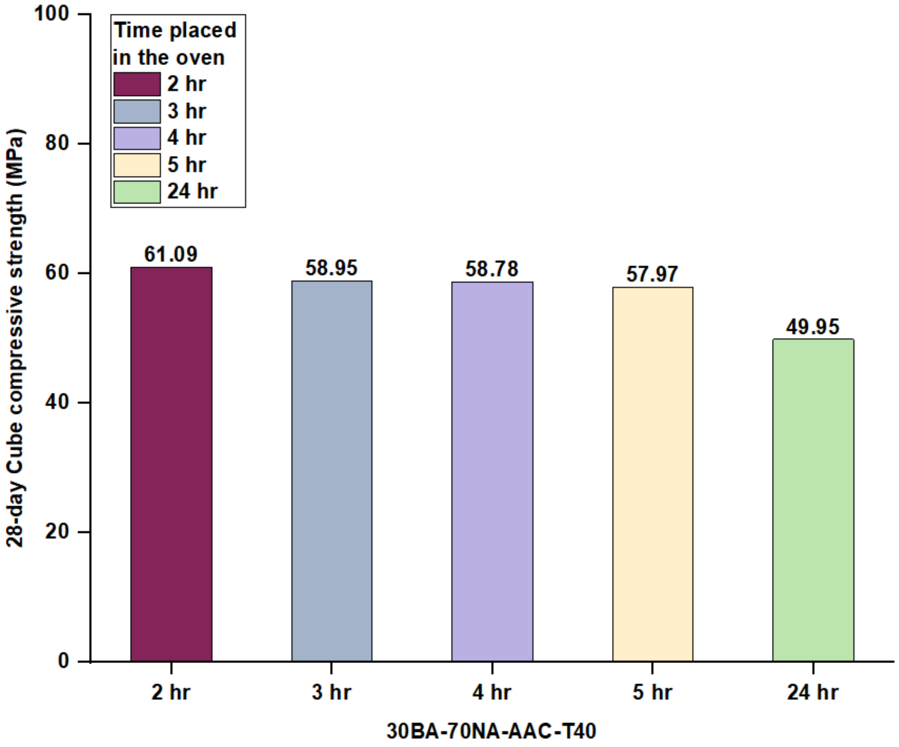

Figure B.2: 28-day cube compressive strength of sample 30BA-70NA-AAC-T40 at different duration's placed inside the oven

C

LCA COMPARISON

The data used for LCA comparison in Chapter 7 consists of mixtures from literature. The activator proportions in AAC majorly influence the environmental impact. In this research, the test sample and the control sample utilized the same amount of activator and aggregate volume. Hence, the effects of the addition of MSWI BA aggregates in concrete can be fully realized. Thus, the AAC control mixture, 100NA-AAC, is compared with the test sample, 30BA-70NA-AAC-T20 mixture in this section.

Table C.1: Environmental cost indicator for 100NA-AAC

100NA-AAC		**GGBFS**	**Na_2SiO_3 solution (37.5% wt% solid)**	**NaOH solution (50% wt% solid)**	**Sand (0-4 mm)**	**Gravel (4-8 mm)**	**Gravel (8-16 mm)**	**Total environmental effect**	**Cost (€)**
		Weight of component in 1 m^3 concrete							
	Shadow cost (€)	314	33.53	25.15	751	557	557		
Global warming potential	€ 0.05	9.5142	11.98464238	10.97777	1.699160735	0.266567	0.266567	34.70891	€ 1.74
Abiotic depletion non-fuel	€ 0.16	0.060916	0.000905914	0.000335	0.000152549	0.000111	0.000111	0.062531	€ 0.01
Abiotic depletion fuel	€ 0.16	0.070964	0.068886352	0.078309	0.011085533	0.001638	0.001638	0.232521	€ 0.04
Ozone layer depletion	€ 30.00	1.09E-06	8.17411E-07	1.03E-05	2.84651E-07	1.72E-08	1.72E-08	1.26E-05	€ 0.00
Photochemical oxidation	€ 2.00	0.001784	0.004277976	0.003531	0.001521838	0.000263	0.000263	0.011641	€ 0.02
Acidification	€ 4.00	0.036738	0.06415493	0.058342	0.011313523	0.001851	0.001851	0.174251	€ 0.70
Eutrophication	€ 9.00	0.005244	0.00668577	0.007599	0.002246421	0.000261	0.000261	0.022298	€ 0.20
Human toxicity	€ 0.09	3.5168	7.733802605	4.92126	1.069234893	0.471651	0.471651	18.1844	€ 1.64
Fresh water aquatic ecotoxicity	€ 0.03	0.06908	0.108467751	0.091301	0.014444956	0.005064	0.005064	0.293422	€ 0.01
Marine aquatic ecotoxicity	€ 0.00	1246.58	431.1638153	391.2239	47.63345597	15.38541	15.38541	2147.372	€ 0.21
Terrestrial ecotoxicity	€ 0.06	0.082268	0.022246586	0.179633	0.005965432	0.002684	0.002684	0.29548	€ 0.02
									€ 4.58

Table C.2: Environmental cost indicator for 30BA-70NA-AAC-T20

30BA-70NA-AAC-T20		**GGBFS**	**Na_2SiO_3 solution (37.5% wt% solid)**	**NaOH solution (50% wt% solid)**	**Sand (0-4 mm)**	**MSWI BA (4-11 mm)**	**Gravel (4-8 mm)**	**Gravel (8-16 mm)**	**Total environmental effect**	**Cost (€)**
		Weight of component in 1 m^3 concrete								
	Shadow cost (€)	314	33.53	25.15	751	151	399	557		
Global warming potential	€ 0.05	9.5142	11.98464238	10.97777	1.699160735	0	0.190952	0.266567	34.63329	€ 1.73
Abiotic depletion non-fuel	€ 0.16	0.060916	0.000905914	0.000335	0.000152549	0	7.95E-05	0.000111	0.0625	€ 0.01
Abiotic depletion fuel	€ 0.16	0.070964	0.068886352	0.078309	0.011085533	0	0.001173	0.001638	0.232056	€ 0.04
Ozone layer depletion	€ 30.00	1.09E-06	8.17411E-07	1.03E-05	2.84651E-07	0	1.23E-08	1.72E-08	1.26E-05	€ 0.00
Photochemical oxidation	€ 2.00	0.001784	0.004277976	0.003531	0.001521838	0	0.000188	0.000263	0.011566	€ 0.02
Acidification	€ 4.00	0.036738	0.06415493	0.058342	0.011313523	0	0.001326	0.001851	0.173726	€ 0.69
Eutrophication	€ 9.00	0.005244	0.00668577	0.007599	0.002246421	0	0.000187	0.000261	0.022224	€ 0.20
Human toxicity	€ 0.09	3.5168	7.733802605	4.92126	1.069234893	0	0.337861	0.471651	18.05061	€ 1.62
Fresh water aquatic ecotoxicity	€ 0.03	0.06908	0.108467751	0.091301	0.014444956	0	0.003628	0.005064	0.291985	€ 0.01
Marine aquatic ecotoxicity	€ 0.00	1246.58	431.1638153	391.2239	47.63345597	0	11.02115	15.38541	2143.008	€ 0.21
Terrestrial ecotoxicity	€ 0.06	0.082268	0.022246586	0.179633	0.005965432	0	0.001922	0.002684	0.294718	€ 0.02
										€ 4.56

D

XRD & XRF

Table D.1: Chemical composition of BFS and MSWI BA obtained from XRF analysis

Compound (wt%)	**MSWI BA**	**BFS**
SiO_2	52.91	34.99
CaO	13.44	36.33
Al_2O_3	10.18	14.32
Fe_2O_3	9.29	0.4
Na_2O	4.24	0.24
K_2O	0.84	0.46
SO_3	0.7	1.36
Cl	0.27	0.02
P_2O_5	1.03	0.01
MgO	2.4	9.42
ZnO	0.55	-
CuO	0.31	0.18
TiO_2	1.12	1.21
MnO	0.21	0.26
PbO	0.09	-
Cr_2O_3	0.07	-
BaO	0.09	0.04
NiO	0.03	-
ZrO_2	-	0.04
SrO	0.04	0.05
SnO_2	0.02	-
Rb_2O	-	-
Nb_2O_5	-	-
Y_2O_3	-	0.01
V_2O_5	-	0.02
CeO_2	-	0.08

REFERENCE

[1] Ayana Ghosh and G. D. Ransinchung. "Performance Evaluation of Fly Ash and Red Mud as Geopolymer Concrete Precursors for Rigid Pavement Application". In: *International Journal of Pavement Research and Technology* (2023). ISSN: 19971400. DOI: `10.1007/s42947-022-00263-x`.

[2] Deveshan L Pillay, Oladimeji B Olalusi, and Mohamed M H Mostafa. "A Review of the Engineering Properties of Concrete with Paper Mill Waste Ash-Towards Sustainable Rigid Pavement Construction". In: (2021). DOI: `10.1007/s12633-020-00664-2/Published`. URL: `https://doi.org/10.1007/s12633-020-00664-2`.

[3] Arunabh Pandey and Brind Kumar. "A comprehensive investigation on application of microsilica and rice straw ash in rigid pavement". In: *Construction and Building Materials* 252 (Aug. 2020). ISSN: 09500618. DOI: `10.1016/j.conbuildmat.2020.119053`.

[4] Ibrahim N.A. Al-Duais et al. "Optimization of alkali-activated binders using natural minerals and industrial waste materials as precursor materials". In: *Journal of Building Engineering* 69 (June 2023), p. 106230. ISSN: 2352-7102. DOI: `10.1016/J.JOBE.2023.106230`.

[5] Isabel Pol et al. "Heliyon Review article A review : Alkali-activated cement and concrete production technologies available in the industry". In: 9.September 2022 (2023). DOI: `10.1016/j.heliyon.2023.e15718`.

[6] Nandipati S.M. Ravi Kumar and S. Venkateswara Rao. "A study on development of pavement quality geopolymer concrete for low volume roads". In: *Materials Today: Proceedings* (2023). ISSN: 22147853. DOI: `10.1016/j.matpr.2023.03.684`.

[7] Tianyu Li et al. "Effect of air void structure and mechanical properties of high strength fiber reinforced mortar composed with different construction sand species based on X-CT technology". In: *Mechanics of Advanced Materials and Structures* (2023). ISSN: 15376532. DOI: `10.1080/15376494.2023.2165743`.

[8] Blessen Skariah Thomas et al. "Geopolymer concrete incorporating recycled aggregates: A comprehensive review". In: *Cleaner Materials* 3 (Mar. 2022), p. 100056. ISSN: 2772-3976. DOI: `10.1016/J.CLEMA.2022.100056`.

[9] Keun Hyeok Yang, Jin Kyu Song, and Keum Il Song. "Assessment of CO2 reduction of alkali-activated concrete". In: *Journal of Cleaner Production* 39 (Jan. 2013), pp. 265–272. ISSN: 0959-6526. DOI: `10.1016/J.JCLEPRO.2012.08.001`.

[10] Bruno Estanqueiro et al. "Environmental life cycle assessment of coarse natural and recycled aggregates for concrete". In: *European Journal of Environmental and Civil Engineering* 22.4 (Apr. 2018), pp. 429–449. ISSN: 19648189. DOI: `10.1080/19648189.2016.1197161`.

[11] Jad Bawab et al. “A review on cementitious materials including municipal solid waste incineration bottom ash (Mswi-ba) as aggregates”. In: *Buildings* 11.5 (2021). ISSN: 20755309. DOI: 10.3390/buildings11050179.

[12] Adrian Ionut Nicoara et al. *End-of-life materials used as supplementary cementitious materials in the concrete industry*. Apr. 2020. DOI: 10.3390/MA13081954.

[13] Hisham Hafez et al. “Data-driven optimization tool for the functional, economic, and environmental properties of blended cement concrete using supplementary cementitious materials”. In: *Journal of Building Engineering* 67 (May 2023). ISSN: 23527102. DOI: 10.1016/j.jobe.2023.106022.

[14] Maria C.G. Juenger and Rafat Siddique. “Recent advances in understanding the role of supplementary cementitious materials in concrete”. In: *Cement and Concrete Research* 78 (2015), pp. 71–80. ISSN: 00088846. DOI: 10.1016/j.cemconres.2015.03.018. URL: http://dx.doi.org/10.1016/j.cemconres.2015.03.018.

[15] Naraindas Bheel et al. “Utilization of millet husk ash as a supplementary cementitious material in eco-friendly concrete: RSM modelling and optimization”. In: *Structures* 49 (Mar. 2023), pp. 826–841. ISSN: 23520124. DOI: 10.1016/j.istruc.2023.02.015.

[16] Yao Ding, Jian Guo Dai, and Cai Jun Shi. “Mechanical properties of alkali-activated concrete: A state-of-the-art review”. In: *Construction and Building Materials* 127 (Nov. 2016), pp. 68–79. ISSN: 0950-0618. DOI: 10.1016/J.CONBUILDMAT.2016.09.121.

[17] Ismail Amer et al. “A review on alkali-activated slag concrete”. In: *Ain Shams Engineering Journal* 12.2 (June 2021), pp. 1475–1499. ISSN: 2090-4479. DOI: 10.1016/J.ASEJ.2020.12.003.

[18] Quan Liu et al. “Dissolved organic matter (DOM) was detected in MSWI plant: An investigation of DOM and potential toxic elements variation in the bottom ash and fly ash”. In: *Science of The Total Environment* 828 (July 2022), p. 154339. ISSN: 0048-9697. DOI: 10.1016/J.SCITOTENV.2022.154339.

[19] Jun Liu et al. “Novel recycling application of high volume municipal solid waste incineration bottom ash (MSWIBA) into sustainable concrete”. In: *Science of The Total Environment* 838 (Sept. 2022), p. 156124. ISSN: 0048-9697. DOI: 10.1016/J.SCITOTENV.2022.156124.

[20] Bram Verbinnen et al. “Recycling of MSWI Bottom Ash: A Review of Chemical Barriers, Engineering Applications and Treatment Technologies”. In: *Waste and Biomass Valorization* 8.5 (July 2017), pp. 1453–1466. ISSN: 1877265X. DOI: 10.1007/s12649-016-9704-0.

[21] Changjun Zhou et al. “Impact of freeze-thaw environment on concrete materials in two-lift concrete pavement”. In: *Construction and Building Materials* 262 (2020), p. 120070. ISSN: 09500618. DOI: 10.1016/j.conbuildmat.2020.120070. URL: https://doi.org/10.1016/j.conbuildmat.2020.120070.

[22] Abdulaziz Alsaif et al. “Freeze-thaw resistance of steel fibre reinforced rubberised concrete”. In: *Construction and Building Materials* 195 (2019), pp. 450–458. ISSN: 09500618. DOI: 10.1016/j.conbuildmat.2018.11.103. URL: https://doi.org/10.1016/j.conbuildmat.2018.11.103.

[23] Judita Gražulytė et al. “The impact of MSWI bottom ash as aggregate on concrete mechanical performance”. In: *International Journal of Pavement Engineering* (2021). ISSN: 1477268X. DOI: 10.1080/10298436.2021.1873333.

[24] Muhammad Faheem Mohd Tahir et al. “Mechanical and Durability Analysis of Fly Ash Based Geopolymer with Various Compositions for Rigid Pavement Applications”. In: *Materials* 15.10 (May 2022). ISSN: 19961944. DOI: 10.3390/ma15103458.

[25] “NEN en 1338- Requirments for concrete pavers”. In: ().

[26] E. E. Keijzer et al. “Carbon footprint comparison of innovative techniques in the construction and maintenance of road infrastructure in The Netherlands”. In: *Environmental Science and Policy* 54 (Dec. 2015), pp. 218–225. ISSN: 18736416. DOI: 10.1016/j.envsci.2015.06.010.

[27] Paola Di Mascio, Giuseppe Loprencipe, and Laura Moretti. “Technical and economic criteria to select pavement surfaces of port handling plants”. In: *Coatings* 9.2 (2019). ISSN: 20796412. DOI: 10.3390/coatings9020126.

[28] Tatiana García-Segura, Víctor Yepes, and Julián Alcalá. “Life cycle greenhouse gas emissions of blended cement concrete including carbonation and durability”. In: *International Journal of Life Cycle Assessment* 19.1 (Jan. 2014), pp. 3–12. ISSN: 09483349. DOI: 10.1007/s11367-013-0614-0.

[29] Zehrudin Osmanovic, Nedžad Haračić, and Jelica Zelić. “Properties of blastfurnace cements (CEM III/A, B, C) based on Portland cement clinker, blastfurnace slag and cement kiln dusts”. In: *Cement and Concrete Composites* 91.October 2016 (2018), pp. 189–197. ISSN: 09589465. DOI: 10.1016/j.cemconcomp.2018.05.006.

[30] Rob B Polder et al. *Innovation based on tradition: blast furnace slag cement for durable concrete structures in Norway?* Tech. rep.

[31] Barbara Lothenbach et al. “Hydration of a low-alkali CEM III/B–SiO2 cement (LAC)”. In: *Cement and Concrete Research* 42.2 (Feb. 2012), pp. 410–423. ISSN: 0008-8846. DOI: 10.1016/J.CEMCONRES.2011.11.008.

[32] Anya Vollpracht, Marios Soutsos, and Fragkoulis Kanavaris. “Strength development of GGBS and fly ash concretes and applicability of fib model code’s maturity function – A critical review”. In: *Construction and Building Materials* 162 (Feb. 2018), pp. 830–846. ISSN: 0950-0618. DOI: 10.1016/J.CONBUILDMAT.2017.12.054.

[33] Erdoan Özbay, Mustafa Erdemir, and Halil Ibrahim Durmuş. “Utilization and efficiency of ground granulated blast furnace slag on concrete properties – A review”. In: *Construction and Building Materials* 105 (Feb. 2016), pp. 423–434. ISSN: 0950-0618. DOI: 10.1016/J.CONBUILDMAT.2015.12.153.

[34] Ahmad L. Almutairi et al. “Potential applications of geopolymer concrete in construction: A review”. In: *Case Studies in Construction Materials* 15 (Dec. 2021), e00733. ISSN: 2214-5095. DOI: 10.1016/J.CSCM.2021.E00733.

[35] M. Talha Ghafoor et al. "Influence of alkaline activators on the mechanical properties of fly ash based geopolymer concrete cured at ambient temperature". In: *Construction and Building Materials* 273 (2021), p. 121752. ISSN: 09500618. DOI: 10.1016/j.conbuildmat.2020.121752. URL: https://doi.org/10.1016/j.conbuildmat.2020.121752.

[36] Louise K. Turner and Frank G. Collins. "Carbon dioxide equivalent (CO2-e) emissions: A comparison between geopolymer and OPC cement concrete". In: *Construction and Building Materials* 43 (June 2013), pp. 125–130. ISSN: 0950-0618. DOI: 10.1016/J.CONBUILDMAT.2013.01.023.

[37] Qiang Mao et al. "Mechanism, characterization and factors of reaction between basalt and alkali: Exploratory investigation for potential application in geopolymer concrete". In: *Cement and Concrete Composites* 130 (July 2022), p. 104526. ISSN: 0958-9465. DOI: 10.1016/J.CEMCONCOMP.2022.104526.

[38] Kamal Neupane. "High-Strength Geopolymer Concrete- Properties, Advantages and Challenges". In: *Advances in Materials* 7.2 (2018), p. 15. ISSN: 2327-2503. DOI: 10.11648/j.am.20180702.11.

[39] H. Tchakoute Kouamo et al. "The effect of adding alumina-oxide to metakaolin and volcanic ash on geopolymer products: A comparative study". In: *Construction and Building Materials* 35 (Oct. 2012), pp. 960–969. ISSN: 0950-0618. DOI: 10.1016/J.CONBUILDMAT.2012.04.023.

[40] Md Manjur A. Elahi et al. "A review on alkali-activated binders: Materials composition and fresh properties of concrete". In: *Construction and Building Materials* 260 (Nov. 2020), p. 119788. ISSN: 0950-0618. DOI: 10.1016/J.CONBUILDMAT.2020.119788.

[41] Pradip Nath and Prabir Kumar Sarker. "Effect of GGBFS on setting, workability and early strength properties of fly ash geopolymer concrete cured in ambient condition". In: *Construction and Building Materials* 66 (Sept. 2014), pp. 163–171. ISSN: 0950-0618. DOI: 10.1016/J.CONBUILDMAT.2014.05.080.

[42] P. Duxson. "Geopolymer precursor design". In: *Geopolymers: Structures, Processing, Properties and Industrial Applications* (Jan. 2009), pp. 37–49. DOI: 10.1533/9781845696382.1.37.

[43] H. S. Abhishek et al. "Fresh mechanical and durability properties of alkali-activated fly ash-slag concrete: a review". In: *Innovative Infrastructure Solutions* 7.1 (2022), pp. 1–14. ISSN: 23644184. DOI: 10.1007/s41062-021-00711-w. URL: https://doi.org/10.1007/s41062-021-00711-w.

[44] Mehrab Nodehi and Vahid Mohamad Taghvaee. "Alkali-Activated Materials and Geopolymer: a Review of Common Precursors and Activators Addressing Circular Economy". In: *Circular Economy and Sustainability* 2.1 (2022), pp. 165–196. ISSN: 2730-597X. DOI: 10.1007/s43615-021-00029-w.

[45] Jixiang Wang et al. "Effects of fly ash on the properties and microstructure of alkali-activated FA/BFS repairing mortar". In: *Fuel* 256 (Nov. 2019), p. 115919. ISSN: 0016-2361. DOI: 10.1016/J.FUEL.2019.115919.

[46] Ghina M. Zannerni, Kazi P. Fattah, and Adil K. Al-Tamimi. “Ambient-cured geopolymer concrete with single alkali activator”. In: *Sustainable Materials and Technologies* 23 (Apr. 2020), e00131. ISSN: 2214-9937. DOI: 10.1016/J.SUSMAT.2019.E00131.

[47] Muhammad N.S. Hadi, Haiqiu Zhang, and Shelley Parkinson. “Optimum mix design of geopolymer pastes and concretes cured in ambient condition based on compressive strength, setting time and workability”. In: *Journal of Building Engineering* 23 (May 2019), pp. 301–313. ISSN: 2352-7102. DOI: 10.1016/J.JOBE.2019.02.006.

[48] W. K. Part, M. Ramli, and C. B. Cheah. “An Overview on the Influence of Various Factors on the Properties of Geopolymer Concrete Derived From Industrial Byproducts”. In: *Handbook of Low Carbon Concrete* (Jan. 2017), pp. 263–334. DOI: 10.1016/B978-0-12-804524-4.00011-7.

[49] C. Ruiz-Santaquiteria et al. “Alkaline solution/binder ratio as a determining factor in the alkaline activation of aluminosilicates”. In: *Cement and Concrete Research* 42.9 (Sept. 2012), pp. 1242–1251. ISSN: 0008-8846. DOI: 10.1016/J.CEMCONRES.2012.05.019.

[50] Ahmad L. Almutairi et al. “Potential applications of geopolymer concrete in construction: A review”. In: *Case Studies in Construction Materials* 15 (Dec. 2021), e00733. ISSN: 2214-5095. DOI: 10.1016/J.CSCM.2021.E00733.

[51] Osama Ahmed Mohamed. “A review of durability and strength characteristics of alkali-activated slag concrete”. In: *Materials* 12.8 (2019). ISSN: 19961944. DOI: 10.3390/ma12081198.

[52] F. Puertas et al. “Alkali-activated fly ash/slag cements. Strength behaviour and hydration products”. In: *Cement and Concrete Research* 30.10 (2000), pp. 1625–1632. ISSN: 00088846. DOI: 10.1016/S0008-8846(00)00298-2.

[53] Isabella Bianco, Branwen Ap Dafydd Tomos, and Raffaele Vinai. “Analysis of the environmental impacts of alkali-activated concrete produced with waste glass-derived silicate activator – A LCA study”. In: *Journal of Cleaner Production* 316 (Sept. 2021), p. 128383. ISSN: 0959-6526. DOI: 10.1016/J.JCLEPRO.2021.128383.

[54] Parham Shoaei et al. “Difference between geopolymers and alkali-activated materials”. In: *Handbook of Sustainable Concrete and Industrial Waste Management: Recycled and Artificial Aggregate, Innovative Eco-friendly Binders, and Life Cycle Assessment* (Jan. 2022), pp. 421–435. DOI: 10.1016/B978-0-12-821730-6.00018-8.

[55] N. K. Lee and H. K. Lee. “Setting and mechanical properties of alkali-activated fly ash/slag concrete manufactured at room temperature”. In: *Construction and Building Materials* 47 (Oct. 2013), pp. 1201–1209. ISSN: 0950-0618. DOI: 10.1016/J.CONBUILDMAT.2013.05.107.

[56] Aneeta Mary Joseph et al. “Pre-treatment and utilisation of municipal solid waste incineration bottom ashes towards a circular economy”. In: *Construction and Building Materials* 260 (Nov. 2020), p. 120485. ISSN: 0950-0618. DOI: 10.1016/J.CONBUILDMAT.2020.120485.

[57] O. Ginés et al. “Combined use of MSWI bottom ash and fly ash as aggregate in concrete formulation: Environmental and mechanical considerations”. In: *Journal of Hazardous Materials* 169.1-3 (Sept. 2009), pp. 643–650. ISSN: 0304-3894. DOI: 10.1016/J.JHAZMAT.2009.03.141.

[58] Dongxing Xuan, Pei Tang, and Chi Sun Poon. “Limitations and quality upgrading techniques for utilization of MSW incineration bottom ash in engineering applications – A review”. In: *Construction and Building Materials* 190 (Nov. 2018), pp. 1091–1102. ISSN: 0950-0618. DOI: 10.1016/J.CONBUILDMAT.2018.09.174.

[59] Yating Zhu et al. “Physicochemical characterization and heavy metals leaching potential of municipal solid waste incinerated bottom ash (MSWI-BA) when utilized in road construction”. In: (). DOI: 10.1007/s11356-020-08007-9/Published. URL: https://doi.org/10.1007/s11356-020-08007-9.

[60] Yun Cao et al. “Effect of SiO 2 , Al 2 O 3 and CaO on characteristics of lightweight aggregates produced from MSWI bottom ash sludge (MSWI-BAS)”. In: *Construction and Building Materials* 205 (2019), pp. 368–376. ISSN: 0950-0618. DOI: 10.1016/j.conbuildmat.2019.01.104. URL: https://doi.org/10.1016/j.conbuildmat.2019.01.104.

[61] Emanuele Toraldo et al. “Use of stabilized bottom ash for bound layers of road pavements”. In: *Journal of Environmental Management* 121 (May 2013), pp. 117–123. ISSN: 0301-4797. DOI: 10.1016/J.JENVMAN.2013.02.037.

[62] Peiliang Shen et al. “Utilization of municipal solid waste incineration bottom ash (IBA) aggregates in high-strength pervious concrete”. In: *Resources, Conservation and Recycling* 174 (Nov. 2021), p. 105736. ISSN: 0921-3449. DOI: 10.1016/J.RESCONREC.2021.105736.

[63] Yibing Zuo. “Experimental Study and Numerical Simulation of the Reaction Process and Microstructure Formation of Alkali-Activated Materials”. In: (). DOI: 10.4233/uuid:193a4016-5fc7-401b-babe-722ff6a95a6c. URL: https://doi.org/10.4233/uuid:193a4016-5fc7-401b-babe-722ff6a95a6c.

[64] Wen Ten Kuo, Chih Chien Liu, and De Sin Su. “Use of washed municipal solid waste incinerator bottom ash in pervious concrete”. In: *Cement and Concrete Composites* 37.1 (Mar. 2013), pp. 328–335. ISSN: 0958-9465. DOI: 10.1016/J.CEMCONCOMP.2013.01.001.

[65] Trong Phuoc Huynh and Si Huy Ngo. “Waste incineration bottom ash as a fine aggregate in mortar: An assessment of engineering properties, durability, and microstructure”. In: *Journal of Building Engineering* 52 (July 2022), p. 104446. ISSN: 2352-7102. DOI: 10.1016/J.JOBE.2022.104446.

[66] Sabrina Sorlini, Alessandro Abbà, and Carlo Collivignarelli. “Recovery of MSWI and soil washing residues as concrete aggregates”. In: *Waste Management* 31.2 (Feb. 2011), pp. 289–297. ISSN: 0956-053X. DOI: 10.1016/J.WASMAN.2010.04.019.

[67] A. Keulen et al. “High performance of treated and washed MSWI bottom ash granulates as natural aggregate replacement within earth-moist concrete”. In: *Waste Management* 49 (Mar. 2016), pp. 83–95. ISSN: 0956-053X. DOI: 10.1016/J.WASMAN.2016.01.010.

[68] R. Forteza et al. "Characterization of bottom ash in municipal solid waste incinerators for its use in road base". In: *Waste Management* 24.9 (Jan. 2004), pp. 899–909. ISSN: 0956-053X. DOI: 10.1016/J.WASMAN.2004.07.004.

[69] Ngoc Hung Le et al. "Evaluation of physicochemical and hydromechanical properties of MSWI bottom ash for road construction". In: *Waste Management* 80 (Oct. 2018), pp. 168–174. ISSN: 0956-053X. DOI: 10.1016/J.WASMAN.2018.09.007.

[70] Urs Müller and Katrin Rübner. "The microstructure of concrete made with municipal waste incinerator bottom ash as an aggregate component". In: *Cement and Concrete Research* 36.8 (Aug. 2006), pp. 1434–1443. ISSN: 0008-8846. DOI: 10.1016/J.CEMCONRES.2006.03.023.

[71] R. Cioffi et al. "Manufacture of artificial aggregate using MSWI bottom ash". In: *Waste Management* 31.2 (Feb. 2011), pp. 281–288. ISSN: 0956-053X. DOI: 10.1016/J.WASMAN.2010.05.020.

[72] Gert Van Der Wegen, Ulbert Hofstra, and John Speerstra. "Upgraded MSWI Bottom Ash as Aggregate in Concrete". In: (). DOI: 10.1007/s12649-013-9255-6.

[73] Nabajyoti Saikia et al. "Pre-treatment of municipal solid waste incineration (MSWI) bottom ash for utilisation in cement mortar". In: *Construction and Building Materials* 96 (Oct. 2015), pp. 76–85. ISSN: 0950-0618. DOI: 10.1016/J.CONBUILDMAT.2015.07.185.

[74] Tao Zhang and Zengzeng Zhao. "Optimal Use of MSWI Bottom Ash in Concrete". In: *International Journal of Concrete Structures and Materials* 8.2 (2014), pp. 173–182. ISSN: 22341315. DOI: 10.1007/s40069-014-0073-4.

[75] Katrin Rübner, F. Haamkens, and O. Linde. "Use of municipal solid waste incinerator bottom ash as aggregate in concrete". In: *Quarterly Journal of Engineering Geology and Hydrogeology* 41.4 (Nov. 2008), pp. 459–464. ISSN: 14709236. DOI: 10.1144/1470-9236/07-036.

[76] Tao Zhang and Zengzeng Zhao. "Optimal Use of MSWI Bottom Ash in Concrete". In: *International Journal of Concrete Structures and Materials* 8.2 (2014), pp. 173–182. ISSN: 22341315. DOI: 10.1007/s40069-014-0073-4.

[77] Matthew L. Schafer et al. "Use of Coal Fly Ash or Glass Pozzolan Addition as a Mitigation Tool for Alkali-Silica Reactivity in Cement Mortars Amended with Recycled Municipal Solid Waste Incinerator Bottom Ash". In: *Waste and Biomass Valorization* 10.9 (2019), pp. 2733–2744. ISSN: 1877265X. DOI: 10.1007/s12649-018-0296-8. URL: http://dx.doi.org/10.1007/s12649-018-0296-8.

[78] J Lynn, Gurmel S Ghataora, and Ravindra K Dhir Obe. "ScienceDirect Municipal incinerated bottom ash (MIBA) characteristics and potential for use in road pavements". In: 10.2017 (2019), pp. 185–201. DOI: 10.1016/j.ijprt.2016.12.003.

[79] Olaf Holm and Franz Georg Simon. "Innovative treatment trains of bottom ash (BA) from municipal solid waste incineration (MSWI) in Germany". In: *Waste Management* 59 (Jan. 2017), pp. 229–236. ISSN: 0956-053X. DOI: 10.1016/J.WASMAN.2016.09.004.

[80] Jinyoung Kim et al. “Effect of chemical treatment of MSWI bottom ash for its use in concrete”. In: *Magazine of Concrete Research* 67.4 (Feb. 2015), pp. 179–186. ISSN: 1751763X. DOI: 10.1680/macr.14.00170.

[81] Philip Van den Heede et al. “Sustainable high-quality recycling of aggregates from waste-to-energy, treated in a wet bottom ash processing installation, for use in concrete products”. In: *Materials* 9.1 (2016), pp. 1–24. ISSN: 19961944. DOI: 10.3390/ma9010009.

[82] Dongxing Xuan and Chi Sun Poon. “Removal of metallic Al and Al/Zn alloys in MSWI bottom ash by alkaline treatment”. In: *Journal of Hazardous Materials* 344 (Feb. 2018), pp. 73–80. ISSN: 0304-3894. DOI: 10.1016/J.JHAZMAT.2017.10.002.

[83] V. Caprai, K. Schollbach, and H. J.H. Brouwers. “Influence of hydrothermal treatment on the mechanical and environmental performances of mortars including MSWI bottom ash”. In: *Waste Management* 78 (Aug. 2018), pp. 639–648. ISSN: 0956-053X. DOI: 10.1016/J.WASMAN.2018.06.030.

[84] Ciarán J. Lynn, Ravindra K. Dhir OBE, and Gurmel S. Ghataora. “Municipal incinerated bottom ash characteristics and potential for use as aggregate in concrete”. In: *Construction and Building Materials* 127 (Nov. 2016), pp. 504–517. ISSN: 0950-0618. DOI: 10.1016/J.CONBUILDMAT.2016.09.132.

[85] Mnaier Saad et al. “Manufacturing of Lightweight Aggregates from Municipal Solid Waste Incineration Bottom Ash and their Impacts on Concrete Properties Thermo-mechanical and physical properties of waste granular cork composite with slag cement View project Manufacturing of L”. In: July (2019). URL: https://www.researchgate.net/publication/334131460.

[86] Shipeng Zhang, Zaid Ghouleh, and Yixin Shao. “Green concrete made from MSWI residues derived eco-cement and bottom ash aggregates”. In: *Construction and Building Materials* 297 (Aug. 2021), p. 123818. ISSN: 0950-0618. DOI: 10.1016/J.CONBUILDMAT.2021.123818.

[87] Kezhen Yan et al. “Assessment and mechanism analysis of municipal solid waste incineration bottom ash as aggregate in cement stabilized macadam”. In: *Journal of Cleaner Production* 244 (Jan. 2020), p. 118750. ISSN: 0959-6526. DOI: 10.1016/J.JCLEPRO.2019.118750.

[88] Nederlands Normalisatie Instituut. “NEN-EN 206+NEN 8005”. In: (2017). ISSN: 8005:2016.

[89] *AEC-granulaat als toeslag-materiaal voor beton.* ISBN: 9789037605327.

[90] “soil_quality_regulation_first_notification_24_311345”. In: ().

[91] Nederlands Normalisatie Instituut. “NEN-EN 206+NEN 8005”. In: (2017). ISSN: 8005:2016.

[92] *NEN-EN 933-1.pdf.*

[93] “NEN-EN 1097-6-Tests for mechanical and physical properties of density and water absorbtion”. In: ().

[94] “NEN 1097-3-Determination of loose bulk density and voids”. In: ().

[95] “NEN 1097-1999- annex A -Los angeles abrasion”. In: ().

[96] NEN. *NEN 12620:Aggregates for concrete.* Tech. rep. 2008.

[97] Byoung Hooi Cho et al. *Municipal solid waste incineration (MSWI) ashes as construction materials-a review*. 2020. DOI: 10.3390/ma13143143.

[98] Peiliang Shen et al. “Feasible use of municipal solid waste incineration bottom ash in ultra-high performance concrete”. In: *Cement and Concrete Composites* 114 (Nov. 2020), p. 103814. ISSN: 0958-9465. DOI: 10.1016/J.CEMCONCOMP.2020.103814.

[99] Nikolina Poranek et al. “Green Deal and Circular Economy of Bottom Ash Waste Management in Building Industry—Alkali (NaOH) Pre-Treatment”. In: *Materials* 15.10 (May 2022). ISSN: 19961944. DOI: 10.3390/ma15103487.

[100] A. Keulen et al. “High performance of treated and washed MSWI bottom ash granulates as natural aggregate replacement within earth-moist concrete”. In: *Waste Management* 49 (Mar. 2016), pp. 83–95. ISSN: 0956-053X. DOI: 10.1016/J.WASMAN.2016.01.010.

[101] J. M. Chimenos et al. “Short-term natural weathering of MSWI bottom ash”. In: *Journal of Hazardous Materials* 79.3 (Dec. 2000), pp. 287–299. ISSN: 0304-3894. DOI: 10.1016/S0304-3894(00)00270-3.

[102] J. Pera et al. “Use of incinerator bottom ash in concrete”. In: *Cement and Concrete Research* 27.1 (Jan. 1997), pp. 1–5. ISSN: 0008-8846. DOI: 10.1016/S0008-8846(96)00193-7.

[103] “12390-3-Compressive strength”. In: ().

[104] “12390-6-Split tensile strength test”. In: ().

[105] “NEN EN 14651-for the flexural strength test”. In: ().

[106] “12390-9-freeze and thaw-De icing salt”. In: ().

[107] Amin Noushini and Arnaud Castel. “The effect of heat-curing on transport properties of low-calcium fly ash-based geopolymer concrete”. In: *Construction and Building Materials* 112 (June 2016), pp. 464–477. ISSN: 0950-0618. DOI: 10.1016/J.CONBUILDMAT.2016.02.210.

[108] Mohamed Rabie, Mohammad R. Irshidat, and Nasser Al-Nuaimi. “Ambient and Heat-Cured Geopolymer Composites: Mix Design Optimization and Life Cycle Assessment”. In: *Sustainability (Switzerland)* 14.9 (2022). ISSN: 20711050. DOI: 10.3390/su14094942.

[109] Ankur Mehta et al. “Fly ash and ground granulated blast furnace slag-based alkali-activated concrete: Mechanical, transport and microstructural properties”. In: *Construction and Building Materials* 257 (Oct. 2020), p. 119548. ISSN: 0950-0618. DOI: 10.1016/J.CONBUILDMAT.2020.119548.

[110] Nguyen Van Chanh et al. *RECENT RESEARCH GEOPOLYMER CONCRETE*. Tech. rep. 2008.

[111] A. Maldonado-Alameda et al. “Municipal solid waste incineration bottom ash as alkali-activated cement precursor depending on particle size”. In: *Journal of Cleaner Production* 242 (Jan. 2020), p. 118443. ISSN: 0959-6526. DOI: 10.1016/J.JCLEPRO.2019.118443.

[112] Jiaqi Li. *Municipal solid waste incineration ash-incorporated concrete: One step towards environmental justice*. Nov. 2021. DOI: 10.3390/buildings11110495.

[113] K. L. Lin, W. C. Chang, and D. F. Lin. “Pozzolanic characteristics of pulverized incinerator bottom ash slag”. In: *Construction and Building Materials* 22.3 (Mar. 2008), pp. 324–329. ISSN: 09500618. DOI: `10.1016/j.conbuildmat.2006.08.012`.

[114] Sasui Sasui et al. “Effects of waste glass as a sand replacement on the strength and durability of fly ash/GGBS based alkali activated mortar”. In: *Ceramics International* 47.15 (Aug. 2021), pp. 21175–21196. ISSN: 0272-8842. DOI: `10.1016/J.CERAMINT.2021.04.121`.

[115] Kezhen Yan et al. “Assessment and mechanism analysis of municipal solid waste incineration bottom ash as aggregate in cement stabilized macadam”. In: *Journal of Cleaner Production* 244 (Jan. 2020), p. 118750. ISSN: 0959-6526. DOI: `10.1016/J.JCLEPRO.2019.118750`.

[116] Aneeta Mary Joseph et al. “Pre-treatment and utilisation of municipal solid waste incineration bottom ashes towards a circular economy”. In: *Construction and Building Materials* 260 (2020), p. 120485. ISSN: 09500618. DOI: `10.1016/j.conbuildmat.2020.120485`. URL: `https://doi.org/10.1016/j.conbuildmat.2020.120485`.

[117] T. Bakharev, J. G. Sanjayan, and Y. B. Cheng. “Effect of admixtures on properties of alkali-activated slag concrete”. In: *Cement and Concrete Research* 30.9 (Sept. 2000), pp. 1367–1374. ISSN: 0008-8846. DOI: `10.1016/S0008-8846(00)00349-5`.

[118] X. Huang et al. “Preparation and properties of geopolymer from blast furnace slag”. In: *Materials Research Innovations* 19 (Dec. 2015), pp. 413–419. ISSN: 1433075X. DOI: `10.1179/1432891715Z.0000000002210`.

[119] Ali A. Aliabdo, Abd Elmoaty M. Abd Elmoaty, and Mohammed A. Emam. “Factors affecting the mechanical properties of alkali activated ground granulated blast furnace slag concrete”. In: *Construction and Building Materials* 197 (Feb. 2019), pp. 339–355. ISSN: 0950-0618. DOI: `10.1016/J.CONBUILDMAT.2018.11.086`.

[120] Wen Cheng Liao et al. “An innovative test method for tensile strength of concrete by applying the strut-and-tie methodology”. In: *Materials* 13.12 (June 2020), pp. 1–20. ISSN: 19961944. DOI: `10.3390/ma13122776`.

[121] D S Lane. *FINAL REPORT EVALUATION OF CONCRETE CHARACTERISTICS FOR RIGID PAVEMENTS*. Tech. rep. 1998.

[122] Fa Yang et al. “Estimating the Effect of Vibration Mixing Process on Air Pore Size Distributions in Concrete Using Digital Image Analysis”. In: *Buildings* 12.8 (2022). ISSN: 20755309. DOI: `10.3390/buildings12081142`.

[123] M. Cyr and R. Pouhet. “The frost resistance of alkali-activated cement-based binders”. In: *Handbook of Alkali-Activated Cements, Mortars and Concretes* (Jan. 2015), pp. 293–318. DOI: `10.1533/9781782422884.3.293`.

[124] Khashayar Ebrahimi et al. “A review of the impact of micro- and nanoparticles on freeze-thaw durability of hardened concrete: Mechanism perspective”. In: *Construction and Building Materials* 186 (Oct. 2018), pp. 1105–1113. ISSN: 0950-0618. DOI: `10.1016/J.CONBUILDMAT.2018.08.029`.

[125] J. Alexandre Bogas, J. De Brito, and Duarte Ramos. “Freeze-thaw resistance of concrete produced with fine recycled concrete aggregates”. In: *Journal of Cleaner Production* 115 (2016), pp. 294–306. ISSN: 09596526. DOI: 10.1016/j.jclepro.2015.12.065. URL: http://dx.doi.org/10.1016/j.jclepro.2015.12.065.

[126] Cong Zhu et al. “Effect of aggregate saturation degree on the freeze–thaw resistance of high performance polypropylene fiber lightweight aggregate concrete”. In: *Construction and Building Materials* 145 (Aug. 2017), pp. 367–375. ISSN: 0950-0618. DOI: 10.1016/J.CONBUILDMAT.2017.04.039.

[127] Ruijun Wang, Qingjun Zhang, and Yang Li. “Deterioration of concrete under the coupling effects of freeze–thaw cycles and other actions: A review”. In: *Construction and Building Materials* 319 (Feb. 2022), p. 126045. ISSN: 0950-0618. DOI: 10.1016/J.CONBUILDMAT.2021.126045.

[128] Peng Zhang et al. “Effect of Air Entrainment on the Mechanical Properties, Chloride Migration, and Microstructure of Ordinary Concrete and Fly Ash Concrete”. In: *Journal of Materials in Civil Engineering* 30.10 (2018), pp. 1–9. ISSN: 0899-1561. DOI: 10.1061/(asce)mt.1943-5533.0002456.

[129] Thang T. Nguyen et al. “Experimental and numerical investigation of influence of air-voids on the compressive behaviour of foamed concrete”. In: *Materials & Design* 130 (Sept. 2017), pp. 103–119. ISSN: 0264-1275. DOI: 10.1016/J.MATDES.2017.05.054.

[130] E. K.Kunhanandan Nambiar and K. Ramamurthy. “Air-void characterisation of foam concrete”. In: *Cement and Concrete Research* 37.2 (Feb. 2007), pp. 221–230. ISSN: 0008-8846. DOI: 10.1016/J.CEMCONRES.2006.10.009.

[131] Jakub Holan et al. “Experimental investigation of the compressive strength of normal-strength air-entrained concrete at high temperatures”. In: *Construction and Building Materials* 248 (2020), p. 118662. ISSN: 09500618. DOI: 10.1016/j.conbuildmat.2020.118662. URL: https://doi.org/10.1016/j.conbuildmat.2020.118662.

[132] Michael Henry, Ivan Sandi Darma, and Takafumi Sugiyama. “Analysis of the effect of heating and re-curing on the microstructure of high-strength concrete using X-ray CT”. In: *Construction and Building Materials* 67 (2014), pp. 37–46. ISSN: 09500618. DOI: 10.1016/j.conbuildmat.2013.11.007. URL: http://dx.doi.org/10.1016/j.conbuildmat.2013.11.007.

[133] Jing Hu et al. “Influence of aggregate particles on mastic and air-voids in asphalt concrete”. In: *Construction and Building Materials* 93 (Sept. 2015), pp. 1–9. ISSN: 0950-0618. DOI: 10.1016/J.CONBUILDMAT.2015.05.031.

[134] Bo Chen et al. “Detect concrete cracks based on OTSU algorithm with differential image”. In: *The Journal of Engineering* 2019.23 (Dec. 2019), pp. 9088–9091. ISSN: 2051-3305. DOI: 10.1049/joe.2018.9191.

[135] R. C.K. Wong and K. T. Chau. “Estimation of air void and aggregate spatial distributions in concrete under uniaxial compression using computer tomography scanning”. In: *Cement and Concrete Research* 35.8 (Aug. 2005), pp. 1566–1576. ISSN: 0008-8846. DOI: 10.1016/J.CEMCONRES.2004.08.016.

[136] Yujun Che et al. “Influences of air-voids on the performance of 3d printing cementitious materials”. In: *Materials* 14.16 (Aug. 2021). ISSN: 19961944. DOI: 10.3390/ma14164438.

[137] Hammad Ahmed Shah, Qiang Yuan, and Shenghao Zuo. *Air entrainment in fresh concrete and its effects on hardened concrete-a review*. Mar. 2021. DOI: 10.1016/j.conbuildmat.2020.121835.

[138] Ruijun Wang et al. “Review on the deterioration and approaches to enhance the durability of concrete in the freeze–thaw environment”. In: *Construction and Building Materials* 321 (Feb. 2022), p. 126371. ISSN: 0950-0618. DOI: 10.1016/J.CONBUILDMAT.2022.126371.

[139] Ruben Villarreal et al. “An Alternative Test Method for Determining Hardened Air Void Parameters for Concrete Pavement”. In: *Journal of Civil Engineering and Construction* 12.1 (Feb. 2023), pp. 19–39. DOI: 10.32732/jcec.2023.12.1.19.

[140] V. Caprai et al. “Investigation of the hydrothermal treatment for maximizing the MSWI bottom ash content in fine lightweight aggregates”. In: *Construction and Building Materials* 230 (Jan. 2020), p. 116947. ISSN: 0950-0618. DOI: 10.1016/J.CONBUILDMAT.2019.116947.

[141] Shipeng Zhang, Zaid Ghouleh, and Yixin Shao. “Green concrete made from MSWI residues derived eco-cement and bottom ash aggregates”. In: *Construction and Building Materials* 297 (Aug. 2021), p. 123818. ISSN: 0950-0618. DOI: 10.1016/J.CONBUILDMAT.2021.123818.

[142] R. del Valle-Zermeño et al. “Material characterization of the MSWI bottom ash as a function of particle size. Effects of glass recycling over time”. In: *Science of the Total Environment* 581-582 (2017), pp. 897–905. ISSN: 18791026. DOI: 10.1016/j.scitotenv.2017.01.047. URL: http://dx.doi.org/10.1016/j.scitotenv.2017.01.047.

[143] Jessica Giro-paloma and Joan Formosa. “GLASS CONTENT IN MSWI BOTTOM ASH : EFFECTIVENESS ASSESSMENT OF”. In: May (2014).

[144] Yunmei Wei et al. “Geoenvironmental weathering/deterioration of landfilled MSWI-BA glass”. In: *Journal of Hazardous Materials* 278 (Aug. 2014), pp. 610–619. ISSN: 0304-3894. DOI: 10.1016/J.JHAZMAT.2014.05.093.

[145] R. del Valle-Zermeño et al. “Aggregate material formulated with MSWI bottom ash and APC fly ash for use as secondary building material”. In: *Waste Management* 33.3 (Mar. 2013), pp. 621–627. ISSN: 0956-053X. DOI: 10.1016/J.WASMAN.2012.09.015.

[146] Qadeer Alam et al. “In-depth mineralogical quantification of MSWI bottom ash phases and their association with potentially toxic elements”. In: *Waste Management* 87 (2019), pp. 1–12. ISSN: 0956-053X. DOI: 10.1016/j.wasman.2019.01.031. URL: https://doi.org/10.1016/j.wasman.2019.01.031.

[147] P M F Van De Wouw et al. “Compositional modelling and crushing behaviour of MSWI bottom ash material classes”. In: *Waste Management* 101 (2020), pp. 268–282. ISSN: 0956-053X. DOI: 10.1016/j.wasman.2019.10.013. URL: https://doi.org/10.1016/j.wasman.2019.10.013.

[148] X Gao et al. "Characterization and application of municipal solid waste incineration (MSWI) bottom ash and waste granite powder in alkali activated slag". In: 164 (2017), pp. 410–419. DOI: 10.1016/j.jclepro.2017.06.218.

[149] Troy Hottle et al. "Environmental life-cycle assessment of concrete produced in the United States". In: *Journal of Cleaner Production* 363 (Aug. 2022), p. 131834. ISSN: 0959-6526. DOI: 10.1016/J.JCLEPRO.2022.131834.

[150] *Environmental management-Life cycle assessment-Principles and framework Management environnemental-Analyse du cycle de vie-Principes et cadre.* Tech. rep. 2006. URL: www.iso.org.

[151] NIBE EPD. *R<THiNK your environmental impact, our concern.* 2021. URL: https://www.rethink-epd.com/en.

[152] Daman K. Panesar, Karina E. Seto, and Cameron J. Churchill. "Impact of the selection of functional unit on the life cycle assessment of green concrete". In: *International Journal of Life Cycle Assessment* 22.12 (Dec. 2017), pp. 1969–1986. ISSN: 16147502. DOI: 10.1007/s11367-017-1284-0.

[153] Bing Xia, Tao Ding, and Jianzhuang Xiao. "Life cycle assessment of concrete structures with reuse and recycling strategies: A novel framework and case study". In: *Waste Management* 105 (Mar. 2020), pp. 268–278. ISSN: 0956-053X. DOI: 10.1016/J.WASMAN.2020.02.015.

[154] Royal Netherlands Standardization Institute. "NEN-EN 15804". In: (2019).

[155] Muhammad N.S. Hadi, Nabeel A. Farhan, and M. Neaz Sheikh. "Design of geopolymer concrete with GGBFS at ambient curing condition using Taguchi method". In: *Construction and Building Materials* 140 (June 2017), pp. 424–431. ISSN: 0950-0618. DOI: 10.1016/J.CONBUILDMAT.2017.02.131.

[156] Adriana Souto-Martinez et al. "A mathematical model for predicting the carbon sequestration potential of ordinary portland cement (OPC) concrete". In: *Construction and Building Materials* 147 (Aug. 2017), pp. 417–427. ISSN: 09500618. DOI: 10.1016/j.conbuildmat.2017.04.133.

[157] Mohd Shariq, Jagdish Prasad, and Amjad Masood. "Effect of GGBFS on time dependent compressive strength of concrete". In: *Construction and Building Materials* 24.8 (Aug. 2010), pp. 1469–1478. ISSN: 09500618. DOI: 10.1016/j.conbuildmat.2010.01.007.

[158] Nederlandse norm. *NEN 7375.* Tech. rep. 2004.

[159] Jamal Khatib et al. "Effect of municipal solid waste incineration bottom ash (MSWI-BA) on the structural performance of reinforced concrete (RC) beams". In: *Journal of Engineering, Design and Technology* (May 2021). ISSN: 17260531. DOI: 10.1108/JEDT-01-2021-0068.

[160] Ali Jamshidi et al. *State-of-the-art of interlocking concrete block pavement technology in Japan as a post-modern pavement.* Mar. 2019. DOI: 10.1016/j.conbuildmat.2018.11.286.